Electromagnetic Borehole Flowmeter (EBF) Testing in R-area (U)

Westinghouse Savannah River Company
Savannah River Site
Aiken, SC 29808

SRS

SAFETY · RESPONSIBILITY · SECURITY

SAVANNAH RIVER SITE

Electromagnetic Borehole Flowmeter (EBF) Testing in R-area (U)

Gregory P. Flach, Frank C. Sappington, W. Pernell Johnson and Robert A. Hiergesell

Westinghouse Savannah River Company
Savannah River Site
Aiken, SC 29808

SAFETY • RESPONSIBILITY • SECURITY

SRS

SAVANNAH RIVER SITE
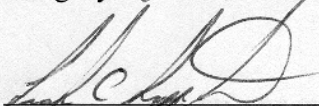
Electromagnetic Borehole Flowmeter Testing in R-area (U)
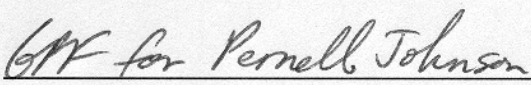
Authentication and Approvals:

(signature)   8/31/00
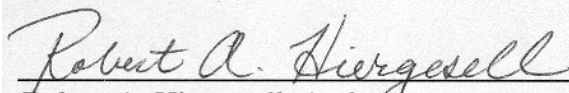
Gregory P. Flach, Author   Date

(signature)   8/31/00
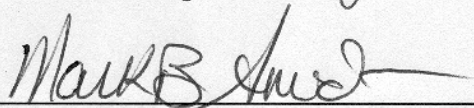
Frank C. Sappington, Author   Date

(signature) for Pernell Johnson   8/31/00
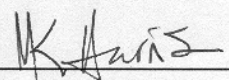
W. Pernell Johnson, Author   Date

(signature)   8/31/00
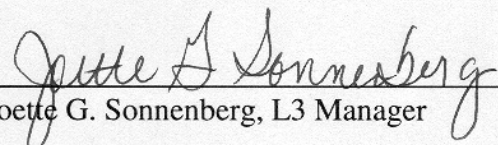
Robert A. Hiergesell, Author   Date

(signature)   9/13/00

Mark B. Amidon, Technical Reviewer   Date

(signature)   9/5/00

Mary K. Harris, L4 Manager   Date

(signature)   9/5/00

Joette G. Sonnenberg, L3 Manager   Date

EXECUTIVE SUMMARY

Six constant-rate, multiple-well aquifer tests were recently conducted in R-area to provide site-specific *in situ* hydraulic parameters for assessing groundwater flow and contaminant transport models of R-Reactor Seepage Basins (RRSB) plume migration and RRSB remedial alternatives. The pumping tests were performed in the Upper Three Runs and Gordon aquifers between December 1999 and February 2000. The tests provide reliable estimates of horizontal conductivity averaged over aquifer thickness, and a relatively large horizontal zone of influence. To complement these results, Electromagnetic Borehole Flowmeter (EBF) testing was subsequently performed to determine the vertical variation of horizontal conductivity for RPC-2PR, RPC-3PW, RPT-2PW, RPT-3PW, RPT-4PW and RPT-30PZ. The EBF data generally indicate significant aquifer heterogeneity over the tested screen intervals (Figures 14, 16-18, 20, 22, 24, 26 and 27-31). The vertical variation of groundwater flow in or out of the well screen under ambient conditions was also measured (Figures 13, 15, 19, 21, 23 and 25). These data have implications for contaminant monitoring.

Regarding future deployments, concerns about bypass flow in filter-packed wells have hindered EBF deployment at the SRS. Recently published analyses of bypass flow, the extensions developed in this report, and R-area EBF testing indicate that bypass flow will not be a serious problem in a typical SRS monitoring well. Furthermore, the head losses that drive bypass flow and cause additional flow redistribution effects can be practically eliminated in future deployments by using the 1" EBF for dynamic testing, lower pumping rates with the ½" EBF, or no EBF packer.

This page intentionally left blank

Contents

Tables

Tables (Continued)

Figures

Figures (cont'd)

Appendices

Introduction

Six constant-rate, multiple-well aquifer tests were recently conducted in R-area to provide site-specific *in situ* hydraulic parameters for assessing groundwater flow and contaminant transport models of R-Reactor Seepage Basins (RRSB) plume migration and RRSB remedial alternatives (Hiergesell, 1999; WSRC, 2000; Hiergesell and others, 2000). The pumping tests were performed in the Upper Three Runs and Gordon aquifers between December 1999 and February 2000. The tests provide reliable estimates of horizontal conductivity averaged over aquifer thickness, and a relatively large horizontal zone of influence. Table 1 summarizes the findings of Hiergesell and others (2000). To complement these results, Electromagnetic Borehole Flowmeter (EBF) testing was subsequently performed to determine the vertical variation of horizontal conductivity about the average determined from the conventional aquifer testing. This report introduces the borehole flowmeter concept and EBF instrument, summarizes field and calculation procedures, presents EBF test results for 7 R-area wells, and provides recommendations for future application of the technology at the Savannah River Site.

Borehole flowmeter designs

The term "borehole flowmeter" in this report refers to any instrument that measures the *vertical* flow inside a well casing, whether under ambient or pumping conditions. Various types of borehole flowmeters have been used in field applications, including heat pulse, tracer release and impeller (spinner) designs. Among these, only impeller flowmeters had been commercially available through the 1980s (Molz and others, 1989). Unfortunately, impeller designs contain fragile moving parts and bearings that are susceptible to degradation/clogging by suspended particles, impacts, etc. Young and Waldrop (1989) analyzed impeller flowmeter calibration data and concluded that the calibration curve is very sensitive to the condition of the bearings; therefore, frequent maintenance and calibration are required to ensure accurate data. Even so, most impeller flowmeters did not accurately measure flows below about 5 L/min (Molz and others, 1989).

To remedy these deficiencies, researchers at the Tennessee Valley Authority (TVA) developed, patented and commercialized a robust, highly-sensitive, borehole flowmeter based on electromagnetic principles in the late 1980s and early 1990s. The Electromagnetic Borehole Flowmeter (EBF) operates according to Faraday's Law of Induction, which states that the voltage induced by a conductor moving at right angles through a magnetic field is directly proportional to the velocity of the moving conductor (Waldrop, 1995). Schematic diagrams of the EBF are shown in Figures 1 and 2 (Molz and Young, 1993). Groundwater acts as the moving conductor, an electromagnet generates the magnetic field, and electrodes measure the induced voltage. The ½" ID EBF has a threshold flowrate of about 5 mL/min, which is 1000 times more sensitive than the typical impeller flowmeter. Flowrates up about 10 L/min can be measured, giving the ½" ID EBF outstanding range. The 1" ID EBF can measure flows from about 40 mL/min to 40 L/min (Waldrop, 1995). Both the ½" and 1" EBF instruments were chosen for aquifer testing in R-area.

Borehole flowmeter testing

The idea behind borehole flowmeter testing is to relate horizontal conductivity as a function of elevation, K(z), to borehole discharge as a function of elevation Q(z). The field procedure is schematically illustrated in Figure 3 (Molz and Young, 1993). Under quasi-steady pumping conditions, borehole discharge (Q) from the bottom of the screen up to the current flowmeter position is measured as a function of elevation (z). As shown in Figure 4, the difference (ΔQ) in borehole discharge Q(z) between at any two locations is the flowrate of groundwater entering the well casing over that interval. This differential flowrate, minus any ambient flow effects, is proportional to the horizontal conductivity of the aquifer over that interval. Ambient flow refers to horizontal flow through the well screen and vertical flow in the casing under natural, undisturbed conditions. In order to rigorously account for potential ambient flow effects, the standard borehole flowmeter test procedure actually involves two series of measurements:

1) under ambient conditions, measure the vertical flowrate inside the well screen at 1 to 2 ft intervals,

2) pump (or inject) at a constant rate above the screen zone and borehole flowmeter,

3) pause until the drawdown becomes quasi-steady-state,

4) under these quasi-steady-state pumping conditions, again measure the vertical flowrate inside the well screen at 1 to 2 ft intervals.

The quasi-steady conditions referred to in step 3) are reported to occur rapidly (e.g. 30 minutes). The ambient flow data is also useful by itself for determining the direction(s) of vertical head gradients in the surrounding aquifer, which has contaminant monitoring implications to be discussed later. Molz and Young (1993) provide a quantitative criterion for determining when quasi-steady conditions have been reached in step 3), and develop methods for analyzing the data as discussed below.

Analysis of borehole flowmeter field data

Molz and others (1989) and Molz and Young (1993) present two methods for estimating the vertical variation of horizontal conductivity from field measurements of borehole discharge as a function of depth, such as those provided by the EBF (see also Rehfeldt and others (1989)). Both methods assume a fully-penetrating well in a confined aquifer. The first method applies the Cooper-Jacob (1946) method to individual sub-intervals of the well screen to estimate conductivity as a function of vertical position. Alternatively, the relative variation of horizontal conductivity about vertically-averaged K can be directly related to the EBF measurements of borehole discharge as a function of depth. If the vertical average is known or can be estimated by other means (e.g. pumping test), then the conductivity profile can be determined. The first method produces conductivity estimates from EBF test data alone, but involves a number of uncertain parameters. The second method is simpler and more precise, but requires an independent estimate of average conductivity. In R-area, a conventional pumping test result is available for each

EBF tested well. Therefore, the second approach presented by Molz and Young (1993) is preferred for the present application. Nevertheless, both methods are presented in order to later compare results.

As discussed previously, the field procedure involves measuring the vertical flowrate within the well casing at regular intervals, typically every 1 to 2 ft, first under ambient conditions and then under pumping conditions. The difference between any two readings is the flow entering the well between the two corresponding elevations. A negative value implies that flow is leaving the well. To develop the first method, the Cooper-Jacob equation is applied to each layer as

$$\Delta h_i(r_w, t) = \frac{(\Delta Q_i - \Delta q_i)}{2\pi K_i \Delta z_i} \ln\left(\frac{1.5}{r_w}\sqrt{\frac{K_i \Delta z_i t}{S_{si} \Delta z_i}}\right) \tag{1}$$

where

$\Delta h_i \equiv$ drawdown

$\Delta Q_i - \Delta q_i \equiv$ net differential flow

$\Delta Q_i \equiv$ difference in EBF flow at the top and bottom of the ith interval under *pumping* conditions

$\Delta q_i \equiv$ difference in EBF flow at the top and bottom of the ith interval under *ambient* conditions

$K_i \equiv$ horizontal conductivity of ith layer

$\Delta z_i \equiv$ thickness of ith layer

$r_w \equiv$ well bore radius

$t \equiv$ elapsed time

$S_{si} \equiv$ specific storage of ith layer

Assuming negligible borehole flowmeter losses under low flow conditions, each layer experiences the same measured drawdown, Δh. The numerical simulations of Javendel and Witherspoon (1969) indicate that the transient drawdown responses of layers in a heterogeneous aquifer quickly merge into a common response described by the Theis solution using averaged aquifer properties. This observation suggests that each layer effectively behaves as if it has the hydraulic diffusivity of the entire aquifer:

$$\frac{K_i \Delta z_i}{S_{si} \Delta z_i} = \frac{T}{S} = \nu \tag{2}$$

In this expression

$\nu \equiv$ hydraulic diffusivity of the entire aquifer

$T \equiv$ transmissivity of the entire aquifer

$S \equiv$ storage coefficient (storativity) of the entire aquifer

With this assumption, one of two proposed by Molz and others (1989), equation (1) becomes after solving for K_i

$$K_i = \frac{(\Delta Q_i - \Delta q_i)}{2\pi\Delta z_i \Delta h} \ln\left(\frac{1.5}{r_w}\sqrt{\frac{Tt}{S}}\right) \tag{3}$$

With a prior estimate of aquifer diffusivity (T/S), equation (3) provides a direct estimate of horizontal conductivity for the ith layer. Fortunately, the Cooper-Jacob estimate is not highly sensitive to the assumed value of T/S for large times, because diffusivity appears within a square-root and logarithm. However, well inefficiencies introduce significant uncertainty in the drawdown experienced by the formation, Δh.

The data analysis procedure for the second method presented by Molz and Young (1993) is summarized by

$$\frac{K_i}{\overline{K}} = \frac{(\Delta Q_i - \Delta q_i)/\Delta z_i}{\sum_i (\Delta Q_i - \Delta q_i)/\sum_i \Delta z_i} \tag{4}$$

where

$K_i \equiv$ horizontal conductivity of the ith interval

$\overline{K} \equiv$ vertically-averaged conductivity

$\Delta Q_i \equiv$ difference in EBF flow at the top and bottom of the ith interval under *pumping* conditions

$\Delta q_i \equiv$ difference in EBF flow at the top and bottom of the ith interval under *ambient* conditions

$\Delta z_i \equiv$ height of the ith interval.

In equation (4), $(\Delta Q_i - \Delta q_i)$ is the net flowrate induced by pumping and accounts for ambient flow effects. Note that the relative conductivity distribution is equal to the relative distribution of net flow entering the well, which is assumed to occur after the initial transient passes and quasi-steady conditions develop. The basis for this assumption is considered further in the next section.

Both methods, summarized by equations (3) and (4), assume that flow approaching the well is horizontal and driven by a vertically-uniform radial head gradient. Any deviations from this assumption in the flow field will introduce systematic biases in the relative conductivity profile computed from either equation. Therefore, pre-testing consideration should be given to identifying, and minimizing if possible, any conditions that will violate the above assumption. For example, non-horizontal flow will occur in an unconfined aquifer if the drawdown is significant, but can be minimized by pumping at a small rate. A partially-penetrating well screen would also create vertical flows. More subtle sources of vertical flow leading to systematic errors are 1) transient effects in the presence of aquifer heterogeneity, 2) a high conductivity filter pack, and 3) head losses across the EBF. Table 2 summarizes peer-reviewed journal articles dealing with these biases, individually and in combination. Each category is discussed in more detail below.

Systematic errors due to transient effects

The most common method of analysing borehole flowmeter data, described by equation (4), depends on the discharge from each layer being proportional to layer transmissivity. This assumption is not valid at early times when transient storage effects dominate, but becomes increasingly accurate at later times. Systematic errors due to transient effects can be mitigated by waiting until "pseudo-steady" conditions are established. Exactly when such conditions are reached is not entirely clear from the literature, but acceptable criteria have been presented in the literature and are further developed in this section, as discussed below.

The data analysis method is based on Javendel and Witherspoon (1969) who conducted an early numerical study of a two-layer confined aquifer with permeability contrasts up to 100:1. Specific storage was assumed to be constant (Kabala, 1994) so the ratio also applies to hydraulic diffusivity. They found that for non-dimensional times

$$t_D \equiv \frac{1}{u} \equiv \frac{4Tt}{Sr^2} \tag{5}$$

exceeding 400 to 4000 (i.e. $Tt/Sr^2 > 100$ to 1000), and a non-dimensional radius r/b exceeding 0.125, the transient drawdown in each layer followed that predicted by Theis (1935) based on average aquifer properties (Javendel and Witherspoon, 1969, Figures 5 and 6). In definition (5) and the non-dimensional radius

   $T \equiv$ transmissivity of entire aquifer (Kb)

   $t \equiv$ time

   $S \equiv$ storage coefficient

   $r \equiv$ radius

   $b \equiv$ entire aquifer thickness

They also observed that "cross-flow near the well bore diminishes with time until finally at large values of time the directions of flow are almost horizontal. Under these conditions the radial gradients along the well bore are uniform and constant, and flux into the well within a given layer is simply proportional to the permeability of that layer" (see Javendel and Witherspoon, 1969, Figures 7 and 8). Figures 7 and 8 in Javendel and Witherspoon (1969) are described in terms of dimensional time. Because specific storage is not specified, the equivalent non-dimensional time when

$$Q_i \propto T_i \tag{6}$$

(flow proportional to transmissivity) is unknown from these figures. However, horizontal flow at the well bore radius can be inferred to occur when the layer drawdown curves in Figures 5 and 6 of Javendel and Witherspoon (1969) merge into a common response. At this point, no head differences exist to drive crossflow.

Rehfeldt and others (1989) and Molz and others (1989) interpreted horizontal flow to imply condition (6) for practical purposes. This condition occurs when $t_D > 400$ to 4000, depending on the permeability contrast between layers and aquifer thickness. At the well bore radius, the criterion is rapidly met. At Savannah River Site (SRS) well RPT-4PW for example, the minimum required time is only

$$t = t_D \frac{Sr_w^2}{T} = (400 \text{ to } 4000) \frac{(1.5 \times 10^{-3})(5/12 \, \text{ft})^2}{0.8 \, \text{ft}^2 / \text{min}} = 8 \, \text{sec to } 1.3 \, \text{min} \tag{7}$$

Analysis of other SRS wells in R-area yields similar results. However, a word of caution is in order. The range of r/b values considered by Javendel and Witherspoon (1969) is not strictly applicable to a typical SRS well (e.g. RPT-4PW). A common example would be a 10 in borehole and a 40 ft screen, or r/b = 0.01. This non-dimensional radius is an order of magnitude smaller than considered, and implies a larger non-dimensional time before drawdown follows the Theis solution.

Molz and others (1989) also state that "pseudo steady state conditions" are required to obtain equation (4), and that these occur when $t_D > 100$, a less restrictive criterion than $t_D > 400$. However in subsequent personal communication (e-mail dated July 12, 2000), Dr. Molz discovered that the intended pseudo-steady-state condition was incorrectly stated in the Molz and others (1989). The error was also reproduced in later papers, such as Molz and Young (1993). Instead of using the well bore radius in equation (5), one should substitute "some estimate of the radius of influence of a flowmeter test" according to Dr. Molz. He does not state a specific formula for radius of influence, but a typical value might be a few feet and produce a dimensional time of at least several minutes before borehole flowmeter testing should begin.

The rigor in assuming that horizontal flow at $t_D > 400$ to 4000 implies condition (6) is not completely clear, and Kabala (1994) subsequently questioned the calculation method summarized by equation (4). He observed however that "since a horizontal flow regime develops in a layered aquifer in the vicinity of a pumped fully penetrating well long

before the quasi-steady state well response is reached [Javendel and Witherspoon, 1968, 1969], it should be possible to design a methodology, based on the Theis [1935] solution, for interpreting flowmeter tests conducted while the well response is still transient." Kabala (1994) assumed that, after a brief initial period (e.g. $t_D > 400$), drawdown in each layer can be described by the Theis solution using layer properties and a contribution, Q_i, to total flow, Q. Equating this drawdown with the Theis drawdown based on aquifer average properties yields

$$\frac{T_i}{T} = \frac{Q_i}{Q}\frac{W\!\left(\dfrac{Sr^2}{4Tt}\dfrac{T/S}{T_i/S_i}\right)}{W\!\left(\dfrac{Sr^2}{4Tt}\right)} = \frac{Q_i}{Q}\frac{W\!\left(\dfrac{1}{t_D}\dfrac{T/S}{T_i/S_i}\right)}{W\!\left(\dfrac{1}{t_D}\right)} \equiv \frac{Q_i}{Q}\frac{W(u\gamma)}{W(u)} \equiv \frac{Q_i}{Q}\eta(u,\gamma) \tag{8}$$

In this expression, layer transmissivity is only strictly proportional to layer flow for infinitely long times or diffusivity equal to the aquifer average ($\gamma = 1$). The bias in omitting the factor η in conventional borehole flowmeter data analysis is therefore $1/\eta$, which is plotted in Figure 5. Figure 5 is therefore the inverse of Figure 1 in Kabala (1994). Incidentally, the curves in Kabala's figure are mislabeled. The upper curve is actually $\gamma = 10^{-2}$ while the lower curve is $\gamma = 10^2$. In Figure 5, "T/S ratio" in the legend is the quantity

$$\log_{10}\frac{T_i/S_i}{T/S} = \log_{10}\frac{1}{\gamma} \tag{9}$$

So, the upper dashed curve corresponds to a low diffusivity layer with $\gamma = 10^2$, while the lower solid curve is high diffusivity and $\gamma = 10^{-2}$. Kabala (1994) observed that the bias is still significant at $t_D = 10^7$, yet borehole data are commonly analyzed for times as early as 10^4. Figure 5 makes sense qualitatively. Consider for example two layers with identical transmissivity, but differing storage coefficient. At early times the layer with the larger storage coefficient (lower diffusivity) would produce more flow in response to a common drawdown. Using the conventional method of data analysis, equation (4), a larger value of conductivity would be computed for this lower diffusivity layer, due to greater layer flow. Thus the estimate would be biased high, as indicated by Figure 5 for low diffusivity. Conversely, estimates for high diffusivity layers would be biased low. Note that the bias is larger for low diffusivity layers than high T/S layers, contrary to Kabala's (1994, p. 686, 2nd column, last full sentence) statement.

While Kabala (1994) attempted a more rigorous analysis of borehole flowmeter testing, the assumption that each layer can be described by the Theis solution using layer properties is contrary to Javendel and Witherspoon (1969), which showed that each layer eventually follows a *common* Theis solution based on aquifer average properties. Equating the layer and aquifer average Theis solutions in Kabala (1994) implies that Q_i must change with time, unless diffusivity is constant, which is a violation of the constant Q assumption of Theis. Therefore, the validity of Figure 5 is unclear. Nevertheless,

Kabala (1994) did establish that condition (6) is at least valid at long times and/or constant diffusivity among layers.

Rudd and Kabala (1996) subsequently performed numerical simulations of borehole flowmeter testing and confirmed that the Theis solution applied to individual layers "does not fully capture the flow dynamics in layered aquifers". The deficiency was attributed to the well face fluxes at layers being transient and vertically non-uniform in their numerical simulations, conditions which violate the assumptions of Theis. Numerical simulations of a two-layer aquifer demonstrated that hydraulic conductivity estimation errors using equation (4) were practically negligible for hydraulic diffusivity contrasts of $10^{-2} <$ $(T/S)_{layer\ 1}/(T/S)_{layer\ 2} < 10^2$, r/b = 0.01 and $t_D > 10^3$ in each layer. This result is surprising given the earlier findings of Kabala (1994) which suggested significant biases persisting for relatively long times. Outside this diffusivity range, the biases are not negligible but usually small for high diffusivity layers. This result is good in that borehole flowmeter testing can only measure high conductivity zones with accuracy anyway, once flow measurement errors are considered. A puzzling aspect of Ruud and Kabala (1996) is that any significant estimation errors are always positive. This result is qualitatively contrary to Kabala (1994) and intuition which indicates that equation (4) should underestimate conductivity for high diffusivity layers.

In summary, the minimum practical conditions under which equation (4) is applicable have not been well defined in general. The conventional analysis is rigorously valid only for infinitely long times and/or constant hydraulic diffusivity among layers (Kabala, 1994). The criterion of Rehfeldt and others (1989) and Molz and others (1989)

$$t_D = \frac{4Tt}{Sr_w^2} = \frac{4\nu t}{r_w^2} > 4\times10^2 \text{ to } 4\times10^3 \tag{10}$$

is commonly used, but may be non-conservative particularly for aquifers of practical thickness. The work of Ruud and Kabala (1996) suggests that equation (4) can be used with good accuracy for $t_D > 10^3$ within each layer, aquifer thicknesses satisfying b < 100r (i.e. r/b > 0.01) and reasonable diffusivity contrasts. To apply this criterion before testing, consider a two layer aquifer with an assumed diffusivity contrast ($\nu_2/\nu_1 > 1$). For the more stringent layer (#1), the criterion at the well bore radius is

$$\frac{4T_1t}{S_1r_w^2} = \frac{4\nu_1 t}{r_w^2} > 10^3 \tag{11}$$

The diffusivity of layer #1 can be related to average diffusivity and diffusivity ratio as

$$\nu_1 = \nu \frac{2}{1 + \nu_2/\nu_1} \tag{12}$$

Substituting equation (12) into (11) produces

$$t_D > 1000 \frac{1 + \nu_2 / \nu_1}{2} \qquad (13)$$

which is generally more conservative than criterion (10). As a third alternative, the corrected criterion of Molz (2000) can be used to define when pseudo-steady conditions are achieved:

$$t_D > 10^2 \left(\frac{r_i}{r_w} \right)^2 \qquad (14)$$

Here r_i is an influence radius measured in feet (m) rather than inches (cm). This criterion would typically be more conservative than (10). A final alternative would be a time beyond which the Theis well function $W(u)$ is slowly changing on an aquifer average basis, such as

$$t_D > 10^6 \qquad (15)$$

which is simply a more conservative version of criterion (10). Equations (10), (13), (14) and (15) provide four possibilities for defining when quasi-steady flow has been reached. The latter three estimates tend to be more conservative. Post-test checks for R-area wells using these criteria are presented later in the report. The safest strategy to minimize systematic errors due to transient effects would be to wait as long as practical after pumping starts before taking borehole flow measurements. In the field, a suggestion would be to wait until the drawdown is observed to be pseudo-steady. Dr. Molz recommends waiting at least 30 minutes after pumping before starting borehole flowmeter testing (Molz, 2000).

Systematic errors due to a well filter pack

Ruud and Kabala (1997) considered the effect of a filter pack annulus on borehole flowmeter estimation under quasi-steady state conditions. In numerical simulations of a two layer aquifer, some groundwater was observed to flow vertically through the filter annulus from the higher conductivity zone and discharge through the well screen adjacent the lower K interval. The artificially-reduced discharge from the high conductivity zone lead to an underestimate of K using equation (4). Conversely, increased discharge from over the screen interval adjacent the low conductivity zone produced an estimate that was biased high. Ruud and others (1999) also considered the effects of a filter pack alone, along the way to analysing the combined effects of a filter pack and flowmeter head losses.

Systematic errors due to EBF head loss

As described by Dinwiddie and others (1999), head losses across the EBF can introduce significant errors in the hydraulic conductivity profile calculated from equation (4). The first of two identified effects for confined aquifers they termed "head-loss-induced flow

redistribution". The second effect involves pump-induced flow bypassing the EBF through the filter pack, and will be discussed in the next section.

The standard calculation procedure for EBF data is based on the assumption that the aquifer is exposed to the same drawdown over the entire well screen length. However, the EBF isolates the portion of the aquifer below the meter from the full drawdown observed at the surface, due to head loss across the meter (Figure 6). That is, the interval below the EBF experiences reduced drawdown. When the head loss caused by flow through the EBF is significant compared to the imposed drawdown, significant biases may be introduced in the calculated relative conductivity profile. Dinwiddie and others (1999) demonstrated that the lower three-quarters of the computed K profile is biased low while the upper quarter is biased high by a greater amount. Head-loss-induced flow redistribution increases with increasing aquifer conductivity for the same pumping rate.

Dinwiddie and others (1999) quantitatively investigated the phenomenon for the ½" ID EBF in a 4" ID, 20 ft long, nonpacked, well screen. Numerical simulations were reported for pumping rates of approximately 20 and 5 L/min, and aquifer conductivities of 0.91, 9.1 and 91 m/day (3, 30 and 300 ft/d). Most of the R-area EBF testing involved 4" wells with active screen lengths of 15 to 40 ft and a pumping rate of roughly 5 L/min. Therefore, the results shown in Figure 16 of Dinwiddie and others (1999), and reproduced here as Figure 7, are most relevant to R-area testing. The aquifer is assumed to have a uniform conductivity of 9.1 m/day (30 ft/day) and the flow rate is 5 L/min. In Figure 7, the calculated K profile is seen to be biased low by as much as 7% in the center, and over-predicted by 27% at the uppermost interval. The biases are demonstrated to increase with increasing aquifer conductivity, and vice versa. The R-area wells that were tested with the EBF have filter packs. Therefore direct comparison of Dinwiddie and others (1999) to the present study has limitations.

Ruud and others (1999) performed similar numerical simulations and observed significant upward flow for the conditions considered. Some flow was observed to leave the well bore just below the flowmeter, enter the aquifer, and then re-enter the well bore just above the flowmeter, thus bypassing the instrument. In wells with a filter pack, bypass flow due to flowmeter head losses is even more significant, as discussed in the next section.

Systematic errors due to combined EBF head loss and filter pack

In wells with a high conductivity filter pack, a second result of head loss across the EBF is bypass flow around the meter, as illustrated in Figures 8 and 9 (Dinwiddie and others, 1999). In this situation, the EBF measures only a fraction of the flow leaving the aquifer below the meter position, generally leading to an under-estimate of the actual conductivity. The exception occurs at the uppermost screen interval, when the EBF passes the top of the screen. Lacking screen above the EBF, bypass flow suddenly ceases and all flow must now pass through the meter. The sudden increase in differential flow for the top interval produces an anomalous high K estimate. Dinwiddie and others (1999) demonstrate that bypass flow increases with filter pack thickness, filter pack conductivity,

and EBF head loss. They also provide a mechanism for estimating bypass flow that can be extended to the R-area test conditions as shown below.

Dinwiddie and others (1999, equation (11)) express bypass flow using a one-dimensional flow concept as

$$Q_{bp}^{*} = K_{fp} A \frac{\Delta h}{L} \tag{16}$$

where

Q_{bp}^{*} $\equiv$ bypass flow (m^3/day)

K_{fp} $\equiv$ filter pack conductivity (m/day)

A $\equiv$ cross-sectional area of filter pack annulus (m^2)

Δh $\equiv$ head loss across EBF (m)

L $\equiv$ effective length of bypass flow through filter pack (m)

Head loss across the ½" EBF was determined through laboratory testing to be (Foley, 1997; Dinwiddie and others, 1999)

$$\Delta h = 0.0012 Q_{m}^{2} + 0.001 Q_{m} \tag{17}$$

where

Q_m $\equiv$ flow through EBF (L/min)

The effective filter pack length, L, can be estimated from numerical simulations performed by Dinwiddie and others (1999). In their simulations, the EBF packer is approximately 5" or 0.127 m in length. For filter pack annular widths of 3.0 and 5.4 cm, the corresponding effective filter pack length was determined through numerical simulations to be 0.18 and 0.21 m, respectively. The effective filter pack length is greater than the EBF packer length because additional distance is required below and above the EBF for the bypass flow to exit and enter the well screen, as shown in Figure 9 (Dinwiddie and others (1999). Assuming these multi-dimensional end effects are controlled mainly by the filter pack thickness, an effective filter pack length can be easily estimated for other packer lengths.

The packer length and effective filter pack length are related by

$$L = L_{EBF} + \Delta L \tag{18}$$

where

$L \equiv$ effective filter pack length (m)

$L_{EBF} \equiv$ EBF packer length (m)

$\Delta L \equiv$ length associated with multi-dimensional end effects (m)

For filter pack annular widths of 3.0 and 5.4 cm, ΔL is 0.053 (0.18-0.127) and 0.083 (0.21-0.127) m, respectively. Assuming a linear variation,

$$\frac{\Delta L - 0.053\,\text{m}}{t_{fp} - 3.0\,\text{cm}} = \frac{0.083 - 0.053\,\text{m}}{5.4 - 3.0\,\text{cm}}$$

or

$$\Delta L = 0.053\,\text{m} + 0.0125\,\frac{\text{m}}{\text{cm}}\left(t_{fp} - 3.0\,\text{cm}\right) \tag{19}$$

where

$t_{fp} \equiv$ thickness of filter pack annulus (cm)

For R-area testing, L_{EBF} is approximately equal to 7" or 0.178 m. Combining this estimate with equations (18) and (19) yields

$$L_{Rarea} = 0.231\,\text{m} + 0.0125\,\frac{\text{m}}{\text{cm}}\left(t_{fp} - 3.0\,\text{cm}\right) \tag{20}$$

for use in equation (16).

FX-50 was used as the filter pack in the R-area wells that were tested with the EBF. The conductivity of FX-50 was estimated through constant-head permeameter testing using the apparatus depicted in Figure 10. The results of 4 trials are listed in Table 3. The average conductivity is 0.12 cm/s, 330 ft/d or 100 m/d. The filter pack area is simply

$$A = \frac{\pi}{4}\left(D_o^2 - D_i^2\right) \tag{21}$$

where D_o and D_i are the inner and outer diameters of the filter pack in meters.

Bypass flow can thus be estimated by combining equations (16), (17), (20) and (21) for the ½" ID EBF. The analysis is the same for the 1" ID EBF, except for head loss. Arnold and Molz (2000) determined that head loss across the 1" EBF is about 16 times lower than for the ½" EBF at the same flowrate, based on analysis of a theoretical nozzle flow equation and laboratory experimentation. Therefore, head loss for the 1" EBF can be approximated as 1/16 of the result from equation (17).

Ruud and others (1999) performed similar numerical simulations considering wells without and with a filter pack, and homogeneous and layered aquifers. Head-loss-induced errors increased for wells with a filter pack and layered aquifer properties, compared to a homogeneous aquifer and no filter pack.

R-area field experience

Beyond the basic field procedure described in an earlier section of this report, a number of practical and logistical issues should be considered during field deployment of the EBF. They include items associated with the power supply, cable, packer and uphole electronics. A notable difficulty specific to the equipment deployed at R-area was an ambient air temperature effect on the uphole electronics.

Power supply: Trial and error experience showed that the EBF performance was greatly influenced by the power supply unit, e.g. generator, inverter, etc. The power supply must have a very constant voltage output. Any fluctuations other than small changes in the voltage to the uphole electronics will cause shifts in the meter output readings. This problem can be eliminated by the use of an uninterruptible power supply, a generator with a smooth/constant voltage output, or a power inverter hooked up to a 12 volt power source.

Pumps used during the dynamic testing increase power demand and can also be affected by the power supply. This change in the supply output may affect the actual flows causing changes in the meter output. The generator must be reliable and of the correct size to maintain a constant pump operation. Ideally, separate power supplies would be used for the pump and EBF.

Cable: Two items that would make the unit more user friendly include incorporation of the packer air/nitrogen supply line and incremental foot markings with the electronics cable. Current design requires the addition of a separate air supply line and either a tape or incremental foot markings to be put on the cable by the user. This adds bulk and increases difficulty in handling and deployment time.

The packer supply line and electronics cable must be manually handled by a dedicated field person, in addition to another person who performs most other functions. Lowering and raising the cable can be physically demanding for deep holes. Holding the EBF at a constant, specified depth by hand during testing is tedious. Excess cable must presently be handled by laying it on the ground. As the EBF is advanced deeper into the well, debris such as dirt, grass and/or pine straw can be drawn into the well. These deficiencies could be eliminated with a portable drawworks, such as various models offered by Century Geophysical Corporation that are compatible with contemporary commercial EBF designs.

Packer: The design of the packer includes a stainless steel gear clamp at the top and bottom of the packer. The screw housing on the clamp can be bumped during the insertion of the packer into a well as well as when the packer passes by a joint in the well. If the clamp is bumped/offset a sufficient amount the bladder will leak. This is primarily a

consideration when using the small packer in a 4 inch well where the fit of the deflated packer has a minimal tolerance. Close inspection of the packer is recommended prior to and during each deployment.

Uphole electronics: The uphole electronics box was affected by outside ambient conditions, in that cold temperatures prevented stable display readings. Over the course of two weeks of field testing, it was determined that a steady state "0" reading could not be obtained until the ambient temperature reached approximately 60 ºF.   Unstable readings occurred during three early morning warm up periods when the temperature was below approximately 60 ºF. During the first test the probe was plugged to eliminate any potential for flow through the EBF, lowered into the well, and allowed to warm up for 1 hour per the manufacturers instructions. The instrument display was zeroed and testing started following the appropriate procedural steps. At the completion of the ambient test the instrument had a reading of -0.027 with the probe above the screen in the casing. The probe was removed, plugged, lowered back into the well. With the probe plugged the instrument output was -0.032 and then re-zeroed. At that point the temperature had reached approximately 74 ºF. The following dynamic test started at an instrument reading of 0.000 and ended at -0.005.

Similar behavior were observed on two other occasions. During the second occasion the instrument was warmed up for 1 hour and 45 minutes prior to the start of the test and zeroed. At the completion of the test an offset of -0.015 was recorded. A stable reading could not be obtained and testing did not start on the third occasion until the ambient air temperature had reached approximately 60 ºF. On all other tests conducted the ambient air temperature had reached a minimum of approximately 60 ºF by the end of the warm up period. Following these tests the meter was checked for zero, and observed to read within a few thousands of zero.

The cause of the drift has not been specifically identified. Perhaps a weak electrical component or loose connection was failing at temperatures below approximately 60 ºF, but performing reliably at warmer ambient air temperatures.   The instrument drift observed during cold mornings was significant compared to the ambient flows being measured.   If the ambient flows are of direct interest, future EBF testing should be targeted for ambient air temperatures above 60 ºF. However, the instrument noise under cold conditions was generally not significant compared to differential dynamic flows. Therefore if the non-dimensional conductivity profile is of ultimate interest, then ambient air temperature is probably not a significant issue with respect to future deployments.

EBF calibration results

Calibration data for the ½" ID and 1" ID EBF instruments were obtained from the SRS Experimental Thermal Fluids Laboratory (M&TE ID numbers ES020460 and ES020483 dated 3/24/00). Tables 4 and 5 summarize the calibration data for the ½" and 1" EBF instruments respectively. Figures 11 and 12 display the data and chosen calibration curves for the two EBFs. A quadratic functional form forced to go through the origin (0,0) was chosen for the ½" EBF calibration curve. With this selection an instrument

reading of zero corresponds exactly to zero flow. This feature is desirable when interpreting ambient flow data in the field. The ½" EBF calibration model is

$$Q = 0.0024I^2 + 0.7838I \tag{22}$$

where

$$Q \equiv \text{volumetric flowrate in L/min}$$

$$I \equiv \text{instrument response}$$

The 1" EBF is typically not used for ambient flow testing, and the calibration data were fit with the linear function

$$Q = 0.9797I + 0.1097 \tag{23}$$

where Q and I are defined as before.

R-area conductivity profile results

EBF testing was conducted for seven wells in R-area: RPC-1PW, RPC-2PR, RPC-3PW, RPT-2PW, RPT-3PW, RPT-4PW and RPT-30PZ. For each well that was dynamically tested, the field data were analyzed for vertical variation in horizontal conductivity using equation (4). Bypass flow through the filter pack was estimated from equations (16), (17), (20) and (21). Discussion specific to each well is provided below.

RPC-1PW: RPC-1PW is a 2 inch well with a 15 ft screen in the water table. EBF testing was largely unproductive because only about 2 ft of the screen was saturated at the time. Testing was abandoned after the ambient flows were measured initially. Appendix A contains a record of the ambient test results. The ambient flows readings are negative indicating downward flow in the casing, due to a downward head gradient in the aquifer.

RPC-2PR: RPC-2PR is a 4 inch well with a fully-penetrating 40 ft screen in the "transmissive" zone. The EBF field data for RPC-2PR are provided in Appendix B. Table 6 shows calculations of the non-dimensional conductivity profile based solely on EBF testing, the dimensional conductivity profile based on EBF and conventional aquifer testing, and an estimate of bypass flow through the filter pack. The differential ambient flow and hydraulic conductivity profiles are plotted in Figures 13 and 14 respectively.

Column (4) in Table 6 lists flow inside the well casing under ambient conditions, measured as a function position with the EBF. A positive value indicates upward flow, and a negative value corresponds to downward flow. Overall the ambient data indicate downward flow through the casing due to a downward head gradient in the aquifer. Column (5) lists differential ambient flow, computed as the difference between adjacent EBF measurements. In this column, a positive value means groundwater is entering the casing (leaving the aquifer) while a negative value means water is flowing out the screen (entering the aquifer). These data are plotted in Figure 13. For RPC-2PR, groundwater is

observed to enter the casing over the upper three-quarters of the screen and leave over the bottom quarter, particularly over the interval centered at 233.39 ft msl (see column (12)).

The non-dimensional or relative hydraulic conductivity distribution, K_i/K, based on EBF data alone is shown in column (13). The negative values are not physically possible of course. Negative values of K_i/K, are generally the result of measurement errors and non-ideal test conditions. Expanding on the latter, any artificial reduction in EBF flow when the instrument is passing by a low permeability interval can cause a negative differential net flow in column (9). Examples include a reduction in pump flowrate, which is assumed to be constant in the analysis, and increased flow bypassing the EBF through the filter pack, which also reduces EBF measured flow. These reductions in EBF measured flow are typically small, but can overwhelm the true differential net flow from the aquifer over an interval if the permeability is very low. Therefore, negative values should simply be interpreted as a low permeability zone. The specific cause of negative K_i/K values for RPC-2PR is not known. From inspection of the field data in Appendix B, one possibility is a slight reduction in pumping rate around 16:00 hours on 3/28/00.

The dimensional conductivity profile is obtained by multiplying column (13) by the average conductivity from conventional aquifer testing. Hiergesell and others (2000) report a best-estimate transmissivity of 0.7655 ft^2/min for RPC-2PR (Table 1). Hydraulic conductivity averaged over a 40 ft screen length becomes 27.6 ft/d or 9.72×10^{-3} cm/s. The resulting dimensional conductivity profile is shown in columns (14) and (15) of Table 6, and plotted in Figure 14. The aquifer is seen to be quite heterogeneous over the 40 ft interval tested. Several intervals of high conductivity are seen, with the highest value being 158 ft/d or nearly 6 times higher than average. At the other end of the spectrum, several very low conductivity intervals are also observed.

Estimates of filter pack bypass flow are provided in column (17). Bypass flow relative to EBF flow, column (18), is greatest near the top of the screen. This is because the head losses driving bypass flow increase non-linearly with increasing EBF flow, as indicated by equation (3). The maximum ratio is 6.3%. Although any bypass flow is undesirable, this level should not introduce a large bias in the computed conductivity profile. Fortunately, the bypass flow estimates in Table 6 are probably conservatively high, because the filter pack conductivity was assumed to be that of pristine FX-50. In reality, the in-place FX-50 has certainly been "contaminated" with finer-grained sediments and drilling mud, and exhibits a significantly lower conductivity. As evidence, consider the EBF measured flows for the top two positions. At an elevation of 270.89 ft msl, the EBF is centered above the top of the well screen and is measuring the total pumping rate of 4.30 L/min. One foot lower at 269.89 ft msl, the EBF is centered 0.67 ft or 8 inches below the screen top and measuring 4.22 L/min. The difference between these values is the sum of the flow entering the casing through the top few inches of the screen and any bypass flow. Therefore bypass flow cannot be exceeding 0.08 L/min or 2% of EBF flow. While not definitive, these arguments strongly suggest the maximum bypass flow is well under 6% and not a source of large uncertainty.

Coincidentally, the conditions of this test are similar to one of the "head-loss-induced flow redistribution" numerical simulations of Dinwiddie and others (1999), the results of which are displayed in Figure 7. They compare as follows:

Feature	*RPC-2PR*	*Dinwiddie and others (1999) / Figure 6*
Conductivity (ft/d)	27.6	29.9
Casing diameter (in)	4	4
Filter pack?	yes	no
Screen length (ft)	40	20

The results shown in Figure 7 suggest that biases on the order of several percent are possible for RPC-2PR due to a head-loss-induced flow redistribution effect.

RPC-3PW: This well has a 4 inch casing and a partially-penetrating 40 ft screen in the "lower" aquifer zone of Upper Three Runs aquifer unit (Table 1). Appendix C contains the field data obtained from using both the ½" and 1" EBF instruments for dynamic flow measurements. Data from the ½" EBF are analyzed in Table 7 at 1 ft increments, in the same manner as Table 6 discussed above. The differential ambient flow results are displayed in Figure 15. This figure indicates that flow is mainly entering the casing in the middle of the screen and exiting at the bottom of the screen. Anomalous behavior is observed at the top of the screen where a large negative flow is observed next to a large positive flow. Looking at the ambient flow in column (3) of Table 7, the measurement at 199.98 ft msl is strange in that upward flow in the casing is indicated, whereas all other flows are downward.

The dynamic test results for non-dimensional conductivity are highly variable and contain several negative values. The estimates near 200 ft msl also appear to be aphysical. Looking at the measured flows under dynamic conditions in column (6), an abrupt and unexpected decrease occurred at 199.98 msl. A possible, but highly unlikely, explanation is severe instrument error. The anomaly in the vicinity of 199.98 ft msl occurred at different times under ambient and dynamic conditions, for both the ½" and 1" EBF. Rather, the field data suggest that extraordinarily high bypass flow is occurred at this elevation. Only about ¼ of the anticipated flow is being recorded by the EBF, suggesting that the other ¾ is bypassing the meter. Evidently, filter pack is absent at this elevation creating an extremely low resistance path for flow to bypass the EBF.

Installation of RPC-3PW involved multiple drilling efforts due to lost circulation. Between repeated drilling attempts, addition of special drilling additives in the lost circulation zone, and presence of a persistent lost circulation zone, the filter pack in the suspect area may have settled after well construction. The bentonite seal may have formed a ceiling over the open zone during settling. Intervals of enhanced bypass flow may be occurring elsewhere, although to a lesser degree, and causing the extreme variability and negative conductivity estimates in columns (13) through (15). Nevertheless, the conductivity profile in ft/d is plotted in Figure 16, based on an average conductivity of 47.5 ft/d from conventional aquifer testing (Table 1).

Because much of the variability in Figure 16 is suspected to be an artifact of unusually high bypass flow, the data were re-analyzed over larger intervals in order to smooth the conductivity profile (Tables 8 and 9). The results are plotted in Figures 17 and 18 for 5 and 10 ft intervals respectively. These plots provide more credible estimates of the true conductivity variation, although at a coarser resolution than desired.

The conditions of this test are less similar to those associated with the head-loss-induced flow redistribution results displayed in Figure 7 than for RPC-2PR. They compare as follows:

Feature	RPC-2PR	Dinwiddie and others (1999) / Figure 6
Conductivity (ft/d)	47.5	29.9
Casing diameter (in)	4	4
Filter pack?	yes	no
Screen length (ft)	40	20

Dinwiddie and others (1999) show that biases increase with increasing aquifer conductivity. Therefore, Figure 7 understates the potential head-loss-induced flow redistribution errors for RPC-3PW. Another source of systematic error would be vertical flows caused by partial-penetration of the well screen.

RPC-3PW was also tested at a nominal flow of 15 L/min using the 1" EBF. Tables 10, 11 and 12 present analyses of field data at 1, 5 and 10 ft intervals. The conductivity results are plotted in Figures 16 through 18 along side the ½" EBF results. The 1" EBF conductivity profile at 1 ft resolution has a signature similar to that from the ½" EBF, but shows less variability. The reduced "noise" is probably a result of lower bypass flow for the 1" EBF. Although flowrates are roughly 3 times higher for the 1" EBF compared to the ½" EBF, the head loss is 16 times lower for the 1" EBF at the same flow. Comparing Tables 7 and 10, the net effect is bypass flow for the 1" EBF being only 1/6 of that for the ½" EBF. Therefore, artificial variations in conductivity caused by varying bypass flow conditions should be muted for the 1" EBF compared to the ½" EBF. Figure 16 appears to support this hypothesis. Systematic head-loss-induced flow redistribution errors should also be significantly lower for the 1" EBF results. When the field data are analyzed at coarser 5 ft and 10 ft intervals, even closer agreement is observed between the 1" and ½" EBF results, as shown in Figures 17 and 18.

These results suggest that future dynamic tests should use the 1" EBF, or the ½" EBF at a lower flowrate, to practically eliminate systematic errors due to instrument head loss.

RPT-2PW: This is a 4 inch well with a fully-penetrating 15 ft screen in the "transmissive" zone. Average conductivity was estimated from conventional aquifer testing to be 2.30 ft/d (Table 1). The field data presented in Appendix D were analyzed as shown in Table 13. Unlike RPC-2PR and RPC-3PW, the EBF data for RPT-2PW exhibit no anomalies and can be accepted at face value. The differential ambient flows are small compared to those for RPC-2PR and RPC-3PW, probably due to correspondingly low aquifer conductivity. As shown in Figure 19, groundwater was entering the upper half of the screen and leaving the lower half at the time of the ambient

test. This behavior is consistent with a downward gradient in the aquifer. From a contaminant monitoring perspective, this implies that only groundwater from the upper 7 ft of the screened interval would tend to be sampled, despite the 15 ft screen length.

The conductivity profile is shown in Figure 20. Because the formation conductivity is much lower than the value assumed in Figure 7, head-loss-induced flow redistribution effects are minimal. On the other hand, the borehole diameter for this well was 12 rather than 10 inches as for the preceding wells, which creates a larger annulus of the high conductivity filter pack. Therefore, higher bypass flow is predicted as shown in columns (17) and (18) of Table 13. As was done for RPC-2PR, an upper bound on bypass flow can be computed from the uppermost pair of EBF flows. The result is

$$\left(\frac{Q_{bp}}{Q_{EBF}} \right)_{max} = \frac{4.01 - 3.74}{4.01} \times 100\% = 6.7\% \tag{24}$$

which is lower than 8.2% in Table 13. Therefore, the estimates shown in columns (17) and (18) are certainly too high. As mentioned previously, the conductivity of the in-place filter pack is undoubtedly much lower than the measured value of 100 m/d for pristine FX-50.

RPT-3PW: This is a 4 inch well with a partially-penetrating 40 ft screen in the "lower" UTR aquifer zone. Average conductivity was estimated from conventional aquifer testing to be 5.44 ft/d (Table 1). The field data presented in Appendix E were analyzed as shown in Table 14. The differential ambient flow results in Figure 21 show that groundwater enters the upper third of the screen and exits the bottom two-thirds. A few of the computed conductivities in columns (14) and (15) of Table 14 are slightly negative due to measurement errors and/or non-ideal test conditions. These values should be interpreted as low conductivity. As shown in Figure 22, EBF testing reveals an interval of very high conductivity compared to the average. Because dynamic testing was performed with the 1" EBF, head losses were minimal. Maximum bypass flow is estimated to be only 1.2% of EBF flow. Head-loss-induced flow redistribution errors are probably insignificant, considering usage of the 1" EBF and relatively low aquifer conductivity.

RPT-4PW: This is a 6 inch well with a partially-penetrating 40 ft screen in the Gordon aquifer. Average conductivity was estimated from conventional aquifer testing to be 44.6 ft/d (Table 1). The field data presented in Appendix F were analyzed as shown in Table 15. The current EBF system has a 250 ft cable, which unfortunately limited high-resolution EBF testing to the upper 13 ft of the screen. The bottom 27 ft are necessarily treated as a single interval in the analysis. Considering the precision of the ½" EBF, the ambient data indicate zero flow in the upper 13 ft (Figure 23). The dynamic test results indicate a slightly increasing flowrate as the EBF was raised, which translates into a very low formation conductivity. However, the total pumping rate was also increasingly at the same time. In fact, EBF flow at all elevations appears to be simply measuring the actual pumping rate. Within instrument tolerance, no flow entered the casing over the top 13 ft during both ambient and dynamic testing.   Either the formation is practically

impermeable or the well is not actually screened over this interval. Figure 24 illustrates the resulting conductivity profile.

RPT-30PZ: This is 2 inch water table well with a 40 ft screen in the A and AA horizons. The average conductivity based on conventional aquifer testing is 1.33 ft/d (Table 1). At the time of EBF testing, the water table was about 30½ ft above the bottom of the screen. The field data are presented in Appendix G and analyzed in Table 16. The differential ambient flow results shown in Figure 25 indicate groundwater was entering the casing over the upper three-quarters of the saturated screen and exiting over the lower quarter. For dynamic testing, the pumping was limited to 2 L/min to minimize drawdown. The drawdown was 1½ ft leaving 29 ft of saturated screen. EBF readings were taken every 1 ft up to the final 4 ft, where interference with the pump occurred. In column (6) of Table 16, the total pumping rate of 2.10 L/min was entered at water table elevation during dynamic testing. As seen in Appendix G, the pumping rate fluctuated approximately ±8% about the mean, causing artificial changes in differential net flow. These variations are apparently responsible for the negative conductivities seen in columns (14) and (15). As shown in Figure 26, much higher than average conductivity is observed near the bottom of the screen.

Systematic errors due to head loss across the EBF are likely to be very small given the low pumping rate and low formation conductivity. A packer is not used with the EBF in a 2 inch ID well because the instrument is nearly 2 inches OD. Therefore, flow can bypass the EBF between the meter and casing. Fortunately, this bypass flow occurs regardless of whether the EBF is positioned in or out of the screen, unlike filter pack bypass flow. Therefore, the EBF still responds linearly to the actual well discharge and the calculations summarized by equation (4) are unaffected. In fact, Arnold and Molz (2000) have proposed using the EBF without a packer in larger diameter wells as a way of practically eliminating head loss.

Post-test checks for quasi-steady flow conditions

The estimated conductivity profiles just presented depend on the flow having reached quasi-steady conditions. Four criteria defining the elapsed time required after pumping to achieve such conditions have been given by equations (10), (13), (14) and (15). Tables 17 through 22 evaluate the four criteria for each R-area well. In these tables, the "Ruud and Kabala (1996)" criterion refers to equation (13), "Molz and others (1989)" to equation (14), "Rehfeldt and others (1989)" to equation (10), and "Flach" refers to equation (15). Among these, criterion (13) based on Ruud and Kabala (1996) is preferred because it has a more rigorous basis than equations (10) and (14) and avoids the probable over-conservatism of equation (15). A reasonable assumption for diffusivity contrast is 100:1, considering that flows associated with intervals with conductivity lower than 1/100 of the most permeable layer cannot be accurately measured. In evaluating hydraulic diffusivity (T/S), the transmissivity (T) and storage coefficient (S) estimates are based on the pumping tests of Hiergesell and others (2000, Table 4). Storage coefficients from pumping tests are more uncertain than transmissivity estimates for a heterogeneous

aquifer (Meier and others, 1998; Sanchez-Vila and others, 1999).   Therefore, the diffusivity estimates have similar uncertainty as the storage coefficient estimates.

Table 23 compares the criterion of Ruud and Kabala (1996) assuming a diffusivity contrast of 100:1 to the actual test conditions. Also included are the less conservative measures of Ruud and Kabala (1996) with a 10:1 diffusivity contrast and Rehfeldt and others (1989) ($t_D > 4000$). All tests were conducted beyond the time criterion of Ruud and Kabala (1996) assuming a diffusivity contrast of 100:1, except for RPT-30PZ. However, testing at RPT-30PZ did begin after the two less conservative criteria. Therefore, the EBF conductivity profile results previously presented are valid from the standpoint of having reached pseudo-steady flow.

Comparison of EBF conductivity profiles to Cone Penetration Testing (CPT) data

The dimensional hydraulic conductivity profiles plotted in Figures 14, 18, 20, 22, 24 and 26 are plotted in non-dimensional form in Figures 27 through 31. The non-dimensional profiles are interval conductivity divided by screen-averaged conductivity, column (13) in Tables 6, 12, 13, 14, 15 and 16. The CPT push near RPT-3PW and RPT-4PW did not reach the screen zones for these wells.   At the RPC-3PW site, the CPT log barely overlaps the well screen. At RPC-2PR, RPT-2PW and RPT-30PZ, the CPT logs fully overlap the EBF normalized conductivity profiles. In general, EBF conductivity profiles differ significantly from the conductivity variation suggested by the CPT logs. These comparisons demonstrate the value of EBF measurements, and the difficulty in accurately inferring conductivity from CPT tip resistance, sleeve friction, pore pressure and resistivity data.

Alternative conductivity estimates using Cooper-Jacob analysis

Horizontal conductivity can be estimated directly from data taken during EBF testing, provided the pumping rate is held constant and time-drawdown data are recorded in addition to EBF flowrates.   Under these conditions, a Cooper-Jacob analysis can be applied to each screen interval as summarized by equation (3). Well losses can be introduced by modifying equation (3) as

$$K_i = \frac{(\Delta Q_i - \Delta q_i)}{2\pi \Delta z_i \Delta hE} \ln\left(\frac{1.5}{r_w} \sqrt{\frac{Tt}{S}} \right) \tag{25}$$

where E is well efficiency, defined to be the theoretical drawdown divided by actual drawdown.   If barometric pressure variations are significant, further adjustments to measured drawdown are needed. This approach replaces the need for a prior screen-average conductivity estimate, ideally from a separate multiple well pumping test, with single-well pump testing conducted concurrently with EBF flow measurements. Being a form of single-well aquifer testing, the Cooper-Jacob analysis requires prior estimates for hydraulic diffusivity (T/S) and well efficiency (E). Transmissivity (T) can be determined iteratively from the layer estimates of conductivity (K_i). Therefore, storage coefficient (S) and well efficiency (E) are fundamentally required. Both are difficult to estimate with

accuracy. However, the Cooper-Jacob estimate is not highly sensitive to the assumed value of storage coefficient for large times, because S appears within a square-root and logarithm in equation (24). Unfortunately, the same cannot be said for well efficiency because conductivity is inversely proportional to E in equation (24). Therefore, EBF conductivity estimates from equation (24) have a level of uncertainty similar to conventional single-well pumping test estimates.

The conditions required for Cooper-Jacob analysis were satisfied during EBF testing at RPC-2PR, RPT-2PW and RPT-30PZ. Barometric pressure was not monitored, but probably did not vary substantially over the course of a 1 to 3 hour EBF test. Conductivity calculations using equation (24) are presented in Tables 6, 13 and 14. For these calculations, well efficiency and specific storage coefficient were assumed to be 50% and 10^{-4} ft^{-1}. The Cooper-Jacob conductivity estimates are shown in column (23) of that calculation tables. Column (24) is the ratio of the Cooper-Jacob estimate to the prior estimate in column (14) based on prior multiple-well aquifer testing. Similarly, the Cooper-Jacob estimates are averaged over the screen zone is compared to the prior multiple-well test result beneath column (25). For RPC-2PR, the Cooper-Jacob estimates are about half of the estimates based on equation (4) and multiple-well aquifer testing. For RPT-2PW, the agreement is good with the Cooper-Jacob estimate differing by only 12%. For RPT-3PW, the Cooper-Jacob estimates are two times higher than the prior estimates. Contributors to the discrepancy between the average conductivity computed using Cooper-Jacob and the prior multiple-well test include uncertainty in well efficiency and scale differences.

Considerations and recommendations for future EBF deployment

Based on the experience gained in R-area, the following recommendations and considerations for future EBF deployments are stated.

Existing SRS monitoring wells: Concerns about bypass flow in filter-packed wells have hindered EBF deployment at the SRS in the past. Recently published analyses of bypass flow, the extensions developed in this report, and R-area EBF testing indicate that bypass flow will not be a serious problem in a typical SRS monitoring well. Furthermore, the head losses that drive bypass flow and cause additional flow redistribution effects can be practically eliminated in future deployments by using the 1" EBF for dynamic testing, lower pumping rates with the ½" EBF, or no EBF packer.

Contaminant monitoring implications: The differential ambient flow results for R-area indicate that a well screen functions as a "short-circuit" in the presence of a vertical head gradient in the surrounding aquifer. Usually the gradient is downward as a result of surface recharge. Therefore, groundwater enters the casing over the upper portion of the screen and exits the lower portion. This phenomenon has important implications for contaminant monitoring. Specifically, samples taken from the well will be biased towards groundwater that originated from the upper strata. The extent of the bias depends on the relative strength of the horizontal gradient.

Equipment issues: The present EBF system has a number of shortcomings that should ideally be remedied before extensive, routine application of the technology at the SRS. The specific deficiencies have been identified in an earlier section. Improved EBF systems are now commercially available from Quantum Engineering Corporation and Century Geophysical Corporation.

Optimal EBF testing: Future dynamic testing should be done exclusively with the 1" ID EBF in order to minimize systematic errors due to instrument head losses. Pre-test calculations should be performed to estimate bypass flow using the methods described in this report. Based on this analysis, a pumping rate that reduces bypass flow to an insignificant level should be chosen. Additional effort should be made to ensure the pumping rate is constant, and time-drawdown and barometric data are accurately recorded preferably using a pressure transducer and data logger.

References

Arnold, K. B. and F. J. Molz, 2000, In-well hydraulics of the Electromagnetic Borehole Flowmeter: Further studies, Ground Water Monitoring & Remediation, Winter issue, 52-55.

Cooper, H. H. and C. E. Jacob, 1946, A generalized graphical method for evaluating formation constants and summarizing well-field history, Transactions of the American Geophysical Union, v27, 526-534.

Dinwiddie, C. L., N. A. Foley and F. J. Molz, 1999, In-well hydraulics of the Electromagnetic Borehole Flowmeter, Ground Water, v37 n2, 305-315.

Foley, N. A., 1997, Pressure distribution around an electromagnetic borehole flowmeter in an artificial well, M. S. thesis, Department of Environmental Systems Engineering, Clemson University.

Hiergesell, R. A., 1999, Test plan for conducting aquifer tests near R area reactor, WSRC-RP-99-00419.

Hiergesell, R. A., W. E. Jones and M. K. Harris, 2000, Results of aquifer tests performed near R-area, SRS, WSRC-TR-2000-00180.

Javendel, I., and P. A. Witherspoon, 1969, A method for analyzing transient flow in multilayered aquifers, Water Resources Research, v5 n4, 856-869.

Kabala, Z. J., 1994, Measuring distributions of hydraulic conductivity and specific storativity by the double flowmeter test, Water Resources Research, v30 n3, 685-690.

Meier, P. M., J. Carrera and X. Sanchez-Vila, 1998, An evaluation of Jacob's method for the interpretation of pumping tests in heterogeneous formations, Water Resources Research, v34 n5, 1101-1025.

Molz, F. J., 2000, personal communication, e-mail dated 7/12.

Molz, F. J., R. H. Morin, A. E. Hess, J. G. Melville and O. Guven, 1989, The impeller meter for measuring aquifer permeability variations: evaluation and comparison with other tests, Water Resources Research, v25 n7, 1677-1683.

Molz, F. J. and S. C. Young, 1993, Development and application of borehole flowmeters for environmental assessment, The Log Analyst, v3, Jan.-Feb., 13-23.

Rehfeldt, K. R., P. Hufschmied, L. W. Gelhar and M. E. Schaefer, 1989, The borehole flowmeter technique for measuring hydraulic conductivity variability, report, Electric Power Research Institute, Palo Alto CA.

Riha, B., 1993, Predicting saturated hydraulic conductivity for unconsolidated soils from commonly measured textural properties, M.S. thesis, Clemson University, 87 p.

Ruud, N. C., and Z. J. Kabala, 1996, Numerical evaluation of flowmeter test interpretation methodologies, Water Resources Research, v32 n4, 845-852.

Ruud, N. C., and Z. J. Kabala, 1997, Numerical evaluation of the flowmeter test in a layered aquifer with a skin zone, Journal of Hydrology, v203, 101-108.

Ruud, N. C., Z. J. Kabala and F. J. Molz, 1999, Evaluation of flowmeter-head loss effects in the flowmeter test, Journal of Hydrology, v224, 55-63.

Sanchez-Vila, X., P. M. Meier and J. Carrera, 1999, Pumping tests in heterogeneous aquifers: An analytical study of what can be obtained from their interpretation using Jacob's method, Water Resources Research, v35 n4, 943-952.

Theis, C. V., 1935, The relationship between the lowering of piezometric surface and the rate and duration of discharge using ground-water storage, Trans. Amer. Geophys. Union, v16, 519.

Waldrop, W. R., 1995, A summary of hydrogeologic studies with the Electromagnetic Borehole Flowmeter, report QEC T-102, Quantum Engineering Corporation, 112 Tigitsi Lane, Loudon, Tennessee, 37774, 615-458-0506.

WSRC, 2000, Field summary report for installation of pumping and observation wells in R Area, WSRC-RP-2000-4058.

Young, S. C. and W. R. Waldrop, 1989, An electromagnetic borehole flowmeter for measuring hydraulic conductivity variability, in Molz, F. J., O. Guven and J. G. Melville eds., Proceedings of the conference on new field techniques for quantifying the physical and chemical properties of heterogeneous aquifers: Water Resources Research Institute, Auburn University, Alabama.

Table 1   R-area well information.

Well	SRS N (ft)	SRS E (ft)	Pad Elevation (ft msl)	TOC Elev (ft msl)	Top of Screen (ft msl)	Bottom of Screen (ft msl)	Screen Length (ft)	Borehole Diameter (in)	Casing Diameter (in)	Filter Pack	Hydro-stratigraphic unit	Unit Thickness (ft)	Average Trans-missivity (ft^2/min)	Average Conductivity (ft/d)
RPC-1PW	57938.27	74187.63	305.24	307.56	285.41	270.41	15	8	2	FX-50			-	
RPC-2PR	57918.93	73976.10	309.02	311.51	270.56	230.56	40	10	4	FX-50	transmissive	39	0.679	24.4
RPC-3PW	57913.93	74069.58	307.58	309.14	202.25	162.25	40	10	4	FX-50	"lower" UTR	101	1.75	25.0
RPT-2PW	56089.13	76789.92	287.66	289.91	209.33	194.33	15	12	4	FX-50	transmissive	15	0.024	2.3
RPT-3PW	56127.15	76565.66	287.64	289.83	138.31	98.31	40	10	4	FX-50	"lower" UTR	74	0.102	2.0
RPT-4PW	56106.15	76566.26	287.50	289.72	55.77	15.77	40	10	6	FX-50	Gordon	86	0.871	14.6
RPT-30PZ	56067.92	76753.77	287.52	289.66	272.19	232.19	40	8	2	FX-50	A/AA	34	0.038	1.4

Table 2   Peer-reviewed journal publications addressing systematic errors in borehole flowmeter analyses.

Transient flow	Filter pack	Flowmeter head losses	References
×			Molz and others (1989) Kabala (1994) Ruud and Kabala (1996)
	×		Ruud and Kabala (1997) Ruud and others (1999)
		×	Dinwiddie and others (1999)
	×	×	Dinwiddie and others (1999) Ruud and others (1999)

Table 3 Constant-head permeameter measurements for FX-50 filter pack.

Approx. Start Time	Bucket Vol. (L)	Fill Time Min.	Sec.	Total Time (sec)	Flow (l/min)	Flow (ft³/min)	Water Level WL (ft) Initial	Final	Sand Column Height SC (ft)	Water Column HeightW C (ft)	ΔH	Head Grad.	A=Pi R^2 (ft^2)	K=Q/iA (ft/min)	K (cm/s)	K (ft/d)	K (m/d)
9:58	16.80	13	53	833	1.21	0.0427	0.1823	0.1823	0.5469	0.7812	1.3281	2.428	0.075	0.233	0.118	336	102
10:52	16.80	14	20	860	1.17	0.0414	0.1875	0.1875	0.5469	0.7760	1.3229	2.419	0.075	0.227	0.115	326	99
11:44	16.80	14	29	869	1.16	0.0410	0.1875	0.1875	0.5469	0.7760	1.3229	2.419	0.075	0.224	0.114	323	98
16:04	16.80	14	8	848	1.19	0.0420	0.1979	0.1979	0.5469	0.7656	1.3125	2.400	0.075	0.232	0.118	334	102
														average	0.116	330	100

Table 4   Calibration data for the 1/2" ID EBF.

	Calibration Data				Calculated Data					$y = 0.0024x^2 + 0.7838x$		
Instrument Response	Water Temp (C)	Water Weight (lbs)	Time Duration (min)	Mass Flow (lbs/min)	Water Density (lb/ft^3)	Volume Flow (ft^3/min)	Volume Flow (Actual) (LPM)	Act-Inst Resp	% Error	Calibrated Meter Flow Rate	Act-Cal Mtr Flow	% Error
0.00							0	0.000		0.000	0.000	
0.029	21.5	0.685	10.00533	0.0685	62.2877	0.0011	0.0311	0.002	6.89	0.023	0.008	27.01
0.036	21.9	0.670	10.0065	0.0670	62.2826	0.0011	0.0304	-0.006	18.25	0.028	0.002	7.30
0.073	22.0	0.667	5.004333	0.1332	62.2813	0.0021	0.0606	-0.012	20.51	0.057	0.003	5.52
0.089	21.8	0.814	5.0035	0.1627	62.2839	0.0026	0.0740	-0.015	20.32	0.070	0.004	5.67
0.506	19.4	4.510	5.009167	0.9003	62.3135	0.0144	0.4091	-0.097	23.68	0.397	0.012	2.91
0.506	19.5	4.500	5.008333	0.8985	62.3123	0.0144	0.4083	-0.098	23.93	0.397	0.011	2.71
0.552	22.2	2.935	3.006833	0.9761	62.2787	0.0157	0.4438	-0.108	24.38	0.433	0.010	2.35
1.007	19.0	17.830	10.01183	1.7809	62.3181	0.0286	0.8092	-0.198	24.44	0.792	0.017	2.16
1.019	20.5	18.020	10.00867	1.8004	62.3003	0.0289	0.8183	-0.201	24.52	0.801	0.017	2.09
4.010	20.8	35.100	5.0065	7.0109	62.2966	0.1125	3.1867	-0.823	25.84	3.182	0.005	0.16
4.030	19.6	35.260	5.0085	7.0400	62.3111	0.1130	3.1992	-0.831	25.97	3.198	0.002	0.05
6.955	21.2	60.990	5.008333	12.1777	62.2916	0.1955	5.5357	-1.419	25.64	5.567	-0.032	0.57
9.860	21.2	52.470	3.0105	17.4290	62.2916	0.2798	7.9227	-1.937	24.45	7.962	-0.039	0.49
9.875	20.5	53.070	3.004667	17.6625	62.3003	0.2835	8.0278	-1.847	23.01	7.974	0.054	0.67
10.015	21.4	53.480	3.005833	17.7921	62.2890	0.2856	8.0881	-1.927	23.82	8.090	-0.002	0.03

Table 5 Calibration data for the 1" ID EBF.

	Calibration Data				Calculated Data					Calibrated Meter Flow y = 0.9797x + 0.1097		
Instrument Response	Water Temp (C)	Water Weight (lbs)	Time Duration (min)	Mass Flow (lbs/min)	Water Density (lb/ft^3)	Volume Flow (ft^3/min)	Volume Flow (Actual) (LPM)	Act-Inst Resp	% Error	Calibrated Meter Flow Rate (L/min)	Act-Cal Mtr Flow (L/min)	% Error
0.00							0	0.00		0.110	-0.110	
0.10	19.0	2.070	5.0065	0.4135	62.3181	0.0066	0.1879	0.09	46.77	0.208	-0.020	10.5
0.10	18.8	2.070	5.006	0.4135	62.3204	0.0066	0.1879	0.09	46.77	0.208	-0.020	10.5
0.10	19.0	2.075	5.0075	0.4144	62.3181	0.0066	0.1883	0.09	46.89	0.208	-0.019	10.3
1.00	22.2	7.255	3.0075	2.4123	62.2787	0.0387	1.0968	0.10	8.83	1.089	0.007	0.7
1.00	22.2	7.280	3.011	2.4178	62.2787	0.0388	1.0993	0.10	9.03	1.089	0.010	0.9
1.00	22.40	7.260	3.006667	2.4146	62.2760	0.0388	1.0979	0.10	8.92	1.089	0.009	0.8
10.02	19.2	66.290	3.0035	22.0709	62.3158	0.3542	10.0289	0.01	0.09	9.926	0.103	1.0
10.23	19.6	68.090	3.0035	22.6702	62.3111	0.3638	10.3020	0.07	0.70	10.132	0.170	1.7
10.40	19.8	68.800	3.005	22.8952	62.3087	0.3674	10.4047	0.00	0.04	10.299	0.106	1.0
20.12	19.2	130.060	3.004667	43.2860	62.3158	0.6946	19.6690	-0.45	2.29	19.821	-0.152	0.8
20.15	19.6	131.500	3.008333	43.7119	62.3111	0.7015	19.8640	-0.29	1.44	19.851	0.013	0.1
20.51	19.8	134.010	3.0075	44.5586	62.3087	0.7151	20.2495	-0.26	1.29	20.203	0.046	0.2
30.00	19.6	161.780	2.509	64.4799	62.3111	1.0348	29.3016	-0.70	2.38	29.501	-0.199	0.7
30.15	19.8	162.290	2.505667	64.7692	62.3087	1.0395	29.4342	-0.72	2.43	29.648	-0.213	0.7
30.30	20.0	163.240	2.5075	65.1007	62.3063	1.0448	29.5860	-0.71	2.41	29.795	-0.209	0.7
35.00	20.0	150.470	2.004167	75.0786	62.3063	1.2050	34.1206	-0.88	2.58	34.399	-0.279	0.8
35.00	19.8	150.510	2.005167	75.0611	62.3087	1.2047	34.1113	-0.89	2.61	34.399	-0.288	0.8
35.00	20.0	156.560	2.007833	77.9746	62.3063	1.2515	35.4367	0.44	1.23	34.399	1.038	2.9

Table 6 Hydraulic conductivity profile and bypass flow estimate for RPC-2PR.

(1)	(2)	(3)	(4)	(5)	(6)	(7)	(8)	(9)	(10)	(11)	(12)	(13)	(14)	(15)	(16)	(17)	(18)	(19)	(20)	(21)	(22)	(23)	(24)	(25)
Depth Below TOC (ft)	Elevation (ft-msl)	Ambient Flow (L/min)	Ambient Flow, q (ft³/min)	Differential Ambient Flow, Δq_i (ft³/min)	Pump Induced Flow (L/min)	Pump Induced Flow, Q (ft³/min)	Net Pumping Flow, Q - q (ft³/min)	Differential Net Flow, $\Delta(Q_i - q_i)$ (ft³/min)	Adjusted Differential Net Flow $\Delta(Q_i - q_i)$ (ft³/min)	Layer Thickness Δz_i (ft)	Mid-point Elevation (ft)	$K_i/K_{bar}=$ $b(\Delta Q_i-\Delta q_i)/(Q_p\Delta z_i)$	K_i (ft/d)	K_i (cms/s)	Check $\Delta z^*K_i/K_{bar}$	Estimated bypass flow (L/min)	Estimated bypass flow ratio (Q_{bp}/Q_{EBF})	Clock Time	Elapsed Time (min)	Water Level (ft)	dh (ft)	Cooper-Jacob K_i (ft/d)	Ratio	$K\Delta z$
37.03	270.89	-0.00044	-0.00002	-0.00017	4.30	0.15178	0.15179	0.00289	0.00289	0.67	270.22	1.14	27.9	9.85E-03	7.618E-01	0.27	0.063	14:30	30	33.85	0.80	12.9	0.46	8.60
38.03	269.89	0.00449	0.00016	0.00005	4.22	0.14906	0.14890	0.01314	0.01314	1.00	269.39	3.46	84.7	2.99E-02	3.463E+00	0.26	0.062	14:33	33	33.85	0.80	39.4	0.46	39.35
39.03	268.89	0.00315	0.00011	0.00010	3.85	0.13588	0.13577	0.00354	0.00354	1.00	268.39	0.93	22.8	8.06E-03	9.342E-01	0.22	0.058	14:37	37	33.85	0.80	10.7	0.47	10.70
40.03	267.89	0.00024	0.00001	-0.00001	3.74	0.13223	0.13223	0.00046	0.00046	1.00	267.39	0.12	3.0	1.05E-03	1.222E-01	0.21	0.056	14:40	40	33.86	0.81	1.4	0.47	1.41
41.03	266.89	0.00047	0.00002	0.00004	3.73	0.13176	0.13176	-0.00007	-0.00007	1.00	266.39	-0.02	-0.4	-1.50E-04	-1.740E-02	0.21	0.056	14:42	42	33.86	0.81	-0.2	0.47	-0.20
42.03	265.89	-0.00059	-0.00002	0.00006	3.73	0.13181	0.13183	-0.00049	-0.00049	1.00	265.39	-0.13	-3.1	-1.11E-03	-1.285E-01	0.21	0.056	14:44	44	33.86	0.81	-1.5	0.47	-1.49
43.03	264.89	-0.00230	-0.00008	-0.00004	3.74	0.13223	0.13232	-0.00056	-0.00056	1.00	264.39	-0.15	-3.6	-1.28E-03	-1.483E-01	0.21	0.056	14:46	46	33.86	0.81	-1.7	0.47	-1.72
44.03	263.89	-0.00129	-0.00005	0.00010	3.76	0.13283	0.13288	-0.00015	-0.00015	1.00	263.39	-0.04	-1.0	-3.52E-04	-4.080E-02	0.21	0.056	14:48	48	33.86	0.81	-0.5	0.48	-0.48
45.03	262.89	-0.00406	-0.00014	0.00005	3.76	0.13289	0.13303	0.00049	0.00049	1.00	262.39	0.13	3.2	1.12E-03	1.302E-01	0.21	0.057	14:50	50	33.86	0.81	1.5	0.48	1.53
46.03	261.89	-0.00540	-0.00019	0.00010	3.75	0.13235	0.13254	0.00442	0.00442	1.00	261.39	1.17	28.5	1.01E-02	1.166E+00	0.21	0.056	14:52	52	33.86	0.81	13.7	0.48	13.73
47.03	260.89	-0.00831	-0.00029	0.00013	3.62	0.12782	0.12812	0.00246	0.00246	1.00	260.39	0.65	15.8	5.59E-03	6.480E-01	0.20	0.055	14:54	54	33.86	0.81	7.7	0.48	7.67
48.03	259.89	-0.01200	-0.00042	0.00032	3.55	0.12523	0.12566	0.00329	0.00329	1.00	259.39	0.87	21.2	7.47E-03	8.663E-01	0.19	0.054	14:56	56	33.86	0.81	10.3	0.49	10.29
49.03	258.89	-0.02118	-0.00075	0.00008	3.44	0.12162	0.12237	0.00180	0.00180	1.00	258.39	0.47	11.6	4.09E-03	4.745E-01	0.18	0.053	14:58	58	33.85	0.80	5.7	0.49	5.66
50.03	257.89	-0.02330	-0.00082	-0.00004	3.39	0.11975	0.12057	-0.00078	-0.00078	1.00	257.39	-0.21	-5.0	-1.78E-03	-2.065E-01	0.18	0.052	15:00	60	33.85	0.80	-2.5	0.49	-2.47
51.03	256.89	-0.02215	-0.00078	0.00022	3.41	0.12057	0.12136	0.00211	0.00211	1.00	256.39	0.56	13.6	4.80E-03	5.564E-01	0.18	0.052	15:03	63	33.85	0.80	6.7	0.49	6.71
52.03	255.89	-0.02834	-0.00100	-0.00012	3.35	0.11825	0.11925	-0.00022	-0.00022	1.00	255.39	-0.06	-1.4	-4.94E-04	-5.724E-02	0.17	0.051	15:06	66	33.85	0.80	-0.7	0.50	-0.69
53.03	254.89	-0.02484	-0.00088	0.00013	3.36	0.11859	0.11946	-0.00010	-0.00010	1.00	254.39	-0.03	-0.6	-2.21E-04	-2.559E-02	0.17	0.052	15:08	68	33.85	0.80	-0.3	0.50	-0.31
54.03	253.89	-0.02839	-0.00100	0.00019	3.36	0.11856	0.11956	0.00912	0.00912	1.00	253.39	2.40	58.8	2.07E-02	2.404E+00	0.17	0.052	15:10	70	33.85	0.80	29.2	0.50	29.20
55.03	252.89	-0.03365	-0.00119	0.00035	3.09	0.10925	0.11044	0.00551	0.00551	1.00	252.39	1.45	35.5	1.25E-02	1.453E+00	0.15	0.048	15:13	73	33.86	0.81	17.6	0.50	17.58
56.03	251.89	-0.04361	-0.00154	0.00002	2.93	0.10339	0.10493	0.00321	0.00321	1.00	251.39	0.85	20.7	7.29E-03	8.452E-01	0.14	0.046	15:16	76	33.87	0.82	10.2	0.49	10.19
57.03	250.89	-0.04416	-0.00156	0.00004	2.84	0.10017	0.10173	0.00352	0.00352	1.00	250.39	0.93	22.7	8.00E-03	9.280E-01	0.13	0.045	15:19	79	33.87	0.82	11.1	0.49	11.15
58.03	249.89	-0.04537	-0.00160	0.00021	2.74	0.09660	0.09821	0.00191	0.00191	1.00	249.39	0.50	12.3	4.34E-03	5.038E-01	0.12	0.044	15:22	82	33.88	0.83	6.0	0.49	6.03
59.03	248.89	-0.05127	-0.00181	-0.00012	2.68	0.09448	0.09629	0.00151	0.00151	1.00	248.39	0.40	9.7	3.43E-03	3.975E-01	0.12	0.043	15:25	85	33.88	0.83	4.7	0.49	4.74
60.03	247.89	-0.04777	-0.00169	0.00021	2.64	0.09310	0.09479	0.00173	0.00173	1.00	247.39	0.46	11.2	3.94E-03	4.574E-01	0.11	0.043	15:27	87	33.89	0.84	5.4	0.49	5.44
61.03	246.89	-0.05381	-0.00190	-0.00015	2.58	0.09115	0.09305	0.00094	0.00094	1.00	246.39	0.25	6.1	2.14E-03	2.478E-01	0.11	0.042	15:32	92	33.90	0.85	2.9	0.48	2.93
62.03	245.89	-0.04958	-0.00175	0.00018	2.56	0.09036	0.09211	0.00005	0.00005	1.00	245.39	0.01	0.3	1.09E-04	1.269E-02	0.11	0.042	15:37	97	33.91	0.86	0.1	0.48	0.15
63.03	244.89	-0.05461	-0.00193	0.00004	2.55	0.09014	0.09206	0.00321	0.00321	1.00	244.39	0.85	20.7	7.29E-03	8.451E-01	0.11	0.042	15:39	99	33.91	0.86	9.9	0.48	9.88
64.03	243.89	-0.05572	-0.00197	0.00004	2.46	0.08689	0.08886	0.00644	0.00644	1.00	243.39	1.70	41.5	1.46E-02	1.699E+00	0.10	0.040	15:42	102	33.92	0.87	19.8	0.48	19.78
65.03	242.89	-0.05684	-0.00201	0.00004	2.28	0.08041	0.08242	0.00249	0.00249	1.00	242.39	0.66	16.1	5.67E-03	6.578E-01	0.09	0.038	15:45	105	33.92	0.87	7.6	0.47	7.63
66.03	241.89	-0.05795	-0.00205	0.00001	2.21	0.07788	0.07992	0.00097	0.00097	1.00	241.39	0.26	6.3	2.21E-03	2.558E-01	0.08	0.037	15:47	107	33.93	0.88	3.0	0.47	2.96
67.03	240.89	-0.05837	-0.00206	0.00001	2.18	0.07689	0.07895	0.00314	0.00314	1.00	240.39	0.83	20.2	7.13E-03	8.269E-01	0.08	0.037	15:49	109	33.93	0.88	9.5	0.47	9.53
68.03	239.89	-0.05879	-0.00208	0.00001	2.09	0.07374	0.07582	0.01411	0.01411	1.00	239.39	3.72	90.9	3.21E-02	3.720E+00	0.08	0.036	15:54	114	33.94	0.89	42.6	0.47	42.59
69.03	238.89	-0.05921	-0.00209	0.00007	1.69	0.05961	0.06171	0.02175	0.02175	1.00	238.39	5.73	140.2	4.94E-02	5.734E+00	0.05	0.031	15:57	117	33.94	0.89	65.8	0.47	65.79
70.03	237.89	-0.06119	-0.00216	-0.00001	1.07	0.03780	0.03996	0.00203	0.00203	1.00	237.39	0.53	13.1	4.61E-03	5.342E-01	0.03	0.023	16:01	121	33.94	0.89	6.1	0.47	6.15
71.03	236.89	-0.05834	-0.00206	-0.00007	1.92	0.03587	0.03793	0.00227	0.00227	1.00	236.39	0.60	14.6	5.16E-03	5.989E-01	0.02	0.023	16:04	124	33.94	0.89	6.9	0.47	6.90
72.03	235.89	-0.05640	-0.00199	-0.00010	0.95	0.03367	0.03566	0.00249	0.00249	1.00	235.39	0.66	16.1	5.67E-03	6.573E-01	0.02	0.022	16:07	127	33.94	0.89	7.6	0.47	7.59
73.03	234.89	-0.05369	-0.00190	-0.00038	0.89	0.03127	0.03317	0.00959	0.00959	1.00	234.39	2.53	61.8	2.18E-02	2.529E+00	0.02	0.021	16:10	130	33.94	0.89	29.3	0.47	29.28
74.03	233.89	-0.04300	-0.00152	-0.00110	0.62	0.02206	0.02357	0.01897	0.01897	1.00	233.39	5.00	122.3	4.31E-02	5.002E+00	0.01	0.018	16:14	134	33.94	0.89	58.1	0.47	58.05
75.03	232.89	-0.01193	-0.00042	-0.00100	0.12	0.00418	0.00460	0.00105	0.00105	1.00	232.39	0.28	6.8	2.39E-03	2.770E-01	0.00	0.012	16:17	137	33.94	0.89	3.2	0.48	3.22
76.03	231.89	-0.01042	-0.00037	-0.00007	0.09	0.00318	0.00355	0.00077	0.00077	1.00	231.39	0.20	4.9	1.74E-03	2.018E-01	0.00	0.011	16:25	145	33.94	0.89	2.4	0.48	2.36
77.03	230.89	-0.00834	-0.00029	-0.00018	0.07	0.00249	0.00279	0.00270	0.00270	0.33	230.72	2.14	52.3	1.84E-02	7.127E-01	0.00	0.011	16:30	150	33.94	0.89	25.0	0.48	8.35
78.03	229.89	-0.00314	-0.00011		0.00	-0.00003	0.00008																	

37.36	Top of Screen Depth from TOC (ft)		Filter pack:		QP (ft³/min) 0.15171	40.00 b (ft)	
77.36	Bottom of Screen Depth from TOC (ft)	0.254	Do (m)		QP (L/min) 4.30		
40.00	Screen Length (ft)	0.102	Di (m)		uncorr QP 4.30		
307.92	TOC Elevation (ft)	0.043	Area (m²)				
0.679	T pump (ft²/min)	7.62	Thickness (cm)				
39	Formation thickness (ft)	100	Conductivity, K_{gp} (m/d) FX-50				
24.4	K pump (ft/d)		EBF:				
8.62E-03	K pump (cm/s)	0.178	L_{EBF} (m)				
			Bypass flow:				
		0.111	ΔL (m)				
		0.289	L (m)				

Avg K/K_{bar} 1.000000
(Should be exactly 1)

r_w (in)	5
b (ft)	39
K (ft/d)	12
S_s (1/ft)	1.0E-04
T (ft²/d)	468
S (unitless)	3.9E-03
T/S (ft²/d)	1.20E+05
Start of pumping	14:00
Water level (ft)	33.05
Well efficiency	50%

Avg Cooper-Jacob K 11.64
Ratio 0.48

Table 7   Hydraulic conductivity profile and bypass flow estimate for RPC-3PW for ½" EBF, 5 L/min nominal flow and 1 ft increments.

(1)	(2)	(3)	(4)	(5)	(6)	(7)	(8)	(9)	(10)	(11)	(12)	(13)	(14)	(15)	(16)	(17)	(18)
									Adjusted?							Estimated	Estimated
		Ambient	Ambient	Differential Ambient	Pump Induced	Pump Induced	Net Pumping	Differential Net Flow,	Differential Net Flow	Layer	Mid-point	K_i/K_{bar}=			Check	bypass flow	bypass flow ratio
Depth Below TOC (ft)	Elevation (ft-msl)	Flow (L/min)	Flow, q (ft³/min)	Flow, Δq_i (ft³/min)	Flow (L/min)	Flow, Q (ft³/min)	Flow, Q - q (ft³/min)	$\Delta(Q_i - q_i)$ (ft³/min)	$\Delta(Q_i - q_i)$ (ft³/min)	Thickness Δz_i (ft)	Elevation (ft)	$b(\Delta Q_i - \Delta q_i)/$ $(Q_p \Delta z_i)$	K_i (ft/d)	Ki (cm/s)	$\Delta z^* K_i/K_{bar}$	(L/min)	(Q_{bp}/Q_{EBF})
106.16	202.98	-0.00022	-0.00001	0.00001	5.34	0.18863	0.18864	-0.00044	-0.00044	0.27	202.11	-0.35	-8.8	-3.10E-03	-9.380E-02	0.41	0.076
107.16	201.98	-0.00050	-0.00002	0.00001	5.35	0.18906	0.18908	0.00045	0.00045	1.00	201.48	0.10	2.4	8.37E-04	9.508E-02	0.41	0.076
108.16	200.98	-0.00086	-0.00003	-0.00113	5.34	0.18860	0.18863	0.14506	0.14506	1.00	200.48	30.77	767.6	2.71E-01	3.077E+01	0.41	0.076
109.16	199.98	0.03106	0.00110	0.00131	1.26	0.04467	0.04357	-0.11300	-0.11300	1.00	199.48	-23.97	-598.0	-2.11E-01	-2.397E+01	0.03	0.026
110.16	198.98	-0.00606	-0.00021	0.00013	4.43	0.15636	0.15657	-0.01377	-0.01377	1.00	198.48	-2.92	-72.9	-2.57E-02	-2.920E+00	0.29	0.065
111.16	197.98	-0.00970	-0.00034	0.00031	4.81	0.17000	0.17034	-0.00057	-0.00057	1.00	197.48	-0.12	-3.0	-1.06E-03	-1.210E-01	0.33	0.069
112.16	196.98	-0.01854	-0.00065	-0.00005	4.82	0.17025	0.17091	-0.00386	-0.00386	1.00	196.48	-0.82	-20.4	-7.21E-03	-8.186E-01	0.34	0.070
113.16	195.98	-0.01726	-0.00061	-0.00010	4.93	0.17416	0.17477	0.00157	0.00157	1.00	195.48	0.33	8.3	2.92E-03	3.320E-01	0.35	0.071
114.16	194.98	-0.01441	-0.00051	0.00015	4.89	0.17269	0.17320	-0.00328	-0.00328	1.00	194.48	-0.69	-17.3	-6.12E-03	-6.950E-01	0.34	0.070
115.16	193.98	-0.01854	-0.00065	0.00004	4.98	0.17583	0.17648	0.00525	0.00525	1.00	193.48	1.11	27.8	9.79E-03	1.113E+00	0.36	0.071
116.16	192.98	-0.01961	-0.00069	-0.00007	4.83	0.17054	0.17123	0.00027	0.00027	1.00	192.48	0.06	1.4	5.11E-04	5.807E-02	0.34	0.070
117.16	191.98	-0.01755	-0.00062	-0.00008	4.82	0.17034	0.17096	0.00125	0.00125	1.00	191.48	0.27	6.6	2.34E-03	2.661E-01	0.34	0.070
118.16	190.98	-0.01534	-0.00054	0.00012	4.79	0.16916	0.16971	0.00475	0.00475	1.00	190.48	1.01	25.2	8.88E-03	1.008E+00	0.33	0.069
119.16	189.98	-0.01876	-0.00066	0.00004	4.65	0.16429	0.16495	0.00019	0.00019	1.00	189.48	0.04	1.0	3.58E-04	4.062E-02	0.31	0.067
120.16	188.98	-0.01983	-0.00070	-0.00005	4.65	0.16406	0.16476	-0.00205	-0.00205	1.00	188.48	-0.43	-10.8	-3.82E-03	-4.338E-01	0.31	0.067
121.16	187.98	-0.01848	-0.00065	-0.00010	4.71	0.16615	0.16680	-0.00045	-0.00045	1.00	187.48	-0.10	-2.4	-8.39E-04	-9.531E-02	0.32	0.068
122.16	186.98	-0.01578	-0.00056	0.00015	4.72	0.16670	0.16725	0.00653	0.00653	1.00	186.48	1.38	34.5	1.22E-02	1.384E+00	0.32	0.068
123.16	185.98	-0.02005	-0.00071	0.00017	4.53	0.16002	0.16073	-0.00161	-0.00161	1.00	185.48	-0.34	-8.5	-3.00E-03	-3.406E-01	0.30	0.066
124.16	184.98	-0.02497	-0.00088	0.00089	4.57	0.16145	0.16233	0.01410	0.01410	1.00	184.48	2.99	74.6	2.63E-02	2.990E+00	0.30	0.066
125.16	183.98	-0.05206	-0.00177	0.00100	4.15	0.14646	0.14824	0.00619	0.00619	1.00	183.48	1.31	32.7	1.16E-02	1.312E+00	0.25	0.061
126.16	182.98	-0.07868	-0.00278	0.00078	3.94	0.13927	0.14205	0.00190	0.00190	1.00	182.48	0.40	10.0	3.54E-03	4.020E-01	0.23	0.059
127.16	181.98	-0.10089	-0.00356	0.00015	3.87	0.13659	0.14015	-0.00231	-0.00231	1.00	181.48	-0.49	-12.2	-4.32E-03	-4.904E-01	0.22	0.058
128.16	180.98	-0.10502	-0.00371	-0.00007	3.93	0.13876	0.14247	0.00096	0.00096	1.00	180.48	0.20	5.1	1.79E-03	2.029E-01	0.23	0.059
129.16	179.98	-0.10296	-0.00364	0.00007	3.90	0.13788	0.14151	-0.00066	-0.00066	1.00	179.48	-0.14	-3.5	-1.24E-03	-1.409E-01	0.23	0.058
130.16	178.98	-0.10481	-0.00370	-0.00005	3.92	0.13847	0.14217	0.00463	0.00463	1.00	178.48	0.98	24.5	8.65E-03	9.827E-01	0.23	0.058
131.16	177.98	-0.10353	-0.00366	-0.00001	3.79	0.13389	0.13754	0.00408	0.00408	1.00	177.48	0.87	21.6	7.62E-03	8.662E-01	0.22	0.057
132.16	176.98	-0.10318	-0.00364	0.00001	3.68	0.12981	0.13346	0.00096	0.00096	1.00	176.48	0.20	5.1	1.79E-03	2.031E-01	0.20	0.055
133.16	175.98	-0.10347	-0.00365	0.00009	3.65	0.12885	0.13250	0.00201	0.00201	1.00	175.48	0.43	10.7	3.76E-03	4.273E-01	0.20	0.055
134.16	174.98	-0.10603	-0.00374	-0.00002	3.59	0.12674	0.13049	0.00173	0.00173	1.00	174.48	0.37	9.1	3.22E-03	3.661E-01	0.20	0.054
135.16	173.98	-0.10546	-0.00372	-0.00002	3.54	0.12504	0.12876	-0.00248	-0.00248	1.00	173.48	-0.53	-13.1	-4.63E-03	-5.265E-01	0.19	0.054
136.16	172.98	-0.10490	-0.00370	-0.00016	3.61	0.12754	0.13124	0.00513	0.00513	1.00	172.48	1.09	27.2	9.58E-03	1.089E+00	0.20	0.055
137.16	171.98	-0.10041	-0.00355	-0.00005	3.47	0.12256	0.12611	0.00371	0.00371	1.00	171.48	0.79	19.6	6.93E-03	7.873E-01	0.18	0.053
138.16	170.98	-0.09906	-0.00350	-0.00054	3.37	0.11890	0.12240	0.02840	0.02840	1.00	170.48	6.02	150.3	5.30E-02	6.024E+00	0.17	0.052
139.16	169.98	-0.08368	-0.00295	-0.00002	2.58	0.09104	0.09399	0.00603	0.00603	1.00	169.48	1.28	31.9	1.13E-02	1.279E+00	0.11	0.042
140.16	168.98	-0.08311	-0.00293	-0.00010	2.41	0.08503	0.08797	0.00275	0.00275	1.00	168.48	0.58	14.6	5.13E-03	5.832E-01	0.10	0.040
141.16	167.98	-0.08027	-0.00283	0.00007	2.33	0.08238	0.08522	0.00165	0.00165	1.00	167.48	0.35	8.7	3.09E-03	3.506E-01	0.09	0.039
142.16	166.98	-0.08212	-0.00290	-0.00040	2.28	0.08066	0.08356	0.00685	0.00685	1.00	166.48	1.45	36.2	1.28E-02	1.452E+00	0.09	0.038
143.16	165.98	-0.07073	-0.00250	-0.00035	2.10	0.07422	0.07672	0.01117	0.01117	1.00	165.48	2.37	59.1	2.08E-02	2.368E+00	0.08	0.036
144.16	164.98	-0.06083	-0.00215	-0.00049	1.80	0.06340	0.06555	0.01520	0.01520	1.00	164.48	3.22	80.4	2.84E-02	3.223E+00	0.06	0.032
145.16	163.98	-0.04701	-0.00166	-0.00063	1.38	0.04869	0.05035	0.01878	0.01878	1.00	163.48	3.98	99.4	3.51E-02	3.982E+00	0.04	0.027
146.16	162.98	-0.02921	-0.00103	-0.00088	0.87	0.03055	0.03158	0.03153	0.03153	0.73	162.61	9.12	227.6	8.03E-02	6.688E+00	0.02	0.021
147.16	161.98	-0.00434	-0.00015		0.00	-0.00011	0.00004	0.18904	0.18904								

106.89	Top of Screen Depth from TOC (ft)	
146.89	Bottom of Screen Depth from TOC (ft)	
40.00	Screen Length (ft)	
309.14	TOC Elevation (ft)	
1.75	T pump (ft2/min)	
101	Formation thickness (ft)	
25.0	K pump (ft/d)	
8.80E-03	K pump (cm/s)	

Filter pack:

0.254	Do (m)
0.102	Di (m)
0.043	Area (m^2)
7.62	Thickness (cm)
100	Conductivity, K_{gp} (m/d) FX-50

EBF:

0.178	L_{EBF} (m)

Bypass flow:

0.111	ΔL (m)
0.289	L (m)

QP (ft3/min)	0.18859
QP (L/min)	5.34
uncorr QP	5.34

40.00 b (ft)

Avg K_i/K_{bar} 1.000000

(Should be exactly 1)

Table 8   Hydraulic conductivity profile and bypass flow estimate for RPC-3PW for ½" EBF, 5 L/min nominal flow and 5 ft increments.

(1)	(2)	(3)	(4)	(5)	(6)	(7)	(8)	(9)	(10) Adjusted?	(11)	(12)	(13)	(14)	(15)	(16)	(17)	(18)
Depth Below TOC (ft)	Elevation (ft-msl)	Ambient Flow (L/min)	Ambient Flow, q (ft³/min)	Differential Ambient Flow, Δq_i (ft³/min)	Pump Induced Flow (L/min)	Pump Induced Flow, Q (ft³/min)	Net Pumping Flow, Q - q (ft³/min)	Differential Net Flow, $\Delta(Q_i - q_i)$ (ft³/min)	Differential Net Flow $\Delta(Q_i - q_i)$ (ft³/min)	Layer Thickness Δz_i (ft)	Mid-point Elevation (ft)	$K_i/K_{bar=}$ $b(\Delta Q_i-\Delta q_i)/$ $(Q_p\Delta z_i)$	K_i (ft/d)	Ki (cm/s)	Check $\Delta z^*K_i/K_{bar}$	Estimated bypass flow (L/min)	Estimated bypass flow ratio (Q_{bp}/Q_{EBF})
106.16	202.98	-0.00022	-0.00001	0.00033	5.34	0.18863	0.18864	0.01830	0.01830	4.27	200.11	0.91	43.2	1.52E-02	3.881E+00	0.41	0.076
111.16	197.98	-0.00970	-0.00034	0.00035	4.81	0.17000	0.17034	-0.00090	-0.00090	5.00	195.48	-0.04	-1.8	-6.37E-04	-1.899E-01	0.33	0.069
116.16	192.98	-0.01961	-0.00069	-0.00004	4.83	0.17054	0.17123	0.00443	0.00443	5.00	190.48	0.19	8.9	3.15E-03	9.394E-01	0.34	0.070
121.16	187.98	-0.01848	-0.00065	0.00213	4.71	0.16615	0.16680	0.02475	0.02475	5.00	185.48	1.05	49.9	1.76E-02	5.250E+00	0.32	0.068
126.16	182.98	-0.07868	-0.00278	0.00088	3.94	0.13927	0.14205	0.00451	0.00451	5.00	180.48	0.19	9.1	3.21E-03	9.563E-01	0.23	0.059
131.16	177.98	-0.10353	-0.00366	0.00005	3.79	0.13389	0.13754	0.00630	0.00630	5.00	175.48	0.27	12.7	4.48E-03	1.336E+00	0.22	0.057
136.16	172.98	-0.10490	-0.00370	-0.00087	3.61	0.12754	0.13124	0.04603	0.04603	5.00	170.48	1.95	92.8	3.27E-02	9.762E+00	0.20	0.055
141.16	167.98	-0.08027	-0.00283	-0.00268	2.33	0.08238	0.08522	0.08517	0.08517	5.73	165.11	3.15	149.7	5.28E-02	1.806E+01	0.09	0.039
147.16	161.98	-0.00434	-0.00015		0.00	-0.00011	0.00004	0.18859	0.18859								

106.89	Top of Screen Depth from TOC (ft)			Filter pack:		QP (ft3/min) 0.18859		40.00 b (ft)		Avg K/K_bar 1.000000
146.89	Bottom of Screen Depth from TOC (ft)		0.254	Do (m)		QP (L/min) 5.34				(Should be exactly 1)
40.00	Screen Length (ft)		0.102	Di (m)		uncorr QP 5.34				
309.14	TOC Elevation (ft)		0.043	Area (m^2)						
1.32	T pump (ft2/min)		7.62	Thickness (cm)						
47.5	K pump (ft/d)		100	Conductivity, K_{gp} (m/d) FX-50						
1.68E-02	K pump (cm/s)			EBF:						
			0.178	L_{EBF} (m)						
				Bypass flow:						
			0.111	ΔL (m)						
			0.289	L (m)						

Table 9   Hydraulic conductivity profile and bypass flow estimate for RPC-3PW for ½" EBF, 5 L/min nominal flow and 10 ft increments.

(1)	(2)	(3)	(4)	(5)	(6)	(7)	(8)	(9)	(10) Adjusted?	(11)	(12)	(13)	(14)	(15)	(16)	(17)	(18)
Depth Below TOC (ft)	Elevation (ft-msl)	Ambient Flow (L/min)	Ambient Flow, q (ft³/min)	Differential Ambient Flow, Δq_i (ft³/min)	Pump Induced Flow (L/min)	Pump Induced Flow, Q (ft³/min)	Net Pumping Flow, Q - q (ft³/min)	Differential Net Flow, $\Delta(Q_i - q_i)$ (ft³/min)	Differential Net Flow $\Delta(Q_i - q_i)$ (ft³/min)	Layer Thickness Δz_i (ft)	Mid-point Elevation (ft)	$K_i/K_{bar}=$ $b(\Delta Q_i-\Delta q_i)/$ $(Q_p\Delta z_i)$	K_i (ft/d)	Ki (cm/s)	Check $\Delta z^*K_i/K_{bar}$	Estimated bypass flow (L/min)	Estimated bypass flow ratio (Q_{bp}/Q_{EBF})
106.16	202.98	-0.00022	-0.00001	0.00068	5.34	0.18863	0.18864	0.01740	0.01740	9.27	197.61	0.40	18.9	6.68E-03	3.691E+00	0.41	0.076
116.16	192.98	-0.01961	-0.00069	0.00209	4.83	0.17054	0.17123	0.02918	0.02918	10.00	187.98	0.62	29.4	1.04E-02	6.190E+00	0.34	0.070
126.16	182.98	-0.07868	-0.00278	0.00093	3.94	0.13927	0.14205	0.01081	0.01081	10.00	177.98	0.23	10.9	3.84E-03	2.292E+00	0.23	0.059
136.16	172.98	-0.10490	-0.00370	-0.00355	3.61	0.12754	0.13124	0.13120	0.13120	10.73	167.61	2.59	123.2	4.35E-02	2.783E+01	0.20	0.055
147.16	161.98	-0.00434	-0.00015		0.00	-0.00011	0.00004	0.18859	0.18859								

106.89	Top of Screen Depth from TOC (ft)			Filter pack:		QP (ft3/min) 0.18859		40.00 b (ft)	Avg K_i/K_{bar} 1.000000
146.89	Bottom of Screen Depth from TOC (ft)		0.254	Do (m)		QP (L/min) 5.34			(Should be exactly 1)
40.00	Screen Length (ft)		0.102	Di (m)		uncorr QP 5.34			
309.14	TOC Elevation (ft)		0.043	Area (m^2)					
1.32	T pump (ft2/min)		7.62	Thickness (cm)					
47.5	K pump (ft/d)		100	Conductivity, K_{gp} (m/d) FX-50					
1.68E-02	K pump (cm/s)			EBF:					
			0.178	L_{EBF} (m)					
				Bypass flow:					
			0.111	ΔL (m)					
			0.289	L (m)					

Table 10   Hydraulic conductivity profile and bypass flow estimate for RPC-3PW for 1" EBF, 15 L/min nominal flow and 1 ft increments.

(1)	(2)	(3)	(4)	(5)	(6)	(7)	(8)	(9)	(10) Adjusted?	(11)	(12)	(13)	(14)	(15)	(16)	(17)	(18)
Depth Below TOC (ft)	Elevation (ft-msl)	Ambient Flow (L/min)	Ambient Flow, q (ft³/min)	Differential Ambient Flow, Δq_i (ft³/min)	Pump Induced Flow (L/min)	Pump Induced Flow, Q (ft³/min)	Net Pumping Flow, Q - q (ft³/min)	Differential Net Flow, $\Delta(Q_i - q_i)$ (ft³/min)	Differential Net Flow $\Delta(Q_i - q_i)$ (ft³/min)	Layer Thickness Δz_i (ft)	Mid-point Elevation (ft)	$K_i/K_{bar}=$ b(ΔQ_i-Δq_i)/($Q_p\Delta z_i$)	K_i (ft/d)	Ki (cm/s)	Check $\Delta z{*}K_i/K_{bar}$	Estimated bypass flow (L/min)	Estimated bypass flow ratio (Q_{bp}/Q_{EBF})
106.16	202.98	-0.00022	-0.00001	0.00001	14.56	0.51412	0.51413	-0.00243	-0.00243	0.27	202.11	-0.72	-34.0	-1.20E-02	-1.907E-01	0.17	0.012
107.16	201.98	-0.00050	-0.00002	0.00001	14.63	0.51654	0.51656	-0.00140	-0.00140	1.00	201.48	-0.11	-5.2	-1.84E-03	-1.095E-01	0.17	0.012
108.16	200.98	-0.00086	-0.00003	-0.00113	14.67	0.51793	0.51796	0.23013	0.23013	1.00	200.48	18.05	857.5	3.03E-01	1.805E+01	0.17	0.012
109.16	199.98	0.03106	0.00110	0.00131	8.18	0.28892	0.28782	-0.21198	-0.21198	1.00	199.48	-16.62	-789.9	-2.79E-01	-1.662E+01	0.06	0.007
110.16	198.98	-0.00606	-0.00021	0.00013	14.15	0.49959	0.49981	-0.00878	-0.00878	1.00	198.48	-0.69	-32.7	-1.15E-02	-6.882E-01	0.16	0.012
111.16	197.98	-0.00970	-0.00034	0.00031	14.39	0.50824	0.50859	0.00073	0.00073	1.00	197.48	0.06	2.7	9.54E-04	5.691E-02	0.17	0.012
112.16	196.98	-0.01854	-0.00065	-0.00005	14.36	0.50720	0.50786	-0.00099	-0.00099	1.00	196.48	-0.08	-3.7	-1.30E-03	-7.783E-02	0.17	0.012
113.16	195.98	-0.01726	-0.00061	-0.00010	14.39	0.50824	0.50885	0.00183	0.00183	1.00	195.48	0.14	6.8	2.41E-03	1.435E-01	0.17	0.012
114.16	194.98	-0.01441	-0.00051	0.00015	14.34	0.50651	0.50702	-0.00291	-0.00291	1.00	194.48	-0.23	-10.9	-3.83E-03	-2.285E-01	0.17	0.012
115.16	193.98	-0.01854	-0.00065	0.00004	14.42	0.50928	0.50993	0.00100	0.00100	1.00	193.48	0.08	3.7	1.31E-03	7.842E-02	0.17	0.012
116.16	192.98	-0.01961	-0.00069	-0.00007	14.39	0.50824	0.50893	0.00007	0.00007	1.00	192.48	0.01	0.3	9.58E-05	5.716E-03	0.17	0.012
117.16	191.98	-0.01755	-0.00062	-0.00008	14.39	0.50824	0.50886	0.00077	0.00077	1.00	191.48	0.06	2.9	1.01E-03	6.037E-02	0.17	0.012
118.16	190.98	-0.01534	-0.00054	0.00012	14.37	0.50755	0.50809	0.00368	0.00368	1.00	190.48	0.29	13.7	4.84E-03	2.889E-01	0.17	0.012
119.16	189.98	-0.01876	-0.00066	0.00004	14.27	0.50375	0.50441	-0.00177	-0.00177	1.00	189.48	-0.14	-6.6	-2.32E-03	-1.386E-01	0.17	0.012
120.16	188.98	-0.01983	-0.00070	-0.00005	14.32	0.50548	0.50618	0.00074	0.00074	1.00	188.48	0.06	2.8	9.72E-04	5.800E-02	0.17	0.012
121.16	187.98	-0.01848	-0.00065	-0.00010	14.30	0.50478	0.50544	-0.00060	-0.00060	1.00	187.48	-0.05	-2.2	-7.84E-04	-4.676E-02	0.17	0.012
122.16	186.98	-0.01578	-0.00056	0.00015	14.32	0.50548	0.50603	0.00573	0.00573	1.00	186.48	0.45	21.4	7.53E-03	4.493E-01	0.17	0.012
123.16	185.98	-0.02005	-0.00071	0.00017	14.15	0.49959	0.50030	0.00086	0.00086	1.00	185.48	0.07	3.2	1.14E-03	6.776E-02	0.16	0.012
124.16	184.98	-0.02497	-0.00088	0.00089	14.12	0.49856	0.49944	0.01502	0.01502	1.00	184.48	1.18	56.0	1.97E-02	1.178E+00	0.16	0.011
125.16	183.98	-0.05026	-0.00177	0.00100	13.67	0.48264	0.48442	0.01560	0.01560	1.00	183.48	1.22	58.1	2.05E-02	1.223E+00	0.15	0.011
126.16	182.98	-0.07868	-0.00278	0.00078	13.20	0.46604	0.46882	0.01029	0.01029	1.00	182.48	0.81	38.3	1.35E-02	8.065E-01	0.14	0.011
127.16	181.98	-0.10089	-0.00356	0.00015	12.88	0.45497	0.45853	-0.00188	-0.00188	1.00	181.48	-0.15	-7.0	-2.47E-03	-1.471E-01	0.14	0.011
128.16	180.98	-0.10502	-0.00371	-0.00007	12.93	0.45670	0.46041	0.00111	0.00111	1.00	180.48	0.09	4.1	1.46E-03	8.709E-02	0.14	0.011
129.16	179.98	-0.10296	-0.00364	0.00007	12.90	0.45566	0.45930	-0.00076	-0.00076	1.00	179.48	-0.06	-2.8	-9.95E-04	-5.938E-02	0.14	0.011
130.16	178.98	-0.10481	-0.00370	-0.00005	12.92	0.45635	0.46005	0.00385	0.00385	1.00	178.48	0.30	14.3	5.06E-03	3.019E-01	0.14	0.011
131.16	177.98	-0.10353	-0.00366	-0.00001	12.82	0.45255	0.45620	0.00797	0.00797	1.00	177.48	0.62	29.7	1.05E-02	6.249E-01	0.13	0.010
132.16	176.98	-0.10318	-0.00364	0.00001	12.59	0.44459	0.44823	0.00103	0.00103	1.00	176.48	0.08	3.8	1.35E-03	8.059E-02	0.13	0.010
133.16	175.98	-0.10347	-0.00365	0.00009	12.56	0.44355	0.44721	0.00371	0.00371	1.00	175.48	0.29	13.8	4.88E-03	2.913E-01	0.13	0.010
134.16	174.98	-0.10603	-0.00374	-0.00002	12.45	0.43975	0.44349	0.00348	0.00348	1.00	174.48	0.27	13.0	4.57E-03	2.728E-01	0.13	0.010
135.16	173.98	-0.10546	-0.00372	-0.00002	12.36	0.43629	0.44001	0.00244	0.00244	1.00	173.48	0.19	9.1	3.21E-03	1.915E-01	0.13	0.010
136.16	172.98	-0.10490	-0.00370	-0.00016	12.29	0.43387	0.43757	0.01227	0.01227	1.00	172.48	0.96	45.7	1.61E-02	9.618E-01	0.12	0.010
137.16	171.98	-0.10041	-0.00355	-0.00005	11.94	0.42176	0.42530	0.00524	0.00524	1.00	171.48	0.41	19.5	6.88E-03	4.106E-01	0.12	0.010
138.16	170.98	-0.09906	-0.00350	-0.00054	11.80	0.41657	0.42007	0.07250	0.07250	1.00	170.48	5.68	270.1	9.53E-02	5.685E+00	0.11	0.010
139.16	169.98	-0.08368	-0.00295	-0.00002	9.76	0.34462	0.34757	0.02458	0.02458	1.00	169.48	1.93	91.6	3.23E-02	1.928E+00	0.08	0.008
140.16	168.98	-0.08311	-0.00293	-0.00010	9.06	0.32006	0.32299	0.01428	0.01428	1.00	168.48	1.12	53.2	1.88E-02	1.120E+00	0.07	0.008
141.16	167.98	-0.08027	-0.00283	0.00007	8.66	0.30587	0.30871	0.00443	0.00443	1.00	167.48	0.35	16.5	5.83E-03	3.475E-01	0.06	0.007
142.16	166.98	-0.08212	-0.00290	-0.00040	8.54	0.30138	0.30427	0.02358	0.02358	1.00	166.48	1.85	87.9	3.10E-02	1.849E+00	0.06	0.007
143.16	165.98	-0.07073	-0.00250	-0.00035	7.88	0.27820	0.28070	0.04255	0.04255	1.00	165.48	3.34	158.6	5.59E-02	3.337E+00	0.05	0.007
144.16	164.98	-0.06083	-0.00215	-0.00049	6.68	0.23599	0.23814	0.05895	0.05895	1.00	164.48	4.62	219.7	7.75E-02	4.623E+00	0.04	0.006
145.16	163.98	-0.04701	-0.00166	-0.00063	5.03	0.17753	0.17919	0.06359	0.06359	1.00	163.48	4.99	236.9	8.36E-02	4.986E+00	0.02	0.005
146.16	162.98	-0.02921	-0.00103	-0.00088	3.24	0.11457	0.11560	0.11158	0.11158	0.73	162.61	11.93	567.0	2.00E-01	8.749E+00	0.01	0.003
147.16	161.98	-0.00434	-0.00015		0.11	0.00387	0.00403	0.51010	0.51010								

106.89	Top of Screen Depth from TOC (ft)			Filter pack:		QP (ft3/min) 0.51010	40.00 b (ft)	Avg K/K$_{bar}$ 1.000000
146.89	Bottom of Screen Depth from TOC (ft)		0.254	Do (m)		QP (L/min) 14.45		(Should be exactly 1)
40.00	Screen Length (ft)		0.102	Di (m)		uncorr QP 14.45		
309.14	TOC Elevation (ft)		0.043	Area (m^2)				
1.32	T pump (ft2/min)		7.62	Thickness (cm)				
47.5	K pump (ft/d)		100	Conductivity, K$_{gp}$ (m/d) FX-50				
1.68E-02	K pump (cm/s)			EBF:				
			0.178	L$_{EBF}$ (m)				
				Bypass flow:				
			0.111	ΔL (m)				
			0.289	L (m)				

Table 11 Hydraulic conductivity profile and bypass flow estimate for RPC-3PW for 1" EBF, 15 L/min nominal flow and 5 ft increments.

(1)	(2)	(3)	(4)	(5)	(6)	(7)	(8)	(9)	(10) Adjusted?	(11)	(12)	(13)	(14)	(15)	(16)	(17)	(18)
Depth Below TOC (ft)	Elevation (ft-msl)	Ambient Flow (L/min)	Ambient Flow, q (ft³/min)	Differential Ambient Flow, Δq_i (ft³/min)	Pump Induced Flow (L/min)	Pump Induced Flow, Q (ft³/min)	Net Pumping Flow, Q - q (ft³/min)	Differential Net Flow, $\Delta(Q_i - q_i)$ (ft³/min)	Differential Net Flow $\Delta(Q_i - q_i)$ (ft³/min)	Layer Thickness Δz_i (ft)	Mid-point Elevation (ft)	$K_i/K_{bar=}$ $b(\Delta Q_i - \Delta q_i)/(Q_p \Delta z_i)$	K_i (ft/d)	K_i (cm/s)	Check $\Delta z^* K_i/K_{bar}$	Estimated bypass flow (L/min)	Estimated bypass flow ratio (Q_{bp}/Q_{EBF})
106.16	202.98	-0.00022	-0.00001	0.00033	14.56	0.51412	0.51413	0.00555	0.00555	4.27	200.11	0.10	4.8	1.71E-03	4.349E-01	0.17	0.012
111.16	197.98	-0.00970	-0.00034	0.00035	14.39	0.50824	0.50859	-0.00035	-0.00035	5.00	195.48	-0.01	-0.3	-9.20E-05	-2.744E-02	0.17	0.012
116.16	192.98	-0.01961	-0.00069	-0.00004	14.39	0.50824	0.50893	0.00350	0.00350	5.00	190.48	0.05	2.6	9.20E-04	2.744E-01	0.17	0.012
121.16	187.98	-0.01848	-0.00065	0.00213	14.30	0.50478	0.50544	0.03662	0.03662	5.00	185.48	0.57	27.3	9.63E-03	2.871E+00	0.17	0.012
126.16	182.98	-0.07868	-0.00278	0.00088	13.20	0.46604	0.46882	0.01261	0.01261	5.00	180.48	0.20	9.4	3.32E-03	9.891E-01	0.14	0.011
131.16	177.98	-0.10353	-0.00366	0.00005	12.82	0.45255	0.45620	0.01863	0.01863	5.00	175.48	0.29	13.9	4.90E-03	1.461E+00	0.13	0.010
136.16	172.98	-0.10490	-0.00370	-0.00087	12.29	0.43387	0.43757	0.12886	0.12886	5.00	170.48	2.02	96.0	3.39E-02	1.010E+01	0.12	0.010
141.16	167.98	-0.08027	-0.00283	#REF!	8.66	0.30587	0.30871	0.30468	0.30468	5.73	165.11	4.17	198.0	6.99E-02	2.389E+01	0.06	0.007
147.16	161.98	-0.00434	-0.00015		0.11	0.00387	0.00403	0.51010	0.51010								

106.89	Top of Screen Depth from TOC (ft)			Filter pack:		QP (ft3/min)	0.51010		40.00 b (ft)
146.89	Bottom of Screen Depth from TOC (ft)		0.254	Do (m)		QP (L/min)	14.45		
40.00	Screen Length (ft)		0.102	Di (m)		uncorr QP	14.45		
309.14	TOC Elevation (ft)		0.043	Area (m^2)					
1.32	T pump (ft2/min)		7.62	Thickness (cm)					
47.5	K pump (ft/d)		100	Conductivity, K_{gp} (m/d) FX-50				Avg K_i/K_{bar}	1.000000
1.68E-02	K pump (cm/s)			EBF:					(Should be exactly 1)
			0.178	L_{EBF} (m)					
				Bypass flow:					
			0.111	ΔL (m)					
			0.289	L (m)					

Table 12   Hydraulic conductivity profile and bypass flow estimate for RPC-3PW for 1" EBF, 15 L/min nominal flow and 10 ft increments.

(1)	(2)	(3)	(4)	(5)	(6)	(7)	(8)	(9)	(10) Adjusted?	(11)	(12)	(13)	(14)	(15)	(16)	(17)	(18)
Depth Below TOC (ft)	Elevation (ft-msl)	Ambient Flow (L/min)	Ambient Flow, q (ft³/min)	Differential Ambient Flow, Δq_i (ft³/min)	Pump Induced Flow (L/min)	Pump Induced Flow, Q (ft³/min)	Net Pumping Flow, Q - q (ft³/min)	Differential Net Flow, $\Delta(Q_i - q_i)$ (ft³/min)	Differential Net Flow $\Delta(Q_i - q_i)$ (ft³/min)	Layer Thickness Δz_i (ft)	Mid-point Elevation (ft)	K_i/K_{bar}= $b(\Delta Q_i-\Delta q_i)/(Q_p\Delta z_i)$	K_i (ft/d)	K_i (cm/s)	Check $\Delta z^*K_i/K_{bar}$	Estimated bypass flow (L/min)	Estimated bypass flow ratio (Q_{bp}/Q_{EBF})
106.16	202.98	-0.00022	-0.00001	0.00068	14.56	0.51412	0.51413	0.00520	0.00520	9.27	197.61	0.04	2.1	7.37E-04	4.074E-01	0.17	0.012
116.16	192.98	-0.01961	-0.00069	0.00209	14.39	0.50824	0.50893	0.04012	0.04012	10.00	187.98	0.31	14.9	5.27E-03	3.146E+00	0.17	0.012
126.16	182.98	-0.07868	-0.00278	0.00093	13.20	0.46604	0.46882	0.03125	0.03125	10.00	177.98	0.25	11.6	4.11E-03	2.450E+00	0.14	0.011
136.16	172.98	-0.10490	-0.00370	-0.00355	12.29	0.43387	0.43757	0.43354	0.43354	10.73	167.61	3.17	150.5	5.31E-02	3.400E+01	0.12	0.010
147.16	161.98	-0.00434	-0.00015		0.11	0.00387	0.00403	0.51010	0.51010								

106.89	Top of Screen Depth from TOC (ft)		*Filter pack:*		QP (ft3/min) 0.51010	40.00 b (ft)
146.89	Bottom of Screen Depth from TOC (ft)	0.254	Do (m)		QP (L/min) 14.45	
40.00	Screen Length (ft)	0.102	Di (m)		uncorr QP 14.45	
309.14	TOC Elevation (ft)	0.043	Area (m^2)			
1.32	T pump (ft2/min)	7.62	Thickness (cm)			
47.5	K pump (ft/d)	100	Conductivity, K_{gp} (m/d) FX-50			
1.68E-02	K pump (cm/s)		*EBF:*			
		0.178	L_{EBF} (m)			
			Bypass flow:			
		0.111	ΔL (m)			
		0.289	L (m)			

Avg K_i/K_{bar} 1.000000
(Should be exactly 1)

Table 13 Hydraulic conductivity profile and bypass flow estimate for RPT-2PW.

(1)	(2)	(3)	(4)	(5)	(6)	(7)	(8)	(9)	(10)	(11)	(12)	(13)	(14)	(15)	(16)	(17)	(18)	(19)	(20)	(21)	(22)	(23)	(24)	(25)
Depth Below TOC (ft)	Elevation (ft-msl)	Ambient Flow (L/min)	Ambient Flow, q (ft³/min)	Differential Ambient Flow, Δq_i (ft³/min)	Pump Induced Flow (L/min)	Pump Induced Flow, Q (ft³/min)	Net Pumping Flow, Q - q (ft³/min)	Differential Net Flow, $\Delta(Q_i - q_i)$ (ft³/min)	Adjusted / Differential Net Flow $\Delta(Q_i - q_i)$ (ft³/min)	Layer Thickness Δz_i (ft)	Mid-point Elevation (ft)	K_i/K_{bar}= b$(\Delta Q_i-\Delta q_i)$/ $(Q_p\Delta z_i)$	K_i (ft/d)	K_i (cms/s)	Check $\Delta z \cdot K/K_{bar}$	Estimated bypass flow (L/min)	Estimated bypass flow ratio (Q_{bp}/Q_{EBF})	Clock Time	Elapsed Time (min)	Water Level (ft)	dh (ft)	Cooper-Jacob K_i (ft/d)	Ratio	KΔz
80.58	209.33	0.00000	0.00000	0.00006	4.01	0.14153	0.14153	0.00924	0.00924	1.00	208.83	0.98	2.3	7.98E-04	9.787E-01	0.33	0.082	14:40	110	36.65	8.10	2.6	1.13	2.56
81.58	208.33	-0.00157	-0.00006	0.00006	3.74	0.13223	0.13229	0.01896	0.01896	1.00	207.83	2.01	4.6	1.63E-03	2.009E+00	0.29	0.077	14:37	107	36.65	8.10	5.2	1.13	5.24
82.58	207.33	-0.00314	-0.00011	0.00014	3.21	0.11322	0.11333	0.00457	0.00457	1.00	206.83	0.48	1.1	3.93E-04	4.840E-01	0.22	0.068	14:33	103	36.65	8.10	1.3	1.13	1.26
83.58	206.33	-0.00705	-0.00025	0.00017	3.07	0.10852	0.10877	0.01036	0.01036	1.00	205.83	1.10	2.5	8.92E-04	1.098E+00	0.20	0.066	14:30	100	36.65	8.10	2.8	1.12	2.84
84.58	205.33	-0.01176	-0.00042	0.00019	2.78	0.09799	0.09840	0.00882	0.00882	1.00	204.83	0.93	2.2	7.59E-04	9.342E-01	0.17	0.061	14:23	93	36.65	8.10	2.4	1.12	2.40
85.58	204.33	-0.01724	-0.00061	0.00003	2.52	0.08898	0.08959	0.00854	0.00854	1.00	203.83	0.91	2.1	7.36E-04	9.052E-01	0.14	0.057	14:21	91	36.64	8.09	2.3	1.11	2.32
86.58	203.33	-0.01803	-0.00064	0.00003	2.28	0.08041	0.08105	0.00479	0.00479	1.00	202.83	0.51	1.2	4.12E-04	5.071E-01	0.12	0.052	14:19	89	36.62	8.07	1.3	1.11	1.30
87.58	202.33	-0.01881	-0.00066	-0.00003	2.14	0.07560	0.07626	0.00708	0.00708	1.00	201.83	0.75	1.7	6.10E-04	7.507E-01	0.11	0.050	14:17	87	36.61	8.06	1.9	1.11	1.93
88.58	201.33	-0.01803	-0.00064	-0.00003	1.94	0.06854	0.06918	0.01047	0.01047	1.00	200.83	1.11	2.6	9.01E-04	1.109E+00	0.09	0.047	14:14	84	36.59	8.04	2.8	1.11	2.84
89.58	200.33	-0.01724	-0.00061	-0.00006	1.65	0.05810	0.05871	0.01265	0.01265	1.00	199.83	1.34	3.1	1.09E-03	1.341E+00	0.07	0.042	14:10	80	36.56	8.01	3.4	1.11	3.43
90.58	199.33	-0.01568	-0.00055	-0.00008	1.29	0.04550	0.04606	0.00938	0.00938	1.00	198.83	0.99	2.3	8.08E-04	9.942E-01	0.05	0.036	14:08	78	36.55	8.00	2.5	1.11	2.54
91.58	198.33	-0.01332	-0.00047	-0.00014	1.03	0.03621	0.03668	0.01056	0.01056	1.00	197.83	1.12	2.6	9.10E-04	1.119E+00	0.03	0.031	14:05	75	36.53	7.98	2.9	1.11	2.85
92.58	197.33	-0.00941	-0.00033	-0.00028	0.73	0.02578	0.02612	0.02390	0.02390	1.00	196.83	2.53	5.8	2.06E-03	2.533E+00	0.02	0.026	14:01	71	36.49	7.94	6.5	1.11	6.46
93.58	196.33	-0.00157	-0.00006	-0.00006	0.06	0.00216	0.00221	0.00136	0.00136	1.00	195.83	0.14	0.3	1.17E-04	1.437E-01	0.00	0.015	13:58	68	36.45	7.90	0.4	1.11	0.37
94.58	195.33	0.00000	0.00000	0.00014	0.02	0.00086	0.00086	0.00008	0.00008	0.42	195.12	0.02	0.0	1.70E-05	8.802E-03	0.00	0.014	13:56	66	36.43	7.88	0.1	1.11	0.02
95.00	194.91	-0.00392	-0.00014	-0.00014	0.02	0.00064	0.00077	0.00077	0.00077	0.58	194.62	0.14	0.3	1.15E-04	8.212E-02	0.00	0.014	13:53	63	36.4	7.85	0.4	1.10	0.21
95.58	194.33	0.00000	0.00000	created data	0.00	0.00000	0.00000	0.14153	0.14153															

80.58	Top of Screen Depth from TOC (ft)			Filter pack:		QP (ft3/min)	0.14153	15.00 b (ft)	
95.58	Bottom of Screen Depth from TOC (ft)		0.305	Do (m)		QP (L/min)	4.01		
15.00	Screen Length (ft)		0.102	Di (m)		uncorr QP	4.01		
289.91	TOC Elevation (ft)		0.065	Area (m^2)					
0.024	T pump (ft2/min)		10.16	Thickness (cm)				Avg K_i/K_{bar}	1.000000
15	Formation thickness (ft)		.100	Conductivity, K_{qp} (m/d) FX-50				(Should be exactly 1)	
2.3	K pump (ft/d)			EBF:					
8.13E-04	K pump (cm/s)		0.178	L_{EBF} (m)					
				Bypass flow:					
			0.143	ΔL (m)					
			0.320	L (m)					

r_w (in)	6	
b (ft)	15	Avg Cooper-Jacob K 2.57
K (ft/d)	2.6	Ratio 1.12
S_s (1/ft)	1.0E-04	
T (ft²/d)	39	
S (unitless)	1.5E-03	
T/S (ft²/d)	2.60E+04	
Start of pumping	12:50	
Water level (ft)	28.55	
Well efficiency	50%	

Table 14   Hydraulic conductivity profile and bypass flow estimate for RPT-3PW.

(1) Depth Below TOC (ft)	(2) Elevation (ft-msl)	(3) Ambient Flow (L/min)	(4) Ambient Flow, q (ft³/min)	(5) Differential Ambient Flow, Δq_i (ft³/min)	(6) Pump Induced Flow (L/min)	(7) Pump Induced Flow, Q (ft³/min)	(8) Net Pumping Flow, Q - q (ft³/min)	(9) Differential Net Flow, $\Delta(Q_i - q_i)$ (ft³/min)	(10) Adjusted Differential Net Flow $\Delta(Q_i - q_i)$ (ft³/min)	(11) Layer Thickness Δz_i (ft)	(12) Mid-point Elevation (ft)	(13) $K_i/K_{bar}=b(\Delta Q_i\cdot\Delta q_i)/(Q_p\Delta z_i)$	(14) K_i (ft/d)	(15) K_i (cms/s)	(16) Check $\Delta z^*K_i/K_{bar}$	(17) Estimated bypass flow (L/min)	(18) Estimated bypass flow ratio (Q_{bp}/Q_{EBF})	(19) Clock Time	(20) Elapsed Time (min)	(21) Water Level (ft)	(22) dh (ft)	(23) Cooper-Jacob K_i (ft/d)	(24) Ratio	(25) $K\Delta z$
151.48	138.35	0.00000	0.00000	0.00456	14.16	0.49994	0.49994	0.01204	0.01204	0.96	137.83	1.01	2.0	7.05E-04	9.633E-01	0.16	0.012	14:38	166	61.27	7.70	4.1	2.06	3.94
152.48	137.35	-0.12926	-0.00456	0.00033	13.69	0.48334	0.48790	-0.00137	-0.00137	1.00	136.85	-0.11	-0.2	-7.67E-05	-1.096E-01	0.15	0.011	14:35	163	61.26	7.69	-0.4	2.06	-0.45
153.48	136.35	-0.13866	-0.00490	0.00011	13.72	0.48437	0.48927	0.00300	0.00300	1.00	135.85	0.24	0.5	1.68E-04	2.402E-01	0.15	0.011	14:33	161	61.25	7.68	1.0	2.06	0.98
154.48	135.35	-0.14179	-0.00501	0.00053	13.63	0.48126	0.48627	0.01089	0.01089	1.00	134.85	0.87	1.7	6.10E-04	8.713E-01	0.15	0.011	14:30	158	61.23	7.66	3.6	2.06	3.57
155.48	134.35	-0.15666	-0.00553	0.00011	13.31	0.46984	0.47538	-0.00288	-0.00288	1.00	133.85	-0.23	-0.5	-1.61E-04	-2.303E-01	0.14	0.011	14:27	155	61.22	7.65	-0.9	2.06	-0.94
156.48	133.35	-0.15980	-0.00564	0.00014	13.38	0.47261	0.47825	0.00436	0.00436	1.00	132.85	0.35	0.7	2.44E-04	3.487E-01	0.15	0.011	14:23	151	61.20	7.63	1.4	2.06	1.43
157.48	132.35	-0.16371	-0.00578	0.00044	13.26	0.46811	0.47389	0.01270	0.01270	1.00	131.85	1.02	2.0	7.12E-04	1.016E+00	0.14	0.011	14:16	144	61.17	7.60	4.2	2.06	4.16
158.48	131.35	-0.17623	-0.00622	0.00116	12.88	0.45497	0.46119	0.02963	0.02963	1.00	130.85	2.37	4.7	1.66E-03	2.370E+00	0.14	0.011	14:12	140	61.15	7.58	9.7	2.06	9.70
159.48	130.35	-0.20910	-0.00738	0.00251	12.01	0.42418	0.43156	0.05422	0.05422	1.00	129.85	4.34	8.6	3.04E-03	4.338E+00	0.12	0.010	14:07	135	61.13	7.56	17.7	2.06	17.74
160.48	129.35	-0.28029	-0.00990	0.00287	10.41	0.36745	0.37735	0.05767	0.05767	1.00	128.85	4.61	9.2	3.23E-03	4.614E+00	0.09	0.009	14:03	131	61.11	7.54	18.9	2.06	18.85
161.48	128.35	-0.36160	-0.01277	0.00207	8.69	0.30691	0.31968	0.04359	0.04359	1.00	127.85	3.49	6.9	2.44E-03	3.488E+00	0.06	0.007	13:59	127	61.10	7.53	14.2	2.06	14.24
162.48	127.35	-0.42021	-0.01484	0.00099	7.40	0.26125	0.27608	0.01284	0.01284	1.00	126.85	1.03	2.0	7.20E-04	1.028E+00	0.05	0.006	13:55	123	61.08	7.51	4.2	2.05	4.19
163.48	126.35	-0.44833	-0.01583	0.00019	7.01	0.24741	0.26324	-0.00054	-0.00054	1.00	125.85	-0.04	-0.1	-3.02E-05	-4.312E-02	0.04	0.006	13:52	120	61.07	7.50	-0.2	2.05	-0.18
164.48	125.35	-0.45380	-0.01602	-0.00006	7.02	0.24776	0.26378	0.00386	0.00386	1.00	124.85	0.31	0.6	2.16E-04	3.088E-01	0.04	0.006	13:49	117	61.06	7.49	1.3	2.05	1.26
165.48	124.35	-0.45223	-0.01597	0.00011	6.91	0.24395	0.25992	-0.00011	-0.00011	1.00	123.85	-0.01	0.0	-6.18E-06	-8.825E-03	0.04	0.006	13:46	114	61.05	7.48	0.0	2.05	-0.04
166.48	123.35	-0.45536	-0.01608	0.00006	6.91	0.24395	0.26003	0.00479	0.00479	1.00	122.85	0.38	0.8	2.68E-04	3.830E-01	0.04	0.006	13:44	112	61.04	7.47	1.6	2.05	1.56
167.48	122.35	-0.45692	-0.01613	0.00025	6.77	0.23911	0.25524	0.00044	0.00044	1.00	121.85	0.04	0.1	2.49E-05	3.550E-02	0.04	0.006	13:41	109	61.03	7.46	0.1	2.05	0.14
168.48	121.35	-0.46395	-0.01638	-0.00008	6.75	0.23842	0.25480	0.00735	0.00735	1.00	120.85	0.59	1.2	4.12E-04	5.878E-01	0.04	0.006	13:39	107	61.02	7.45	2.4	2.05	2.39
169.48	120.35	-0.46161	-0.01630	0.00019	6.55	0.23115	0.24745	0.00119	0.00119	1.00	119.85	0.10	0.2	6.67E-05	9.526E-02	0.04	0.006	13:36	104	61.00	7.43	0.4	2.05	0.39
170.48	119.35	-0.46707	-0.01649	-0.00019	6.51	0.22977	0.24626	0.00088	0.00088	1.00	118.85	0.07	0.1	4.96E-05	7.079E-02	0.04	0.006	13:34	102	60.98	7.41	0.3	2.05	0.29
171.48	118.35	-0.46161	-0.01630	-0.00022	6.49	0.22908	0.24537	0.00057	0.00057	1.00	117.85	0.05	0.1	3.17E-05	4.533E-02	0.04	0.006	13:31	99	60.96	7.39	0.2	2.05	0.18
172.48	117.35	-0.45536	-0.01608	-0.00011	6.48	0.22873	0.24481	-0.00127	-0.00127	1.00	116.85	-0.10	-0.2	-7.13E-05	-1.019E-01	0.04	0.006	13:29	97	60.95	7.38	-0.4	2.05	-0.41
173.48	116.35	-0.45223	-0.01597	-0.00066	6.52	0.23011	0.24608	0.00896	0.00896	1.00	115.85	0.72	1.4	5.02E-04	7.172E-01	0.04	0.006	13:27	95	60.93	7.36	2.9	2.05	2.91
174.48	115.35	-0.43349	-0.01531	-0.00055	6.28	0.22181	0.23712	0.01404	0.01404	1.00	114.85	1.12	2.2	7.87E-04	1.123E+00	0.03	0.005	13:24	92	60.91	7.34	4.6	2.05	4.56
175.48	114.35	-0.41786	-0.01475	-0.00036	5.90	0.20832	0.22307	0.01108	0.01108	1.00	113.85	0.89	1.8	6.21E-04	8.866E-01	0.03	0.005	13:22	90	60.90	7.33	3.6	2.04	3.60
176.48	113.35	-0.40771	-0.01440	-0.00047	5.60	0.19760	0.21199	0.00635	0.00635	1.00	112.85	0.51	1.0	3.56E-04	5.080E-01	0.03	0.005	13:20	88	60.89	7.32	2.1	2.04	2.06
177.48	112.35	-0.39443	-0.01393	-0.00055	5.43	0.19171	0.20564	0.00782	0.00782	1.00	111.85	0.63	1.2	4.38E-04	6.253E-01	0.03	0.005	13:18	86	60.88	7.31	2.5	2.04	2.53
178.48	111.35	-0.37880	-0.01338	-0.00039	5.22	0.18445	0.19783	0.01284	0.01284	1.00	110.85	1.03	2.0	7.19E-04	1.027E+00	0.02	0.005	13:16	84	60.87	7.30	4.2	2.04	4.16
179.48	110.35	-0.36786	-0.01299	-0.00102	4.87	0.17200	0.18499	0.02109	0.02109	1.00	109.85	1.69	3.3	1.18E-03	1.687E+00	0.02	0.004	13:13	81	60.86	7.29	6.8	2.04	6.82
180.48	109.35	-0.33894	-0.01197	-0.00102	4.30	0.15193	0.16390	0.02316	0.02316	1.00	108.85	1.85	3.7	1.30E-03	1.853E+00	0.02	0.004	13:11	79	60.85	7.28	7.5	2.03	7.48
181.48	108.35	-0.31001	-0.01095	-0.00064	3.68	0.12979	0.14074	0.01962	0.01962	1.00	107.85	1.57	3.1	1.10E-03	1.570E+00	0.01	0.003	13:09	77	60.83	7.26	6.3	2.03	6.33
182.48	107.35	-0.28342	-0.01001	-0.00022	3.15	0.11111	0.12112	0.00472	0.00472	1.00	106.85	0.38	0.7	2.64E-04	3.775E-01	0.01	0.003	13:07	75	60.82	7.25	1.5	2.03	1.52
183.48	106.35	-0.27716	-0.00979	-0.00017	3.02	0.10662	0.11640	0.00259	0.00259	1.00	105.85	0.21	0.4	1.45E-04	2.070E-01	0.01	0.003	13:05	73	60.80	7.23	0.8	2.03	0.83
184.48	105.35	-0.27247	-0.00962	-0.00055	2.95	0.10419	0.11381	0.00920	0.00920	1.00	104.85	0.74	1.5	5.15E-04	7.361E-01	0.01	0.003	13:02	70	60.78	7.21	3.0	2.03	2.97
185.48	104.35	-0.25683	-0.00907	-0.00240	2.71	0.09555	0.10461	0.02143	0.02143	1.00	103.85	1.71	3.4	1.20E-03	1.714E+00	0.01	0.003	12:59	67	60.75	7.18	6.9	2.03	6.90
186.48	103.35	-0.18876	-0.00666	-0.00249	2.17	0.07652	0.08318	0.02117	0.02117	1.00	102.85	1.69	3.4	1.19E-03	1.694E+00	0.00	0.002	12:56	64	60.73	7.16	6.8	2.03	6.81
187.48	102.35	-0.11830	-0.00418	-0.00119	1.64	0.05784	0.06202	0.01849	0.01849	1.00	101.85	1.48	2.9	1.04E-03	1.479E+00	0.00	0.002	12:54	62	60.71	7.14	5.9	2.02	5.94
188.48	101.35	-0.08462	-0.00299	-0.00058	1.15	0.04054	0.04353	0.00750	0.00750	1.00	100.85	0.60	1.2	4.20E-04	6.000E-01	0.00	0.002	12:51	59	60.69	7.12	2.4	2.02	2.41
189.48	100.35	-0.06817	-0.00241	-0.00075	0.95	0.03362	0.03603	0.01182	0.01182	1.00	99.85	0.95	1.9	6.62E-04	9.454E-01	0.00	0.001	12:49	57	60.67	7.10	3.8	2.02	3.79
190.48	99.35	-0.04702	-0.00166	-0.00166	0.64	0.02255	0.02421	0.02421	0.02421	1.04	98.83	1.86	3.7	1.30E-03	1.937E+00	0.00	0.001	12:46	54	60.67	7.10	7.4	2.01	7.72
191.52	98.31	0.00000	0.00000		0.00	0.00000	0.00000																	

151.52	Top of Screen Depth from TOC (ft)	
191.52	Bottom of Screen Depth from TOC (ft)	
40.00	Screen Length (ft)	
289.83	TOC Elevation (ft)	
0.102	T pump (ft2/min)	
74	Formation thickness (ft)	
2.0	K pump (ft/d)	
7.00E-04	K pump (cm/s)	

Filter pack:

0.254	Do (m)
0.102	Di (m)
0.043	Area (m^2)
7.62	Thickness (cm)
100	Conductivity, K_{gp} (m/d) FX-50

EBF:

0.178	L_{EBF} (m)

Bypass flow:

0.111	ΔL (m)
0.289	L (m)

QP (ft3/min) 0.49994
QP (L/min) 14.16
uncorr QP 14.16

40.00 b (ft)

Avg K/K_{bar} 1.000000
(Should be exactly 1)

r_w (in)	5
b (ft)	74
K (ft/d)	4
S_s (1/ft)	1.0E-04
T (ft²/d)	296
S (unitless)	7.4E-03
T/S (ft²/d)	4.00E+04
Start of pumping	11:52
Water level (ft)	53.57
Well efficiency	50%

Avg Cooper-Jacob K 4.06
Ratio 2.04

Table 15   Hydraulic conductivity profile and bypass flow estimate for RPT-4PW.

(1)	(2)	(3)	(4)	(5)	(6)	(7)	(8)	(9)	(10) Adjusted?	(11)	(12)	(13)	(14)	(15)	(16)	(17)	(18)
Depth Below TOC (ft)	Elevation (ft-msl)	Ambient Flow (L/min)	Ambient Flow, q (ft³/min)	Differential Ambient Flow, Δq_i (ft³/min)	Pump Induced Flow (L/min)	Pump Induced Flow, Q (ft³/min)	Net Pumping Flow, Q - q (ft³/min)	Differential Net Flow, $\Delta(Q_i - q_i)$ (ft³/min)	Differential Net Flow $\Delta(Q_i - q_i)$ (ft³/min)	Layer Thickness Δz_i (ft)	Mid-point Elevation (ft)	$K_i/K_{bar}=$ $b(\Delta Q_i-\Delta q_i)/(Q_p\Delta z_i)$	K_i (ft/d)	K_i (cms/s)	Check $\Delta z \cdot K_i/K_{bar}$	Estimated bypass flow (L/min)	Estimated bypass flow ratio (Q_{bp}/Q_{EBF})
233.82	55.90	0.00000	0.00000	-0.00008	13.55	0.47845	0.47845	0.00073	0.00073	0.87	55.33	0.07	1.0	3.64E-04	6.129E-02	0.13	0.009
234.82	54.90	0.00235	0.00008	-0.00006	13.53	0.47780	0.47772	-0.00133	-0.00133	1.00	54.40	-0.11	-1.6	-5.71E-04	-1.111E-01	0.13	0.009
235.82	53.90	0.00392	0.00014	0.00014	13.57	0.47918	0.47905	-0.00014	-0.00014	1.00	53.40	-0.01	-0.2	-5.95E-05	-1.157E-02	0.13	0.009
236.82	52.90	0.00000	0.00000	0.00000	13.57	0.47918	0.47918	0.00000	0.00000	1.00	52.40	0.00	0.0	0.00E+00	0.000E+00	0.13	0.009
237.82	51.90	0.00000	0.00000	0.00000	13.57	0.47918	0.47918	0.00069	0.00069	1.00	51.40	0.06	0.8	2.98E-04	5.784E-02	0.13	0.009
238.82	50.90	0.00000	0.00000	0.00000	13.55	0.47849	0.47849	-0.00035	-0.00035	1.00	50.40	-0.03	-0.4	-1.49E-04	-2.892E-02	0.13	0.009
239.82	49.90	0.00000	0.00000	0.00014	13.56	0.47884	0.47884	0.00194	0.00194	1.00	49.40	0.16	2.4	8.33E-04	1.620E-01	0.13	0.009
240.82	48.90	-0.00392	-0.00014	-0.00014	13.50	0.47676	0.47690	-0.00055	-0.00055	1.00	48.40	-0.05	-0.7	-2.38E-04	-4.627E-02	0.13	0.009
241.82	47.90	0.00000	0.00000	0.00000	13.52	0.47745	0.47745	-0.00104	-0.00104	1.00	47.40	-0.09	-1.3	-4.46E-04	-8.676E-02	0.13	0.009
242.82	46.90	0.00000	0.00000	0.00000	13.55	0.47849	0.47849	0.00208	0.00208	1.00	46.40	0.17	2.5	8.93E-04	1.735E-01	0.13	0.009
243.82	45.90	0.00000	0.00000	0.00000	13.49	0.47642	0.47642	0.00104	0.00104	1.00	45.40	0.09	1.3	4.46E-04	8.676E-02	0.13	0.009
244.82	44.90	0.00000	0.00000	0.00000	13.46	0.47538	0.47538	0.00035	0.00035	1.00	44.40	0.03	0.4	1.49E-04	2.892E-02	0.13	0.009
245.82	43.90	0.00000	0.00000	0.00000	13.45	0.47503	0.47503	0.00069	0.00069	1.00	43.40	0.06	0.8	2.98E-04	5.784E-02	0.13	0.009
246.82	42.90	0.00000	0.00000	0.00000	13.43	0.47434	0.47434	0.47434	0.47434	27.13	29.33	1.46	21.3	7.52E-03	3.966E+01	0.13	0.009
273.95	15.77	0.00000	0.00000	created date	0.00	0.00000	0.00000										

233.95	Top of Screen Depth from TOC (ft)		
273.95	Bottom of Screen Depth from TOC (ft)		*Filter pack:*
40.00	Screen Length (ft)	0.254	Do (m)
289.72	TOC Elevation (ft)	0.152	Di (m)
0.871	T pump (ft2/min)	0.032	Area (m^2)
86	Formation thickness (ft)	5.08	Thickness (cm)
14.6	K pump (ft/d)	100	Conductivity, K_{gp} (m/d) FX-50
5.14E-03	K pump (cm/s)		*EBF:*
		0.178	L_{EBF} (m)
			Bypass flow:
		0.079	ΔL (m)
		0.257	L (m)

QP (ft3/min) 0.47845   40.00 b (ft)
QP (L/min) 13.55
uncorr QP 13.55

Avg K_i/K_{bar} 1.000000
(Should be exactly 1)

Table 16 Hydraulic conductivity profile and bypass flow estimate for RPT-30PZ.

(1)	(2)	(3)	(4)	(5)	(6)	(7)	(8)	(9)	(10) Adjusted?	(11)	(12)	(13)	(14)	(15)	(16)	(17)	(18)
Depth Below TOC (ft)	Elevation (ft-msl)	Ambient Flow (L/min)	Ambient Flow, q (ft³/min)	Differential Ambient Flow, Δq_i (ft³/min)	Pump Induced Flow (L/min)	Pump Induced Flow, Q (ft³/min)	Net Pumping Flow, Q - q (ft³/min)	Differential Net Flow, $\Delta(Q_i - q_i)$ (ft³/min)	Differential Net Flow $\Delta(Q_i - q_i)$ (ft³/min)	Layer Thickness Δz_i (ft)	Mid-point Elevation (ft)	$K_i/K_{bar}=$ $b(\Delta Q_i-\Delta q_i)/(Q_P\Delta z_i)$	K_i (ft/d)	K_i (cms/s)	Check $\Delta z{*}K_i/K_{bar}$	Estimated bypass flow (L/min)	Estimated bypass flow ratio (Q_{bp}/Q_{EBF})
27.47	262.19	0.00000	0.00000	0.00000													
28.30	261.36	0.00000	0.00000	0.00000	2.10	0.07415	0.07415	0.01285	0.01285	3.17	259.78	1.60	2.8	1.00E-03	5.085E+00	0.05	0.026
28.47	261.19	-0.00078	-0.00003	0.00003													
29.47	260.19	-0.00157	-0.00006	0.00006													
30.47	259.19	-0.00314	-0.00011	-0.00003													
31.47	258.19	-0.00235	-0.00008	0.00011	1.73	0.06121	0.06130	-0.00395	-0.00395	1.00	257.69	-1.56	-2.8	-9.79E-04	-1.565E+00	0.04	0.023
32.47	257.19	-0.00549	-0.00019	0.00008	1.84	0.06506	0.06525	0.00025	0.00025	1.00	256.69	0.10	0.2	6.28E-05	1.004E-01	0.04	0.023
33.47	256.19	-0.00784	-0.00028	-0.00003	1.83	0.06472	0.06500	-0.00093	-0.00093	1.00	255.69	-0.37	-0.7	-2.29E-04	-3.666E-01	0.04	0.023
34.47	255.19	-0.00705	-0.00025	0.00003	1.86	0.06567	0.06592	0.00059	0.00059	1.00	254.69	0.23	0.4	1.46E-04	2.334E-01	0.04	0.024
35.47	254.19	-0.00784	-0.00025	-0.00003	1.84	0.06506	0.06533	-0.00410	-0.00410	1.00	253.69	-1.62	-2.9	-1.01E-03	-1.622E+00	0.04	0.023
36.47	253.19	-0.00705	-0.00025	0.00017	1.96	0.06919	0.06943	-0.00008	-0.00008	1.00	252.69	-0.03	-0.1	-2.02E-05	-3.234E-02	0.05	0.025
37.47	252.19	-0.01176	-0.00042	0.00000	1.96	0.06910	0.06952	-0.00138	-0.00138	1.00	251.69	-0.54	-1.0	-3.41E-04	-5.447E-01	0.05	0.024
38.47	251.19	-0.01176	-0.00042	0.00011	2.00	0.07048	0.07089	0.00542	0.00542	1.00	250.69	2.15	3.8	1.34E-03	2.145E+00	0.05	0.025
39.47	250.19	-0.01489	-0.00053	0.00017	1.84	0.06495	0.06547	0.00127	0.00127	1.00	249.69	0.50	0.9	3.13E-04	5.006E-01	0.04	0.023
40.47	249.19	-0.01959	-0.00069	0.00011	1.80	0.06351	0.06421	0.00267	0.00267	1.00	248.69	1.05	1.9	6.60E-04	1.055E+00	0.04	0.023
41.47	248.19	-0.02273	-0.00080	0.00025	1.72	0.06074	0.06154	0.00211	0.00211	1.00	247.69	0.83	1.5	5.21E-04	8.332E-01	0.04	0.022
42.47	247.19	-0.02978	-0.00105	0.00006	1.65	0.05838	0.05943	-0.00078	-0.00078	1.00	246.69	-0.31	-0.6	-1.94E-04	-3.102E-01	0.04	0.022
43.47	246.19	-0.03135	-0.00111	0.00017	1.67	0.05911	0.06022	-0.00087	-0.00087	1.00	245.69	-0.34	-0.6	-2.15E-04	-3.430E-01	0.04	0.022
44.47	245.19	-0.03605	-0.00127	0.00014	1.69	0.05981	0.06108	0.00042	0.00042	1.00	244.69	0.17	0.3	1.05E-04	1.671E-01	0.04	0.022
45.47	244.19	-0.03997	-0.00141	0.00003	1.68	0.05925	0.06066	0.00081	0.00081	1.00	243.69	0.32	0.6	2.01E-04	3.218E-01	0.04	0.022
46.47	243.19	-0.04075	-0.00144	0.00017	1.65	0.05841	0.05985	0.00062	0.00062	1.00	242.69	0.24	0.4	1.53E-04	2.448E-01	0.04	0.022
47.47	242.19	-0.04545	-0.00160	0.00039	1.63	0.05762	0.05923	0.00281	0.00281	1.00	241.69	1.11	2.0	6.95E-04	1.110E+00	0.04	0.022
48.47	241.19	-0.05642	-0.00199	0.00039	1.54	0.05443	0.05642	0.00247	0.00247	1.00	240.69	0.98	1.7	6.11E-04	9.766E-01	0.03	0.021
49.47	240.19	-0.06739	-0.00238	0.00025	1.46	0.05157	0.05395	0.00140	0.00140	1.00	239.69	0.55	1.0	3.47E-04	5.547E-01	0.03	0.020
50.47	239.19	-0.07444	-0.00263	0.00022	1.41	0.04992	0.05255	0.00123	0.00123	1.00	238.69	0.49	0.9	3.05E-04	4.880E-01	0.03	0.020
51.47	238.19	-0.08071	-0.00285	0.00000	1.37	0.04847	0.05132	0.00238	0.00238	1.00	237.69	0.94	1.7	5.88E-04	9.403E-01	0.03	0.019
52.47	237.19	-0.08071	-0.00285	-0.00058	1.31	0.04609	0.04894	0.01560	0.01560	1.00	236.69	6.17	10.9	3.86E-03	6.170E+00	0.02	0.019
53.47	236.19	-0.06426	-0.00227	-0.00028	0.88	0.03108	0.03334	0.00938	0.00938	1.00	235.69	3.71	6.6	2.32E-03	3.711E+00	0.01	0.015
54.47	235.19	-0.05642	-0.00199	-0.00014	0.62	0.02197	0.02396	0.00136	0.00136	1.00	234.69	0.54	1.0	3.37E-04	5.387E-01	0.01	0.013
55.47	234.19	-0.05250	-0.00185	-0.00011	0.59	0.02075	0.02260	0.00281	0.00281	1.00	233.69	1.11	2.0	6.95E-04	1.110E+00	0.01	0.012
56.47	233.19	-0.04937	-0.00174	-0.00174	0.51	0.01805	0.01980	0.01938	0.01938	1.00	232.69	7.67	13.6	4.80E-03	7.667E+00	0.01	0.012
57.47	232.19	0.00000	0.00000		0.01	0.00042	0.00042										

17.47	Top of Screen Depth from TOC (ft)		*Filter pack:*	QP (ft3/min) 0.07374
57.47	Bottom of Screen Depth from TOC (ft)	0.203	Do (m)	QP (L/min) 2.09
30.85	Saturated Screen Length (ft)	0.051	Di (m)	uncorr QP 2.09
289.66	TOC Elevation (ft)	0.030	Area (m^2)	
0.038	T pump (ft2/min)	7.62	Thickness (cm)	
1.77	K pump (ft/d)	100	Conductivity, K_{gp} (m/d) FX-50	
6.26E-04	K pump (cm/s)		*EBF:*	
26.62	Water Level Depth from TOC (ft) - 12/20/99	0.178	L_{EBF} (m)	
28.30	Water Level Depth from TOC (ft) - EBF dynamic testing		*Bypass flow:*	
		0.111	ΔL (m)	
		0.289	L (m)	

29.17 b (ft)

Avg K/K_bar 1.000000
(Should be exactly 1)

Table 17   Post-test check for quasi-steady flow conditions at RPC-2PR.

Post-test check for valid EBF application (pseudo-steady state & minimal bypass flow)

Site   RPC-2PR

Formation properties

		Ruud and Kabala (1996) pseudo-steady criterion			
estimated K (ft/d)	25	1.0E+03	Non-dimensional time, t_D		
		Diffusivity	Time, t	Time, t	Time, t	Time, t
estimated S_s (1/ft)	2.5E-04	contrast	(d)	(hr)	(min)	(s)
thickness b (ft)	40	1:1	0.0	0.0	0.6	37.5
estimated T (ft²/d)	1000	10:1	0.0	0.1	3.4	206.3
estimated S	1.0E-02	100:1	0.0	0.5	31.6	1893.8
diffusivity ν = T/S (ft²/d)	1.0E+05	1000:1	0.2	5.2	312.8	18768.8

Well properties

		Molz and others (1989) pseudo-steady criterion				
borehole diameter (in)	10	*(but using assumed influence radius per personal comm.)*				
Casing diameter (in)	4	1.0E+02	Non-dimensional time, t_D			
		Influence	Time, t	Time, t	Time, t	Time, t
Borehole radius (in)	5	radius, r (ft)	(d)	(hr)	(min)	(s)
Casing radius (in)	2	1	0.0	0.0	0.4	21.6
Borehole radius (m)	0.1270	2	0.0	0.0	1.4	86.4
Casing radius (m)	0.0508	5	0.0	0.2	9.0	540.0
Annulus area (m²)	0.043	10	0.0	0.6	36.0	2160.0
Annulus thickness (cm)	7.62	20	0.1	2.4	144.0	8640.0
Filter pack conductivity (m/d)	100					

Rehfeldt and others (1989) and Flach criteria

Non-dimensional time, t_D	Time, t (d)	Time, t (hr)	Time, t (min)	Time, t (s)	
4.0E+02	0.0	0.0	0.3	15.0	10:1
4.0E+03	0.0	0.0	2.5	150.0	100:1
4.0E+04	0.0	0.4	25.0	1500.0	r/b<0.125
1.0E+06	0.4	10.4	625.0	37500.0	long time

EBF properties

L_{EBF} (m)   0.178

Bypass properties

ΔL (m)   0.111
L (m)   0.289

Bypass flow estimate

Pumping rate, QP (L/min)	Pumping rate, QP (gal/min)	*1/2" EBF* Bypass (L/min)	Ratio	*1" EBF* Bypass (L/min)	Ratio
0.2	0.05	0.00	1.3%	0.00	0.1%
0.5	0.13	0.01	1.6%	0.00	0.1%
1	0.26	0.02	2.3%	0.00	0.1%
2	0.53	0.07	3.5%	0.00	0.2%
5	1.32	0.36	7.2%	0.02	0.4%
10	2.64	1.33	13.3%	0.08	0.8%
20	5.28	5.12	25.6%	0.32	1.6%
4.3	test block	0.27	6.3%	0.02	0.4%

Table 18   Post-test check for quasi-steady flow conditions at RPC-3PW.

Post-test check for valid EBF application (pseudo-steady state & minimal bypass flow)

Site   RPC-3PW

Formation properties

estimated K (ft/d)	25
estimated S_s (1/ft)	1.0E-04
thickness b (ft)	101
estimated T (ft^2/d)	2525
estimated S	1.0E-02
diffusivity v = T/S (ft^2/d)	2.5E+05

Ruud and Kabala (1996) pseudo-steady criterion

1.0E+03   Non-dimensional time, t_D

Diffusivity contrast	Time, t (d)	Time, t (hr)	Time, t (min)	Time, t (s)
1:1	0.0	0.0	0.3	15.0
10:1	0.0	0.0	1.4	82.5
100:1	0.0	0.2	12.6	757.5
1000:1	0.1	2.1	125.1	7507.5

Well properties

borehole diameter (in)	10
Casing diameter (in)	4
Borehole radius (in)	5
Casing radius (in)	2
Borehole radius (m)	0.1270
Casing radius (m)	0.0508
Annulus area (m^2)	0.043
Annulus thickness (cm)	7.62
Filter pack conductivity (m/d)	100

Molz and others (1989) pseudo-steady criterion
(but using assumed influence radius per personal comm.)

1.0E+02   Non-dimensional time, t_D

Influence radius, r (ft)	Time, t (d)	Time, t (hr)	Time, t (min)	Time, t (s)
1	0.0	0.0	0.1	8.6
2	0.0	0.0	0.6	34.6
5	0.0	0.1	3.6	216.0
10	0.0	0.2	14.4	864.0
20	0.0	1.0	57.6	3456.0

Rehfeldt and others (1989) and Flach criteria

Non-dimensional time, t_D	Time, t (d)	Time, t (hr)	Time, t (min)	Time, t (s)	
4.0E+02	0.0	0.0	0.1	6.0	10:1
4.0E+03	0.0	0.0	1.0	60.0	100:1
4.0E+04	0.0	0.2	10.0	600.0	r/b<0.125
1.0E+06	0.2	4.2	250.0	15000.0	long time

EBF properties

L_{EBF} (m)	0.178

Bypass properties

ΔL (m)	0.111
L (m)	0.289

Bypass flow estimate

Pumping rate, QP (L/min)	Pumping rate, QP (gal/min)	1/2" EBF Bypass (L/min)	Ratio	1" EBF Bypass (L/min)	Ratio
0.2	0.05	0.00	1.3%	0.00	0.1%
0.5	0.13	0.01	1.6%	0.00	0.1%
1	0.26	0.02	2.3%	0.00	0.1%
2	0.53	0.07	3.5%	0.00	0.2%
5	1.32	0.36	7.2%	0.02	0.4%
10	2.64	1.33	13.3%	0.08	0.8%
20	5.28	5.12	25.6%	0.32	1.6%
5.34	test block	0.41	7.6%	0.03	0.5%
14.56	test block	2.76	18.9%	0.17	1.2%

Table 19   Post-test check for quasi-steady flow conditions at RPT-2PW.

Post-test check for valid EBF application (pseudo-steady state & minimal bypass flow)

Site   RPT-2PW

Formation properties

		Ruud and Kabala (1996) pseudo-steady criterion			
estimated K (ft/d)	2.3	1.0E+03	Non-dimensional time, t_D		

		Diffusivity contrast	Time, t (d)	Time, t (hr)	Time, t (min)	Time, t (s)
estimated S_s (1/ft)	1.5E-05	1:1	0.0	0.0	0.6	35.2
thickness b (ft)	15	10:1	0.0	0.1	3.2	193.7
estimated T (ft^2/d)	34.5	100:1	0.0	0.5	29.6	1778.5
estimated S	2.3E-04	1000:1	0.2	4.9	293.8	17626.3
diffusivity ν = T/S (ft^2/d)	1.5E+05					

Well properties

		Molz and others (1989) pseudo-steady criterion				
borehole diameter (in)	12	*(but using assumed influence radius per personal comm.)*				
Casing diameter (in)	4	1.0E+02	Non-dimensional time, t_D			

		Influence radius, r (ft)	Time, t (d)	Time, t (hr)	Time, t (min)	Time, t (s)
Borehole radius (in)	6	1	0.0	0.0	0.2	14.1
Casing radius (in)	2	2	0.0	0.0	0.9	56.3
Borehole radius (m)	0.1524	5	0.0	0.1	5.9	352.2
Casing radius (m)	0.0508	10	0.0	0.4	23.5	1408.7
Annulus area (m^2)	0.065	20	0.1	1.6	93.9	5634.8
Annulus thickness (cm)	10.16					
Filter pack conductivity (m/d)	100					

Rehfeldt and others (1989) and Flach criteria

Non-dimensional time, t_D	Time, t (d)	Time, t (hr)	Time, t (min)	Time, t (s)	
4.0E+02	0.0	0.0	0.2	14.1	10:1
4.0E+03	0.0	0.0	2.3	140.9	100:1
4.0E+04	0.0	0.4	23.5	1408.7	r/b<0.125
1.0E+06	0.4	9.8	587.0	35217.4	long time

EBF properties

L_{EBF} (m)   0.178

Bypass properties

ΔL (m)   0.143
L (m)   0.320

Bypass flow estimate

		1/2" EBF		*1" EBF*	
Pumping rate, QP (L/min)	Pumping rate, QP (gal/min)	Bypass (L/min)	Ratio	Bypass (L/min)	Ratio
0.2	0.05	0.00	1.7%	0.00	0.1%
0.5	0.13	0.01	2.2%	0.00	0.1%
1	0.26	0.03	3.1%	0.00	0.2%
2	0.53	0.10	4.8%	0.01	0.3%
5	1.32	0.49	9.8%	0.03	0.6%
10	2.64	1.83	18.3%	0.11	1.1%
20	5.28	7.03	35.2%	0.44	2.2%
4.01	test block	0.33	8.2%	0.02	0.5%

Table 20   Post-test check for quasi-steady flow conditions at RPT-3PW.

Post-test check for valid EBF application (pseudo-steady state & minimal bypass flow)

Site   RPT-3PW

Formation properties

estimated K (ft/d)	2
estimated S_s (1/ft)	5.0E-06
thickness b (ft)	74
estimated T (ft^2/d)	148
estimated S	3.7E-04
diffusivity v = T/S (ft^2/d)	4.0E+05

Ruud and Kabala (1996) pseudo-steady criterion

1.0E+03   Non-dimensional time, t_D

Diffusivity contrast	Time, t (d)	Time, t (hr)	Time, t (min)	Time, t (s)
1:1	0.0	0.0	0.2	9.4
10:1	0.0	0.0	0.9	51.6
100:1	0.0	0.1	7.9	473.4
1000:1	0.1	1.3	78.2	4692.2

Well properties

borehole diameter (in)	10
Casing diameter (in)	4
Borehole radius (in)	5
Casing radius (in)	2
Borehole radius (m)	0.1270
Casing radius (m)	0.0508
Annulus area (m^2)	0.043
Annulus thickness (cm)	7.62
Filter pack conductivity (m/d)	100

Molz and others (1989) pseudo-steady criterion
(but using assumed influence radius per personal comm.)

1.0E+02   Non-dimensional time, t_D

Influence radius, r (ft)	Time, t (d)	Time, t (hr)	Time, t (min)	Time, t (s)
1	0.0	0.0	0.1	5.4
2	0.0	0.0	0.4	21.6
5	0.0	0.0	2.3	135.0
10	0.0	0.2	9.0	540.0
20	0.0	0.6	36.0	2160.0

Rehfeldt and others (1989) and Flach criteria

Non-dimensional time, t_D	Time, t (d)	Time, t (hr)	Time, t (min)	Time, t (s)	
4.0E+02	0.0	0.0	0.1	3.8	10:1
4.0E+03	0.0	0.0	0.6	37.5	100:1
4.0E+04	0.0	0.1	6.3	375.0	r/b<0.125
1.0E+06	0.1	2.6	156.3	9375.0	long time

EBF properties

L_{EBF} (m)	0.178

Bypass properties

ΔL (m)	0.111
L (m)	0.289

Bypass flow estimate

Pumping rate, QP (L/min)	Pumping rate, QP (gal/min)	*1/2" EBF* Bypass (L/min)	Ratio	*1" EBF* Bypass (L/min)	Ratio
0.2	0.05	0.00	1.3%	0.00	0.1%
0.5	0.13	0.01	1.6%	0.00	0.1%
1	0.26	0.02	2.3%	0.00	0.1%
2	0.53	0.07	3.5%	0.00	0.2%
5	1.32	0.36	7.2%	0.02	0.4%
10	2.64	1.33	13.3%	0.08	0.8%
20	5.28	5.12	25.6%	0.32	1.6%
14.16	test block	2.61	18.4%	0.16	1.2%

Table 21   Post-test check for quasi-steady flow conditions at RPT-4PW.

Post-test check for valid EBF application (pseudo-steady state & minimal bypass flow)

Site   RPT-4PW

Formation properties

		Ruud and Kabala (1996) pseudo-steady criterion			
estimated K (ft/d)	14.6	1.0E+03	Non-dimensional time, t_D		
		Diffusivity	Time, t	Time, t	Time, t	Time, t
estimated S_s (1/ft)	1.6E-05	contrast	(d)	(hr)	(min)	(s)
thickness b (ft)	86	1:1	0.0	0.0	0.1	4.1
estimated T (ft^2/d)	1255.6	10:1	0.0	0.0	0.4	22.6
estimated S	1.4E-03	100:1	0.0	0.1	3.5	207.5
diffusivity ν = T/S (ft^2/d)	9.1E+05	1000:1	0.0	0.6	34.3	2056.8

Well properties

		Molz and others (1989) pseudo-steady criterion				
borehole diameter (in)	10	*(but using assumed influence radius per personal comm.)*				
Casing diameter (in)	6	1.0E+02	Non-dimensional time, t_D			
		Influence	Time, t	Time, t	Time, t	Time, t
Borehole radius (in)	5	radius, r (ft)	(d)	(hr)	(min)	(s)
Casing radius (in)	3	1	0.0	0.0	0.0	2.4
Borehole radius (m)	0.1270	2	0.0	0.0	0.2	9.5
Casing radius (m)	0.0762	5	0.0	0.0	1.0	59.2
Annulus area (m^2)	0.032	10	0.0	0.1	3.9	236.7
Annulus thickness (cm)	5.08	20	0.0	0.3	15.8	946.8
Filter pack conductivity (m/d)	100					

Rehfeldt and others (1989) and Flach criteria

Non-dimensional time, t_D	Time, t (d)	Time, t (hr)	Time, t (min)	Time, t (s)	
4.0E+02	0.0	0.0	0.0	1.6	10:1
4.0E+03	0.0	0.0	0.3	16.4	100:1
4.0E+04	0.0	0.0	2.7	164.4	r/b<0.125
1.0E+06	0.0	1.1	68.5	4109.6	long time

EBF properties

L_{EBF} (m)   0.178

Bypass properties

ΔL (m)   0.079
L (m)   0.257

Bypass flow estimate

		1/2" EBF		***1" EBF***	
Pumping rate, QP (L/min)	Pumping rate, QP (gal/min)	Bypass (L/min)	Ratio	Bypass (L/min)	Ratio
0.2	0.05	0.00	1.1%	0.00	0.1%
0.5	0.13	0.01	1.4%	0.00	0.1%
1	0.26	0.02	1.9%	0.00	0.1%
2	0.53	0.06	3.0%	0.00	0.2%
5	1.32	0.31	6.1%	0.02	0.4%
10	2.64	1.14	11.4%	0.07	0.7%
20	5.28	4.38	21.9%	0.27	1.4%
13.55	test block	2.05	15.1%	0.13	0.9%

Table 22   Post-test check for quasi-steady flow conditions at RPT-30PZ.

Post-test check for valid EBF application (pseudo-steady state & minimal bypass flow)

Site   RPT-30PZ

Formation properties

		Ruud and Kabala (1996) pseudo-steady criterion			
estimated K (ft/d)	1.6	1.0E+03	Non-dimensional time, t_D		

		Diffusivity contrast	Time, t (d)	Time, t (hr)	Time, t (min)	Time, t (s)
estimated S_s (1/ft)	7.5E-05					
thickness b (ft)	34	1:1	0.0	0.0	1.9	112.5
estimated T (ft^2/d)	54.4	10:1	0.0	0.2	10.3	618.8
estimated S	2.6E-03	100:1	0.1	1.6	94.7	5681.3
diffusivity ν = T/S (ft^2/d)	2.1E+04	1000:1	0.7	15.6	938.4	56306.3

Well properties

Molz and others (1989) pseudo-steady criterion
(but using assumed influence radius per personal comm.)

			Non-dimensional time, t_D			
borehole diameter (in)	8	1.0E+02				
Casing diameter (in)	2	Influence radius, r (ft)	Time, t (d)	Time, t (hr)	Time, t (min)	Time, t (s)
Borehole radius (in)	4	1	0.0	0.0	1.7	101.3
Casing radius (in)	1	2	0.0	0.1	6.8	405.0
Borehole radius (m)	0.1016	5	0.0	0.7	42.2	2531.3
Casing radius (m)	0.0254	10	0.1	2.8	168.8	10125.0
Annulus area (m^2)	0.030	20	0.5	11.3	675.0	40500.0
Annulus thickness (cm)	7.62					
Filter pack conductivity (m/d)	100					

Rehfeldt and others (1989) and Flach criteria

		Non-dimensional time, t_D	Time, t (d)	Time, t (hr)	Time, t (min)	Time, t (s)	
EBF properties							
L_{EBF} (m)	0.178	4.0E+02	0.0	0.0	0.8	45.0	10:1
		4.0E+03	0.0	0.1	7.5	450.0	100:1
Bypass properties		4.0E+04	0.1	1.3	75.0	4500.0	r/b<0.125
ΔL (m)	0.111	1.0E+06	1.3	31.3	1875.0	#######	long time
L (m)	0.289						

Bypass flow estimate

Pumping rate, QP (L/min)	Pumping rate, QP (gal/min)	1/2" EBF Bypass (L/min)	Ratio	1" EBF Bypass (L/min)	Ratio
0.2	0.05	0.00	0.9%	0.00	0.1%
0.5	0.13	0.01	1.2%	0.00	0.1%
1	0.26	0.02	1.6%	0.00	0.1%
2	0.53	0.05	2.5%	0.00	0.2%
5	1.32	0.26	5.1%	0.02	0.3%
10	2.64	0.95	9.5%	0.06	0.6%
20	5.28	3.66	18.3%	0.23	1.1%
2.1	test block	0.05	2.6%	0.00	0.2%

Table 23   Summary of post-test checks for quasi-steady flow conditions.

SiteID	Ruud and Kabala (1996) with 100:1 diffusivity contrast	Ruud and Kabala (1996) with 10:1 diffusivity contrast	Rehfeldt and others (1989)	Approximate EBF start (min)	Approximate EBF finish (min)
RPC-2PR	32 min	3.4 min	2.5 min	30 min	2.5 hr
RPC-3PW - 1/2" EBF	13 min	1.4 min	1.0 min	15 min	2.5 hr
RPC-3PW - 1" EBF	14 min	1.4 min	1.0 min	15 min	2 hr
RPT-2PW	30 min	3.2 min	2.3 min	1 hr	2 hr
RPT-3PW	7.9 min	0.9 min	0.6 min	50 min	3 hr
RPT-4PW	3.5 min	0.4 min	0.3 min	20 min	1.5 hr
RPT-30PZ	1.6 hr	10 min	7.5 min	1 hr	2 hr
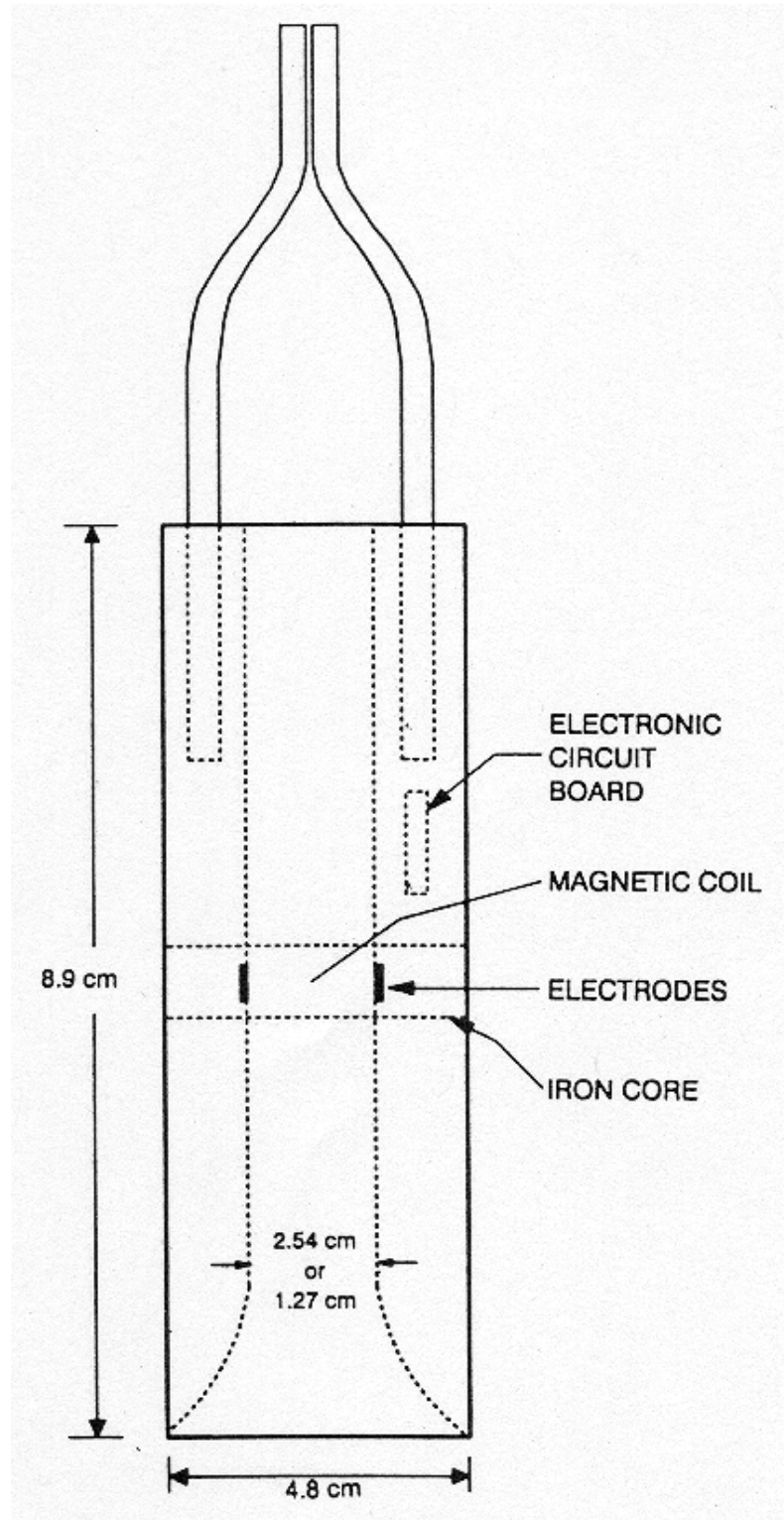
Figure 1   Schematic diagram of the Electromagnetic Borehole Flowmeter; reproduced from Molz and Young (1993).
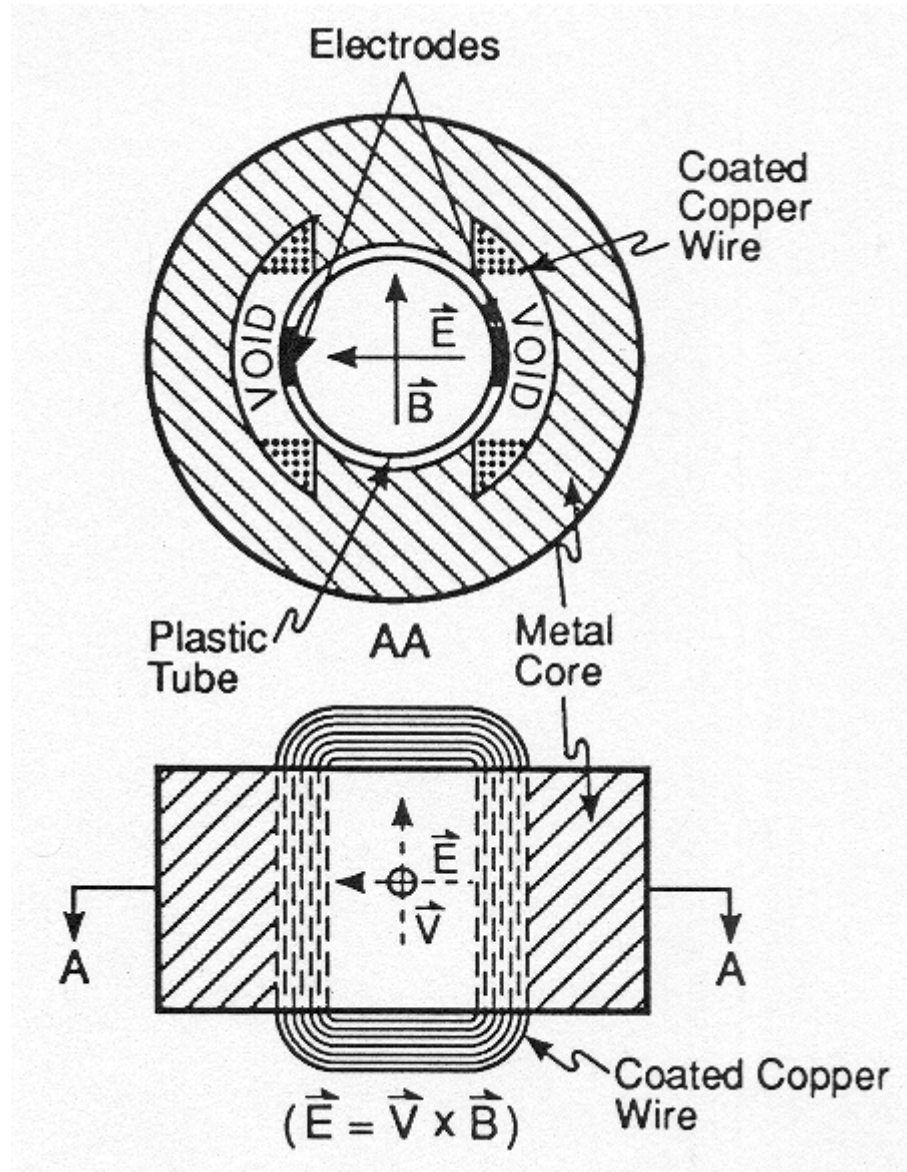
Figure 2   Electromagnetic Borehole Flowmeter (EBF) application of Faraday's Law of Induction; reproduced from Molz and Young (1993).
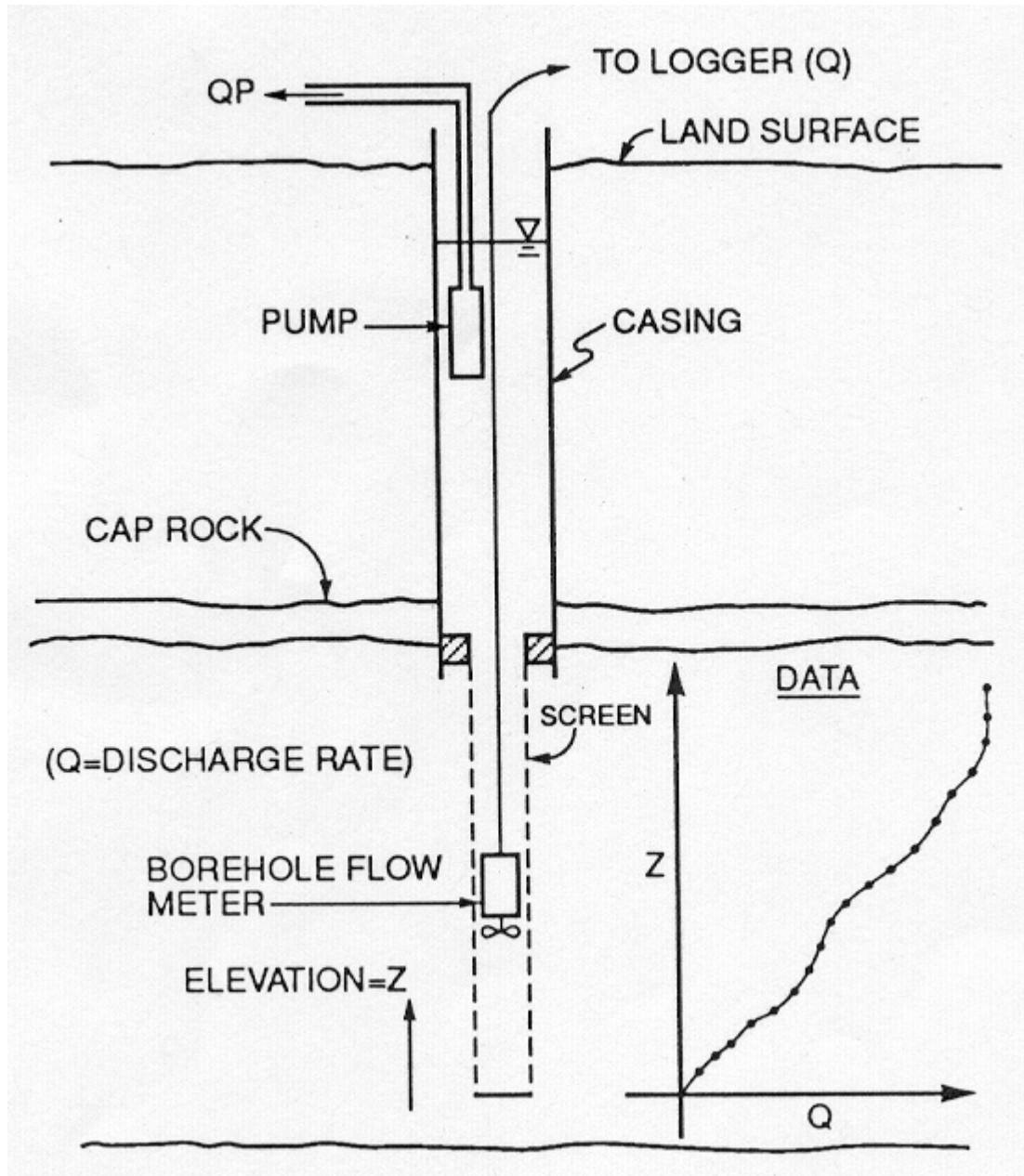
Figure 3   Schematic illustration of borehole flowmeter testing; reproduced from Molz and Young (1993).
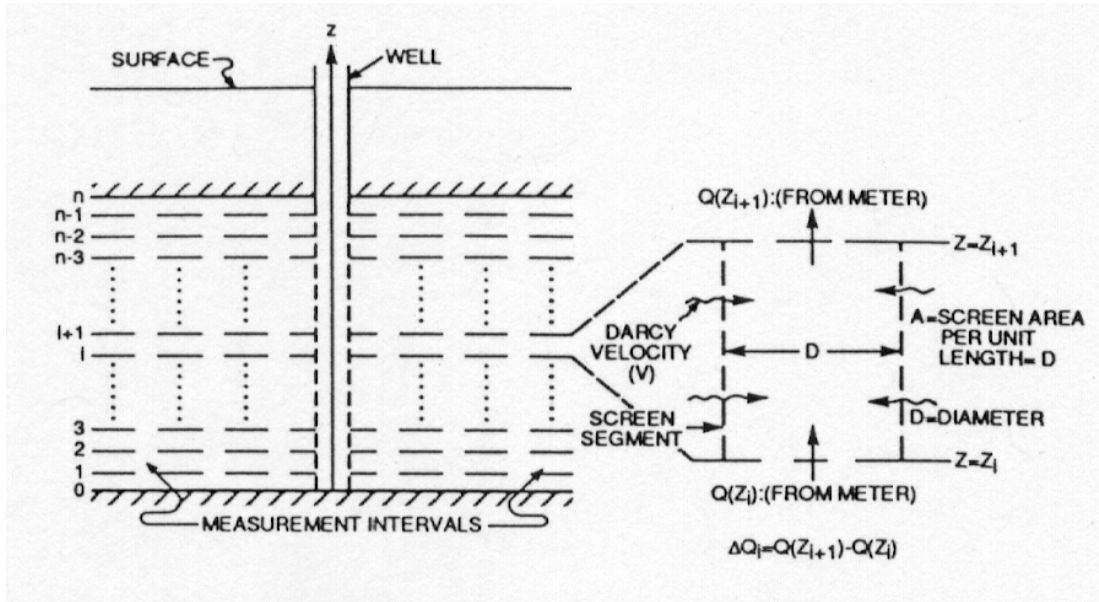
Figure 4   Basic geometry and analysis of borehole flowmeter data; reproduced from Molz and Young (1993).
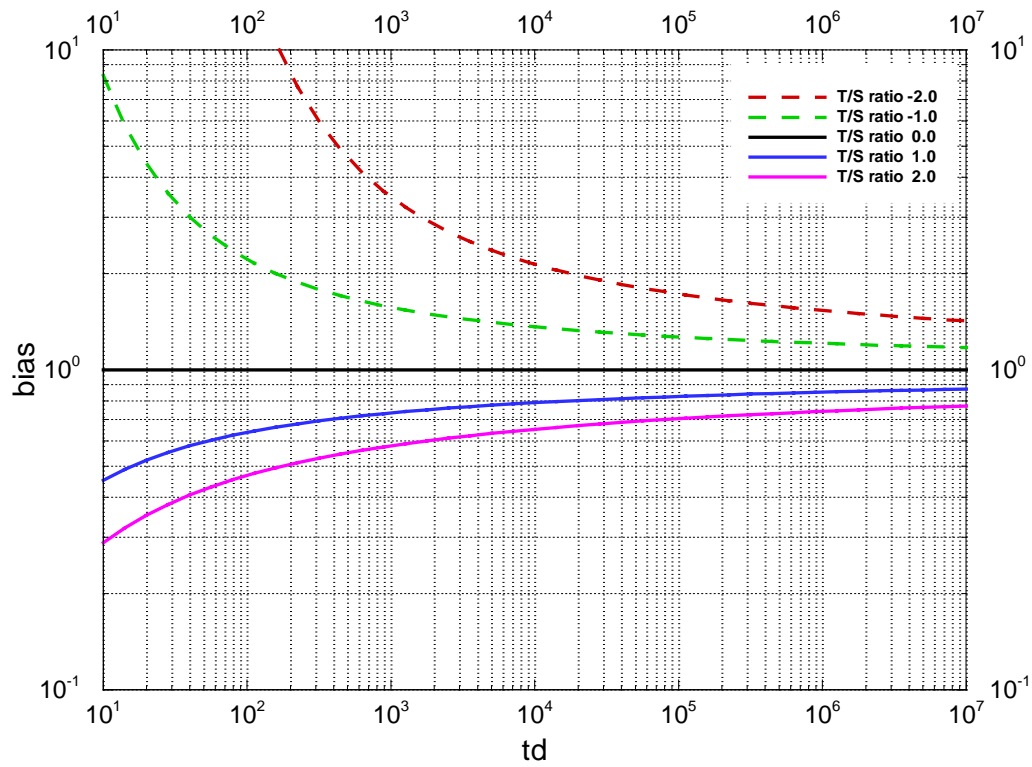
Figure 5   Systematic errors in borehole flowmeter estimation due to transient effects.

$$QP = Q + Q_m$$

Flow entering the well bore above the meter is driven by the observed drawdown, s, between the well radius, r_w, and the radius of influence, r_e.

Q_m

Q $b - z_i$

b

Flow entering the well bore below the meter is driven by the reduced drawdown, $s - h_m$, between the well radius, r_w, and the radius of influence, r_e.

Q_m z_i

r_w r_e
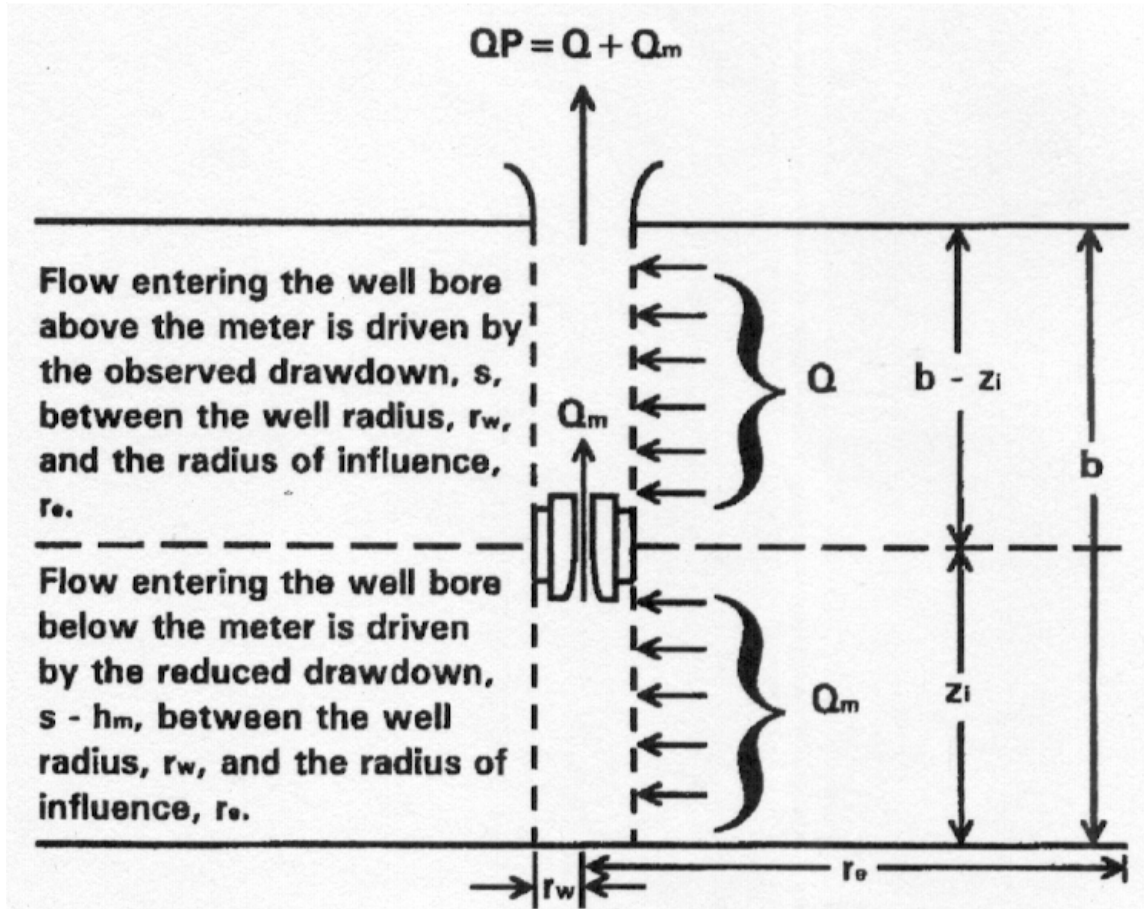
Figure 6   Head-loss-induced flow redistribution; reproduced from Dinwiddie and others (1999).
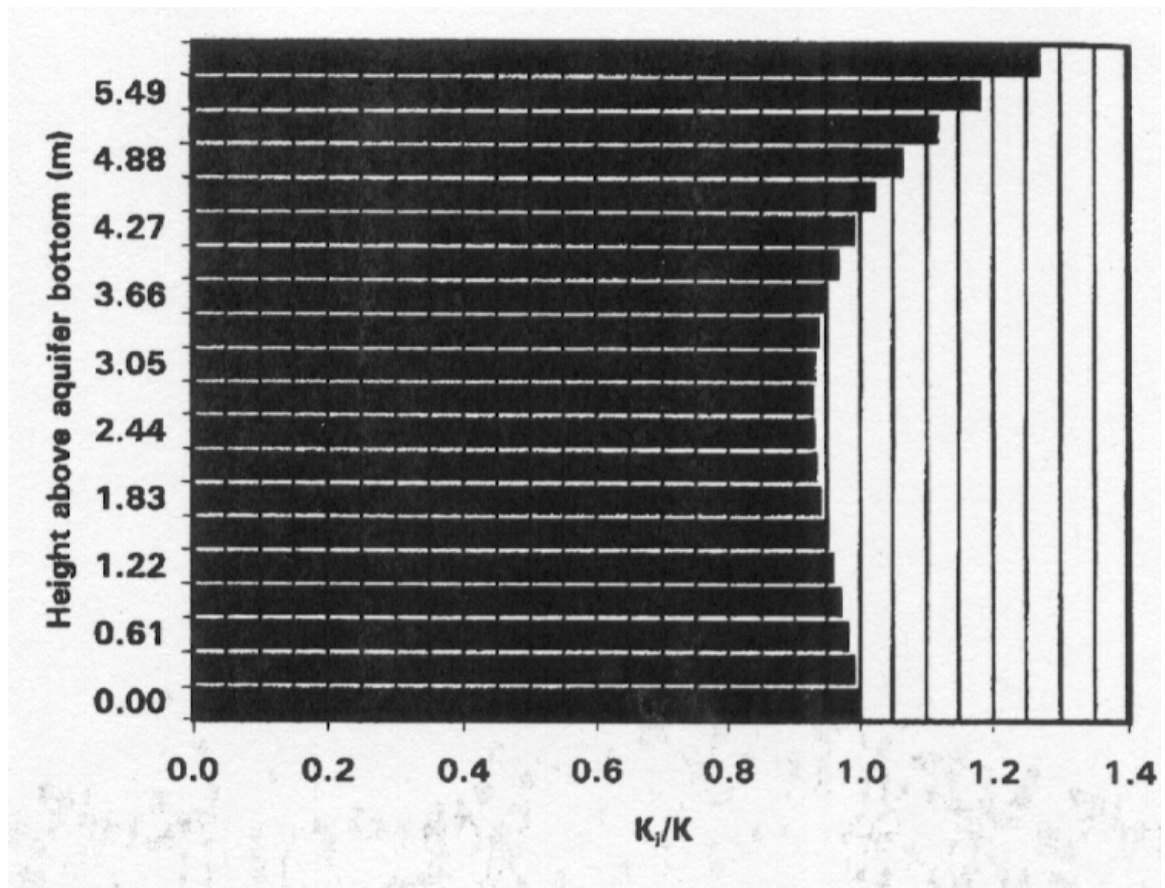
Figure 7   Effect of head-loss-induced flow redistribution for a 4" ID, 20 ft long, nonpacked, well screen; bar graph shows the calculated nondimensional hydraulic conductivity distribution when the true K is 9.1 m/day and the pumping rate is 5 L/min; reproduced from Dinwiddie and others (1999).
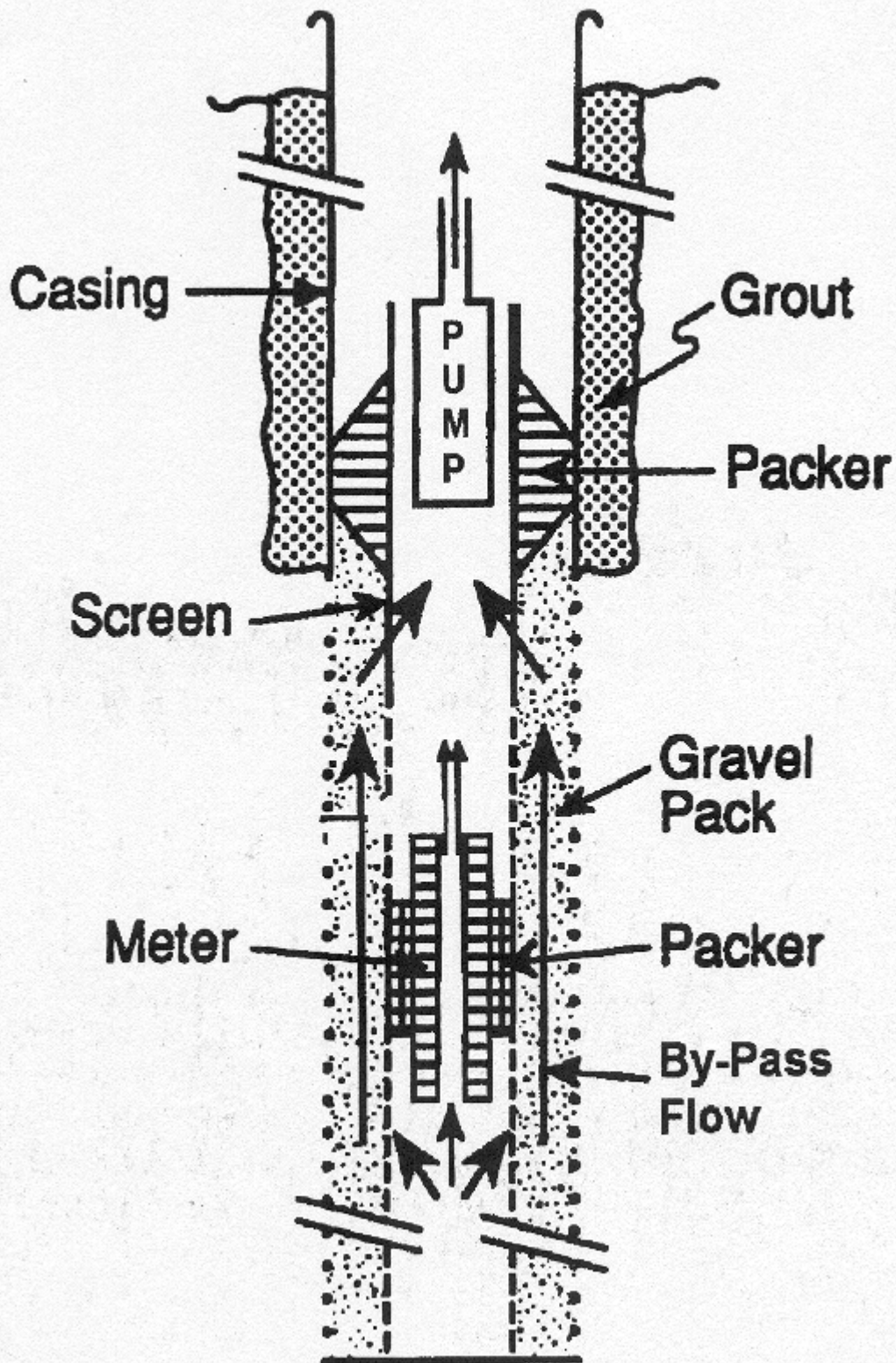
Figure 8   Bypass flow through filter pack induced by EBF head loss; reproduced from Dinwiddie and others (1999).
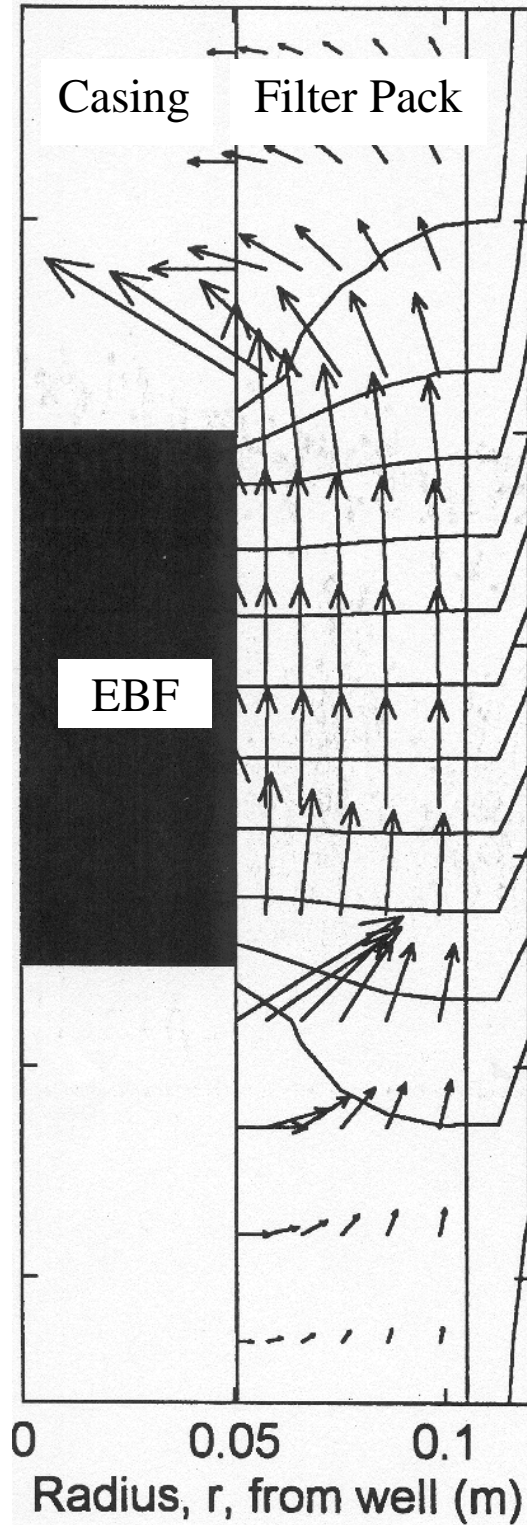
Figure 9   Bypass flow simulation; modified from Dinwiddie and others (1999).
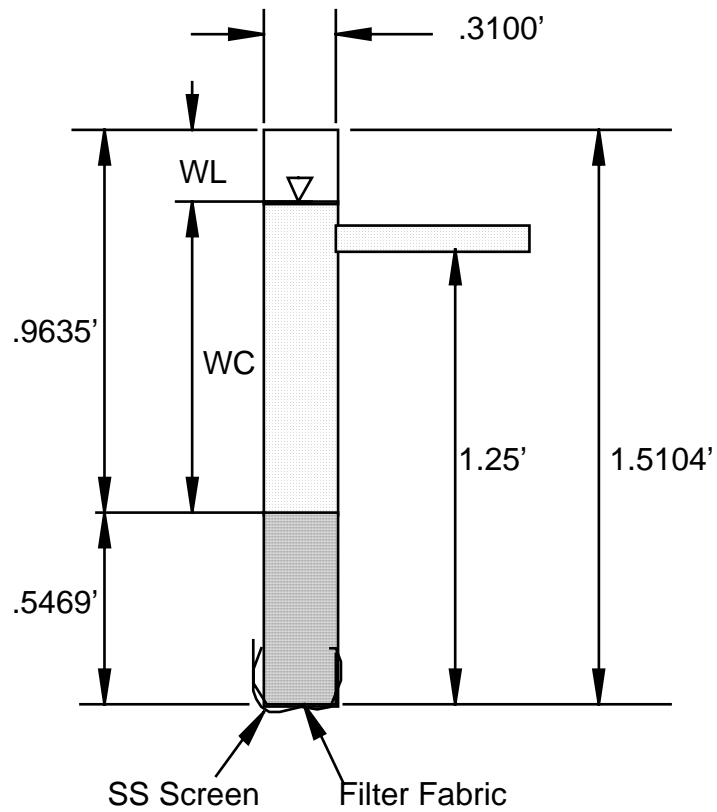
Figure 10   Constant-head permeameter design and dimensions.

Instrument Response .5" Probe Full Scale

$y = 0.0024x^2 + 0.7838x$
$R^2 = 1$
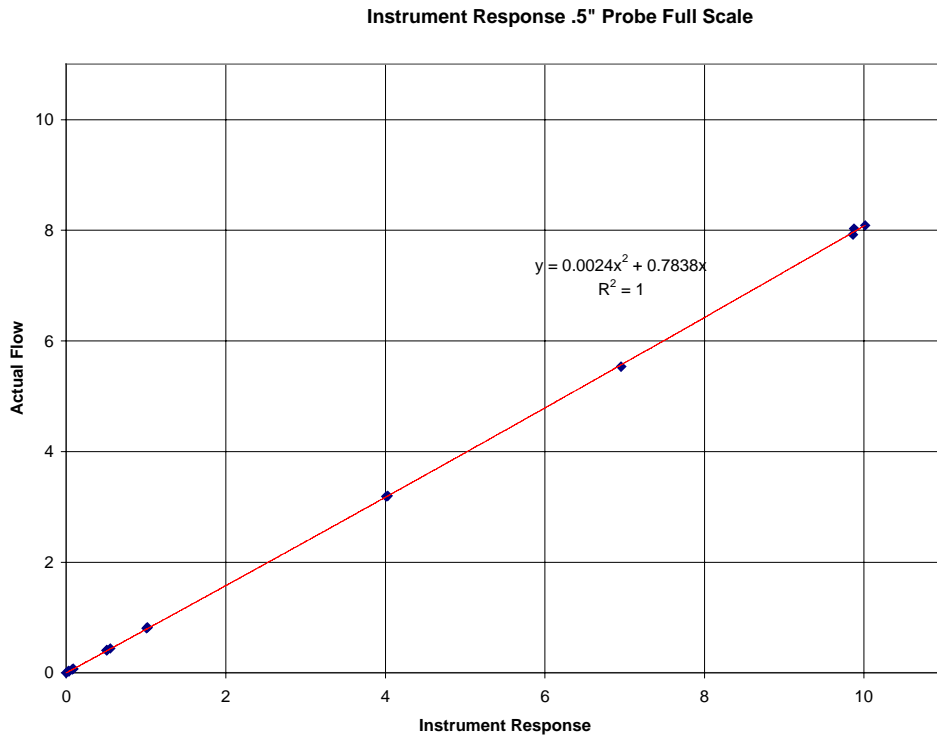
Figure 11   Calibration data and curve for the ½" ID EBF.

Instrument Response 1" Probe

$y = 0.9797x + 0.1097$
$R^2 = 0.9996$
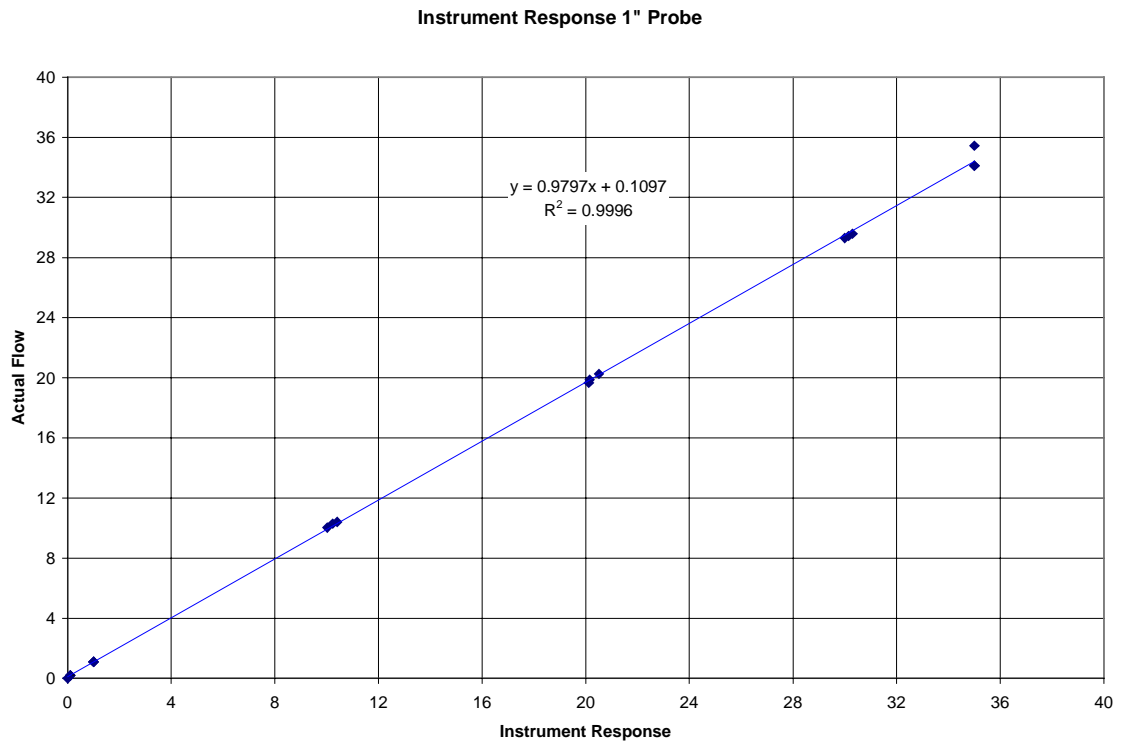
Figure 12   Calibration data and curve for the 1" ID EBF.
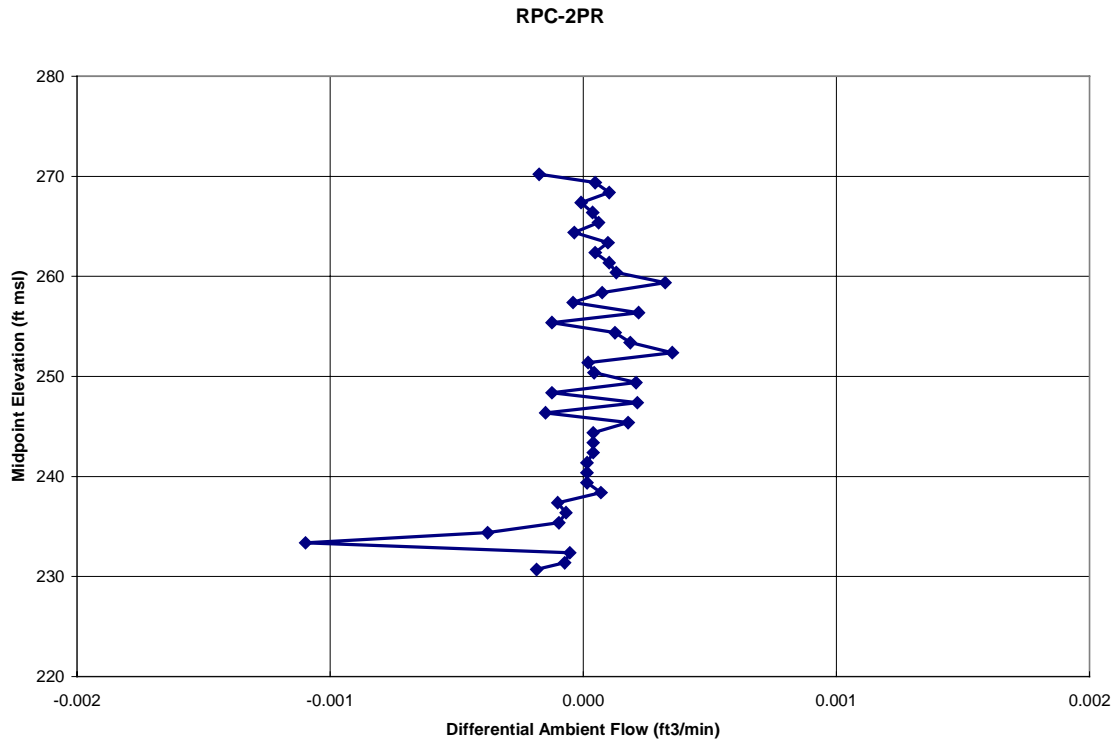
RPC-2PR

Figure 13   Ambient flow measurements for RPC-2PR.
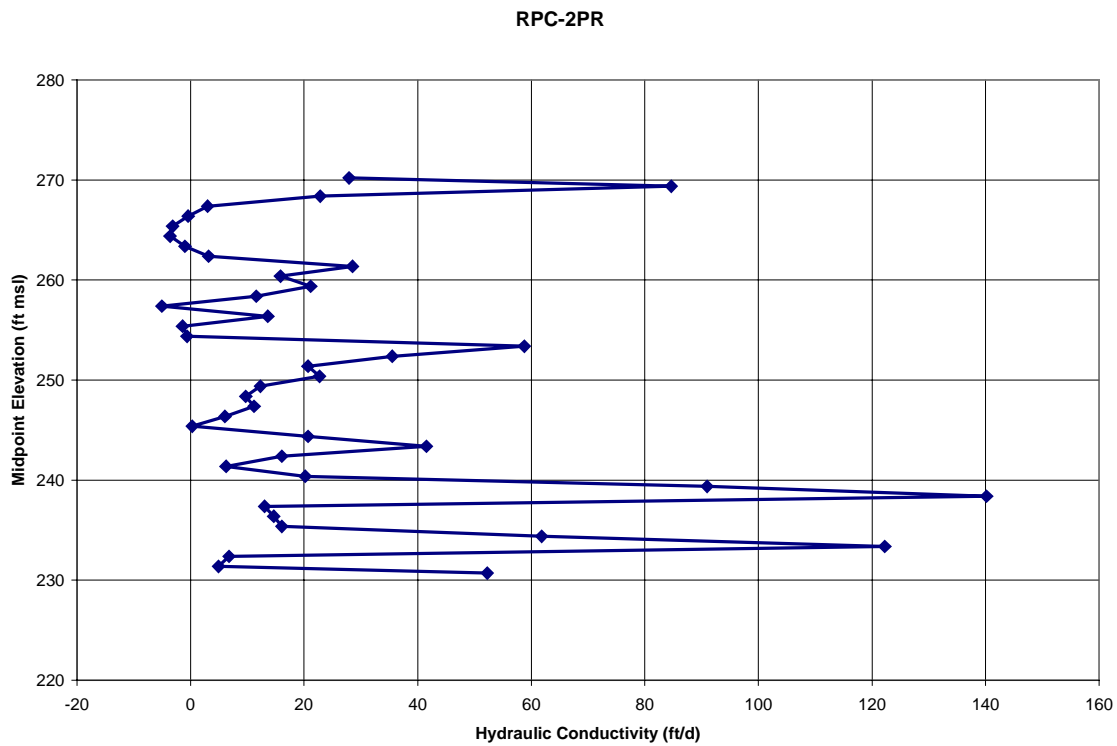
RPC-2PR

Figure 14   Estimated hydraulic conductivity variation for RPC-2PR.
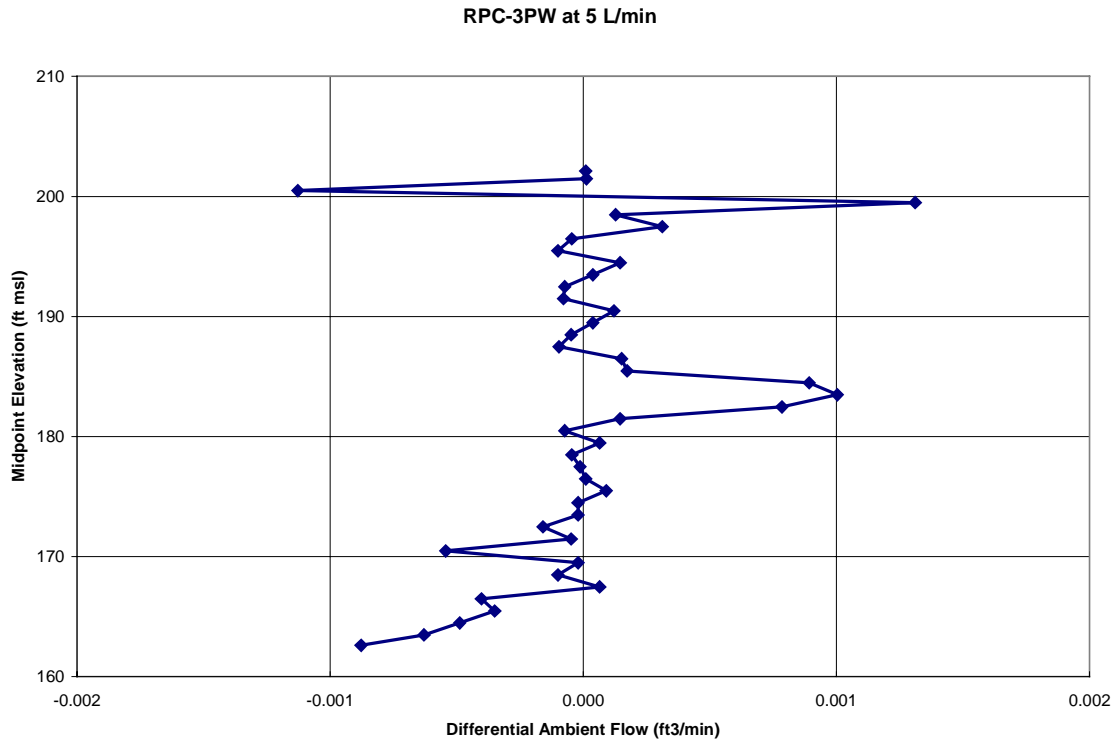
RPC-3PW at 5 L/min

Figure 15   Ambient flow measurements for RPC-3PW.

RPC-3PW at 5 and 15 L/min and 1 ft Increments
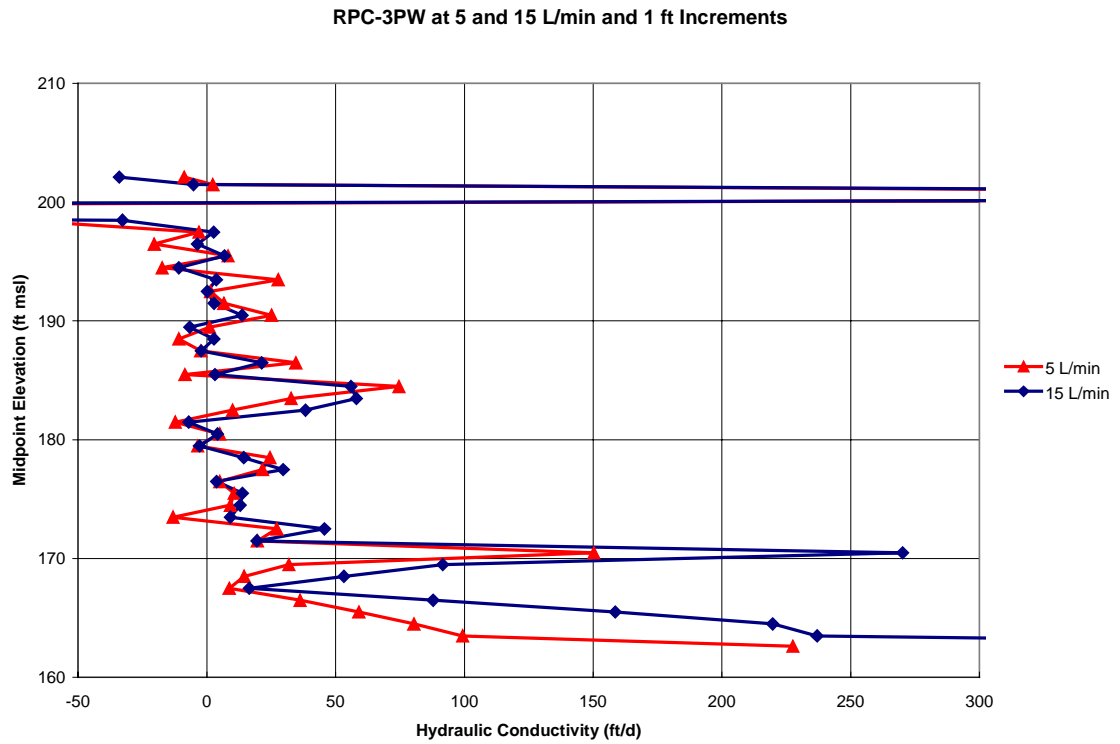
Figure 16   Estimated hydraulic conductivity variation for RPC-3PW at 1 ft intervals using the ½" and 1" ID EBFs.

RPC-3PW at 5 and 15 L/min and 5 ft Increments
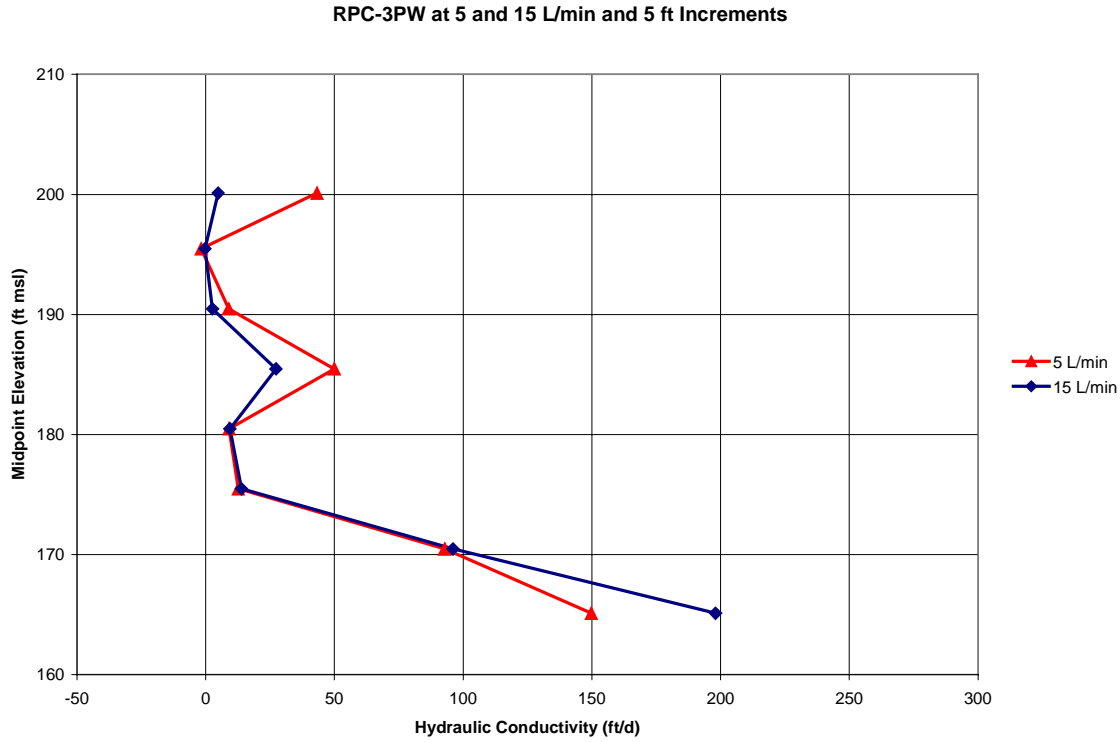
Figure 17   Estimated hydraulic conductivity variation for RPC-3PW at 5 ft intervals
                using the ½" and 1" ID EBFs.

RPC-3PW at 5 and 15 L/min and 10 ft Increments
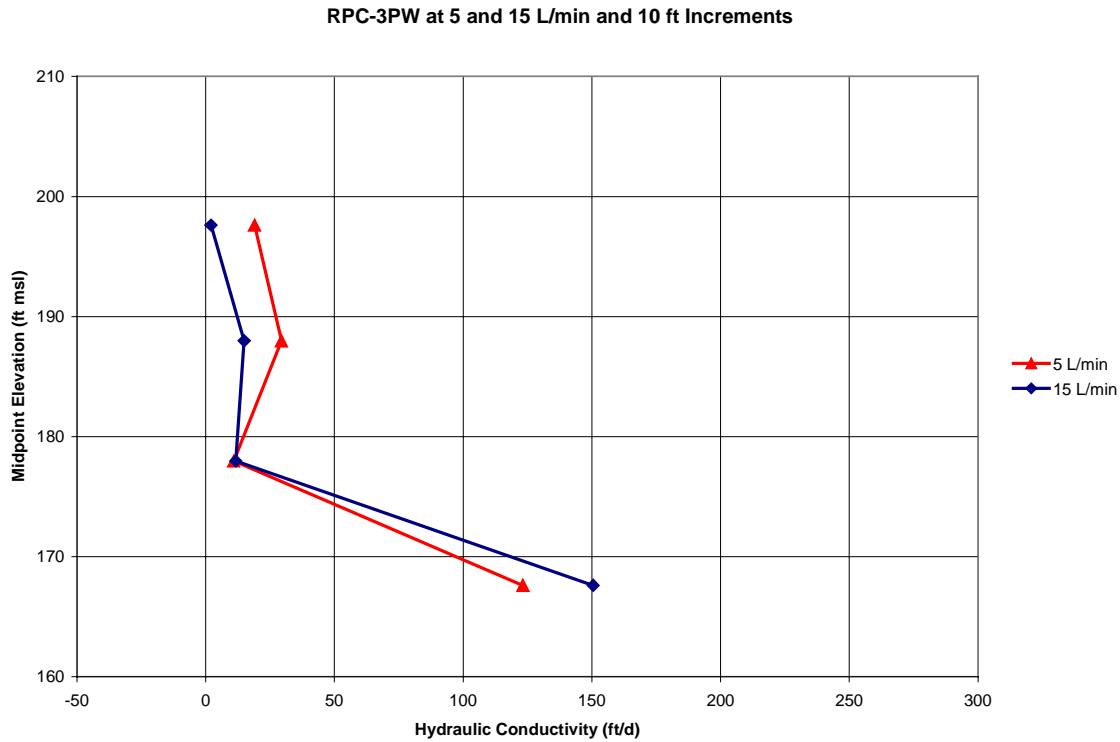
Figure 18   Estimated hydraulic conductivity variation for RPC-3PW at 10 ft intervals
                using the ½" and 1" ID EBFs.
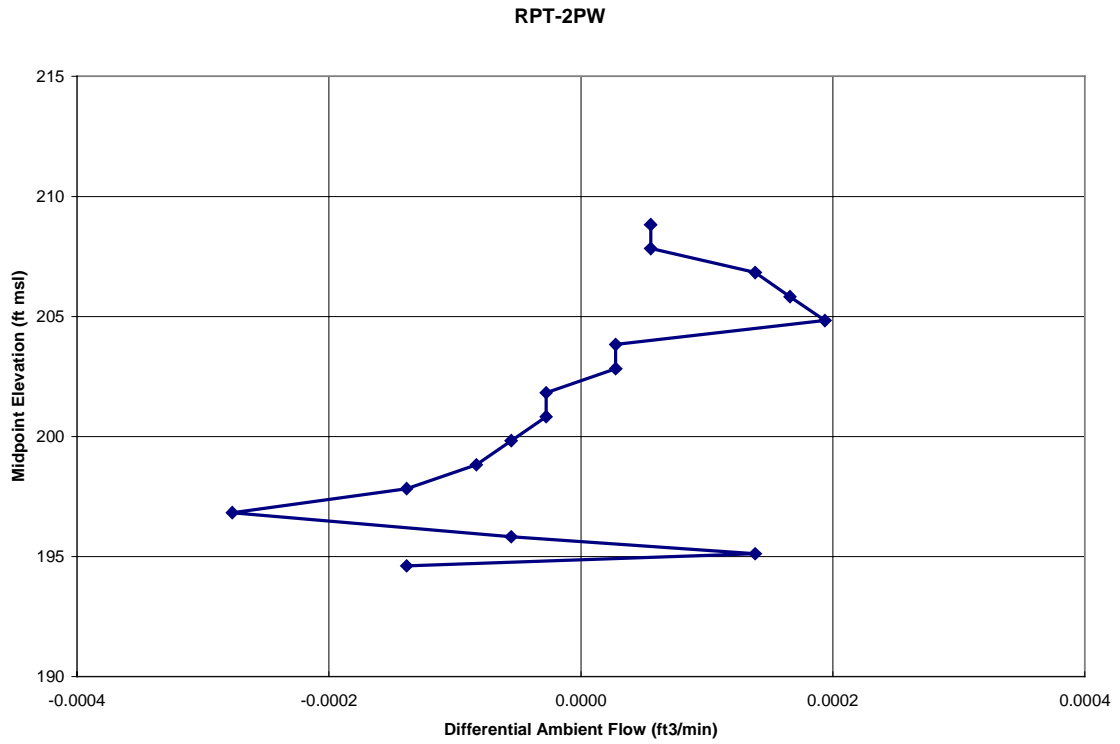
RPT-2PW

Figure 19   Ambient flow measurements for RPT-2PW.
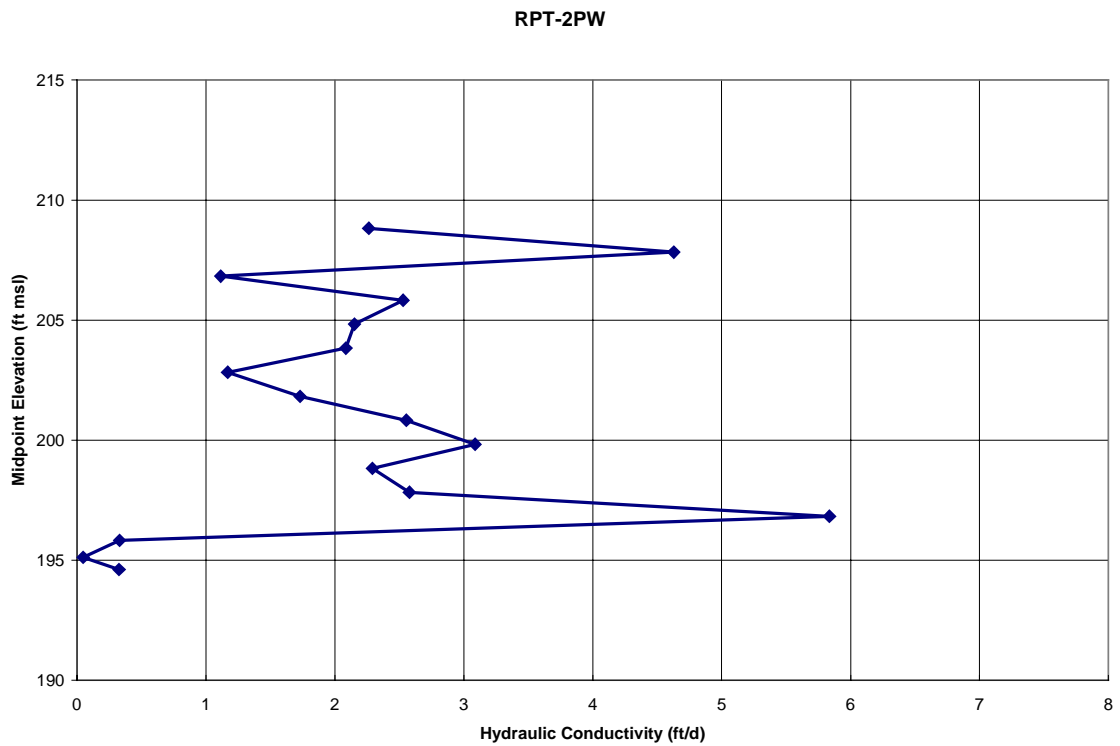
RPT-2PW

Figure 20   Estimated hydraulic conductivity variation for RPT-2PW.

**RPT-3W**
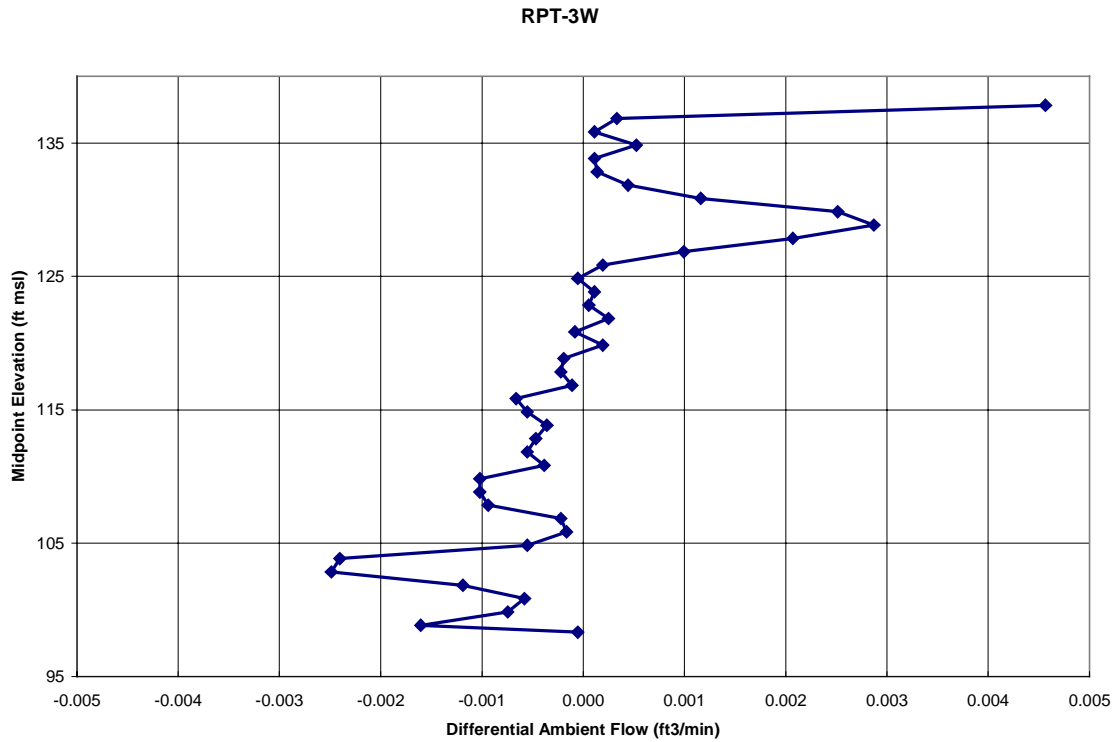
Figure 21   Ambient flow measurements for RPT-3PW.
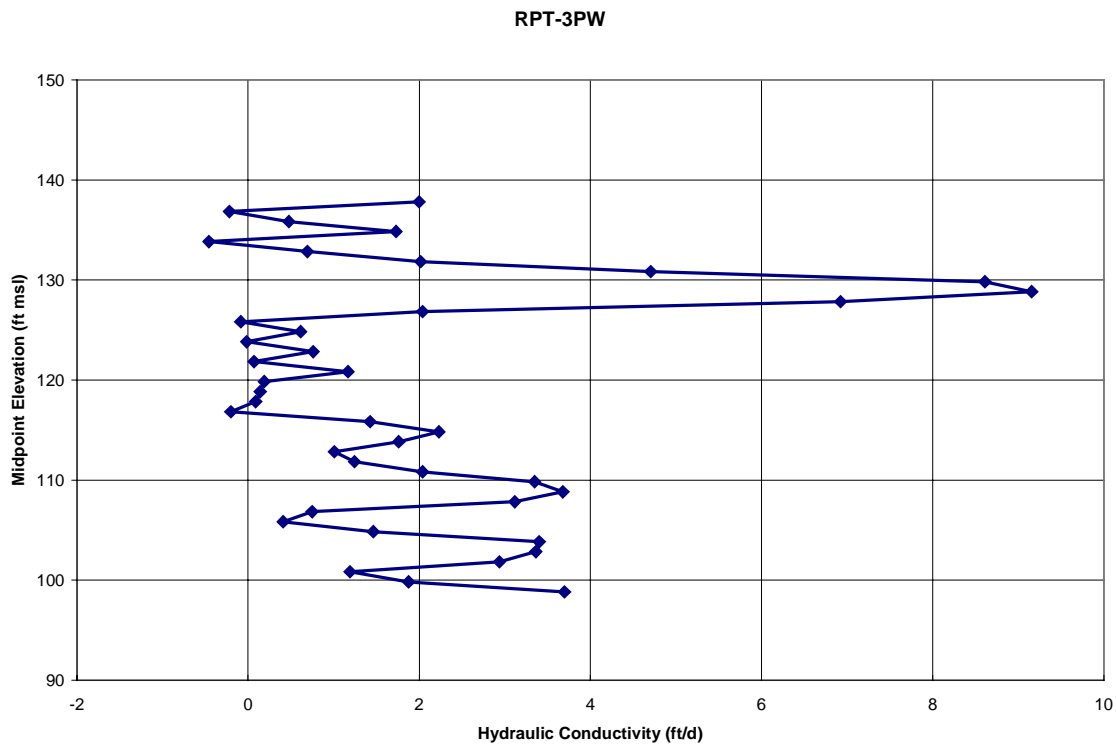
RPT-3PW

Figure 22   Estimated hydraulic conductivity variation for RPT-3PW.
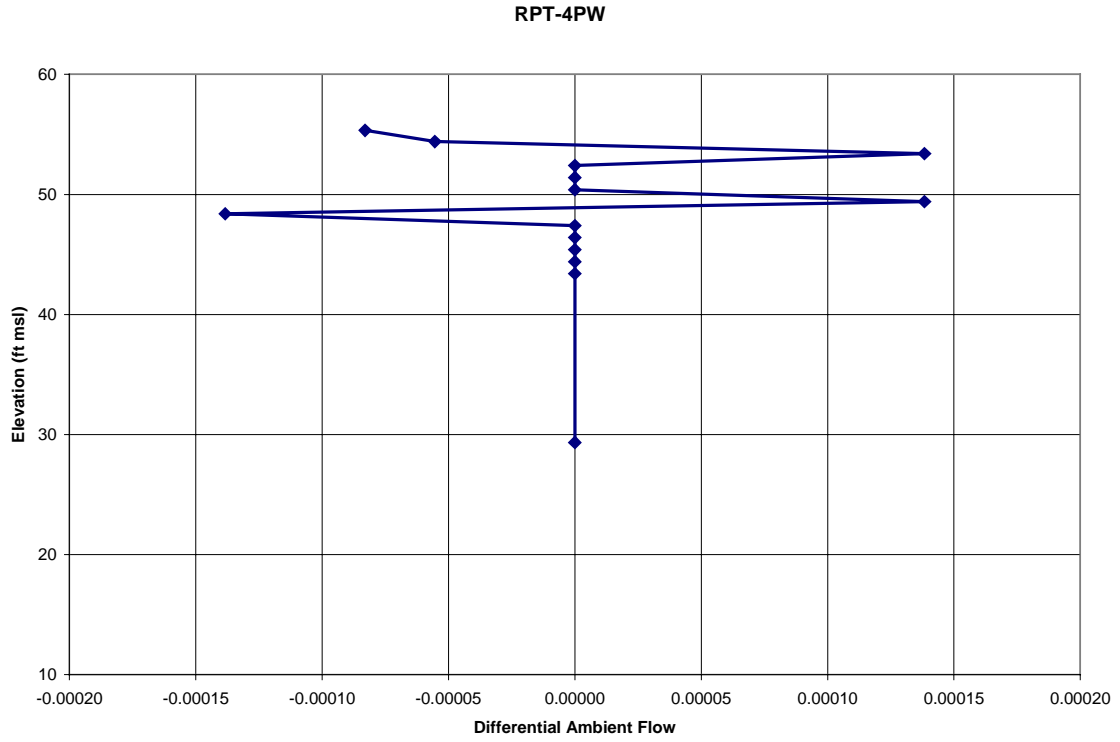
Figure 23   Ambient flow measurements for RPT-4PW.
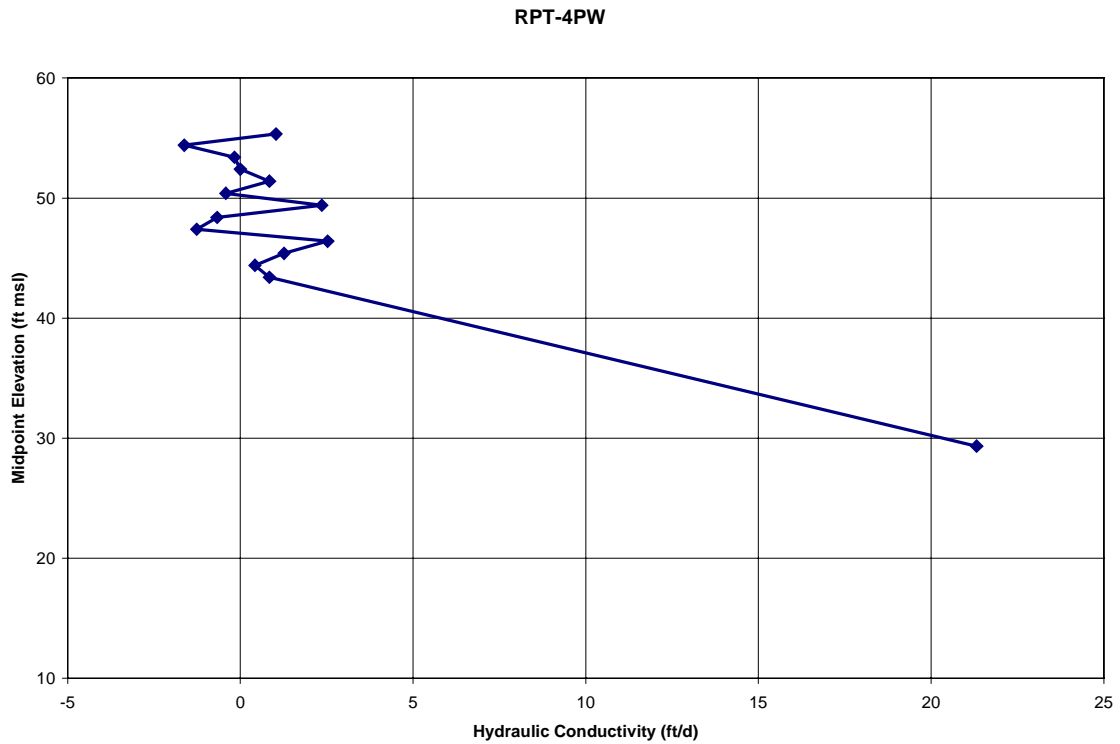
Figure 24   Estimated hydraulic conductivity variation for RPT-4PW.
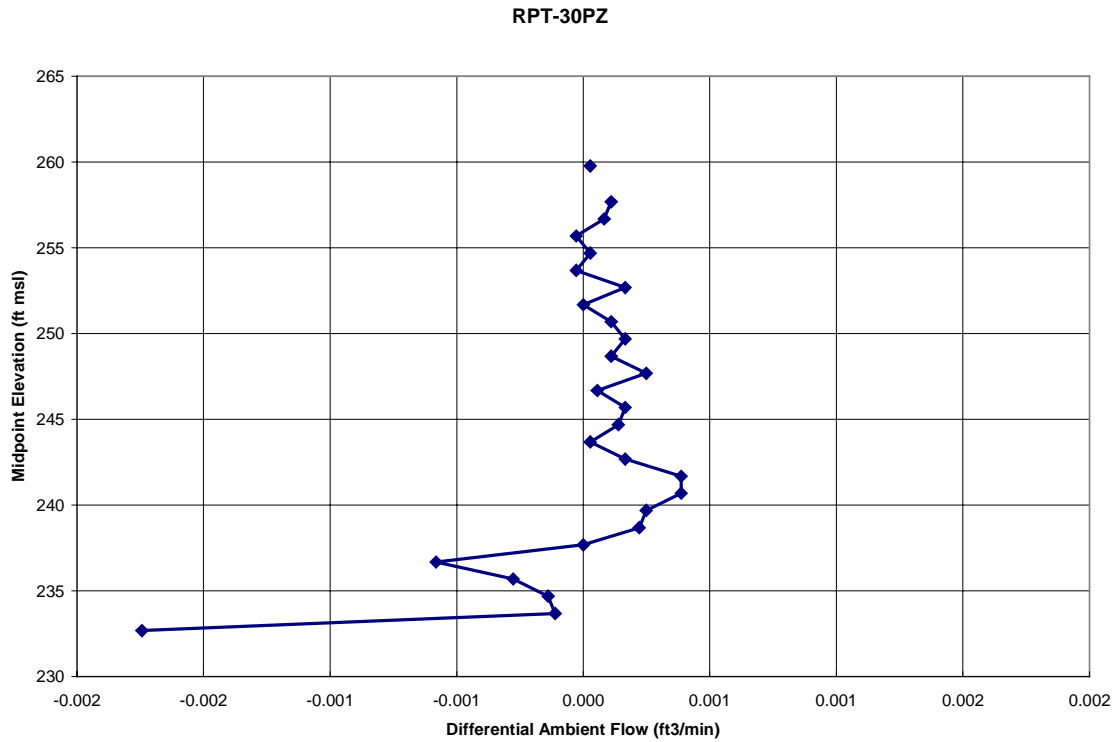
RPT-30PZ

Figure 25   Ambient flow measurements for RPT-30PZ.
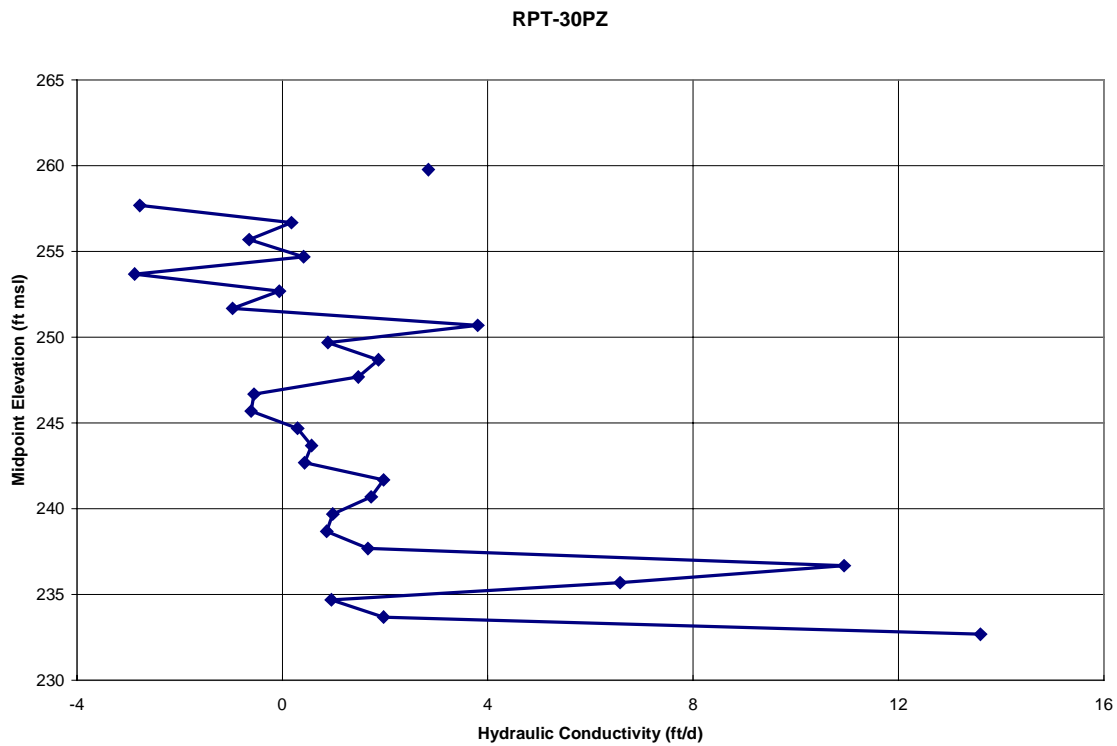
RPT-30PZ

Figure 26   Estimated hydraulic conductivity variation for RPT-30PZ.
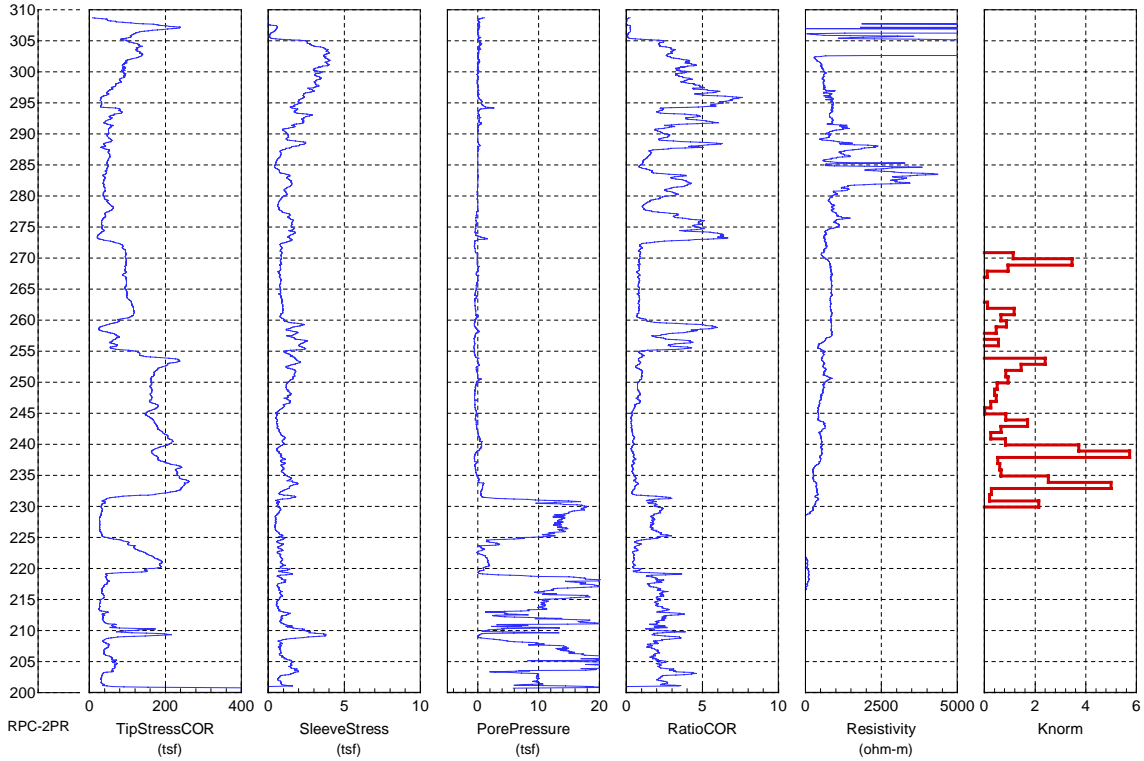
Figure 27   Comparison of CPT data to EBF horizontal conductivity distribution relative to screen-averaged conductivity for RPC-2PR.
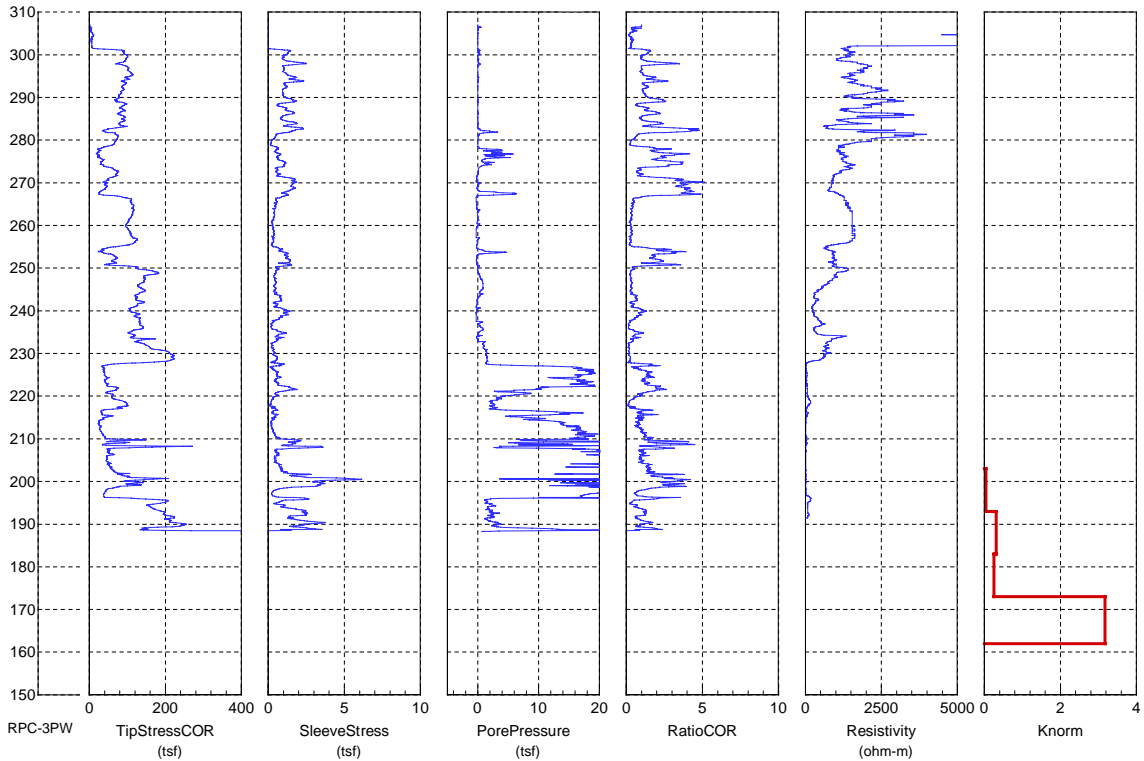
Figure 28   Comparison of CPT data to EBF horizontal conductivity distribution relative to screen-averaged conductivity for RPC-3PW.
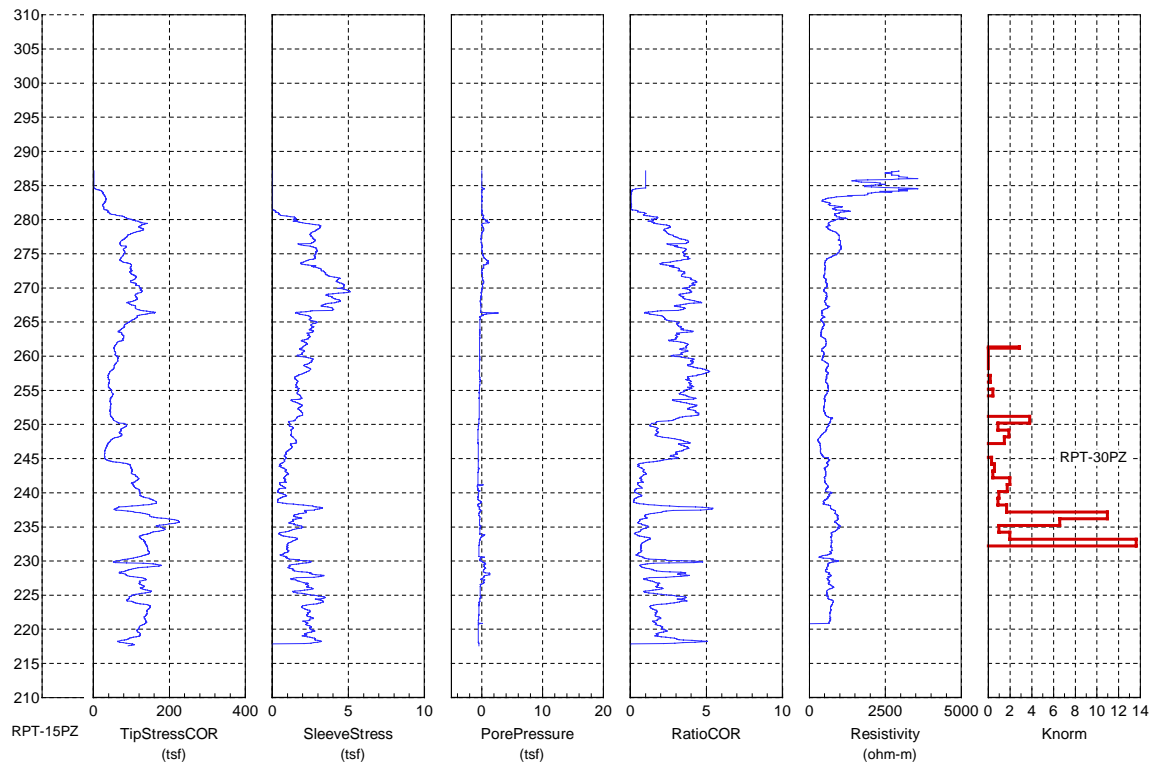
Figure 29   Comparison of CPT data to EBF horizontal conductivity distribution relative to screen-averaged conductivity for RPT-30PZ.
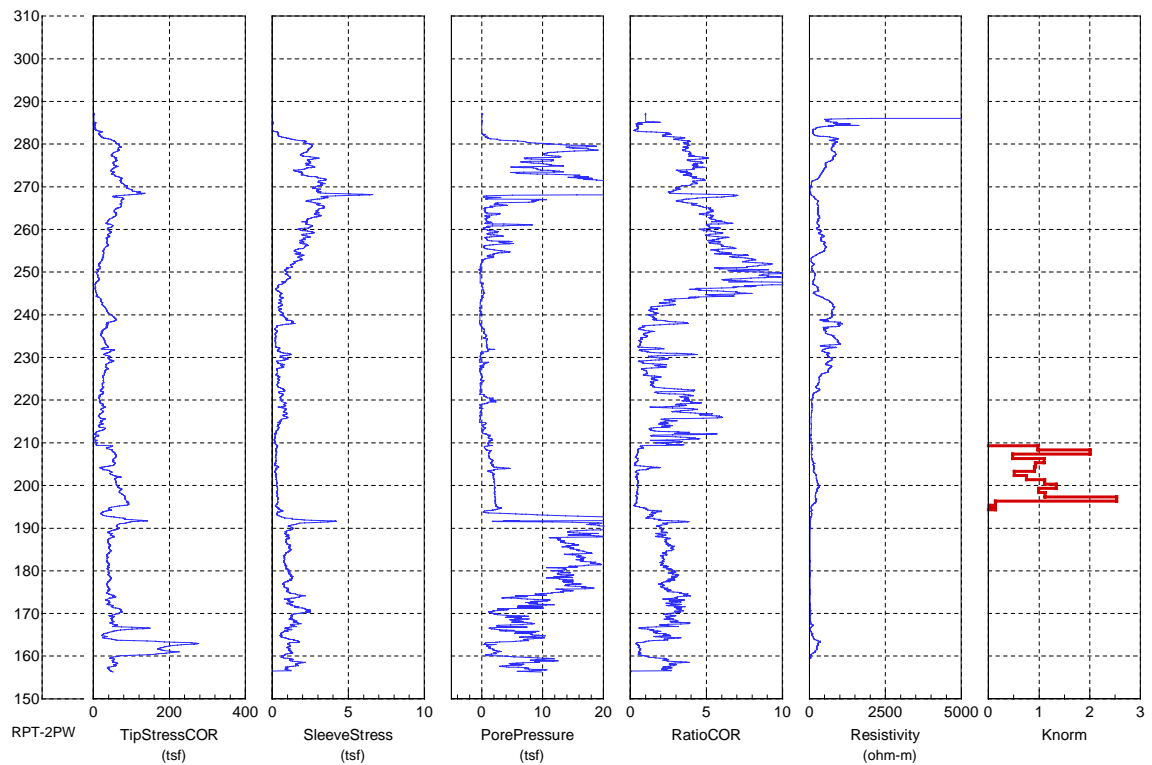
Figure 30   Comparison of CPT data to EBF horizontal conductivity distribution relative to screen-averaged conductivity for RPT-2PW.
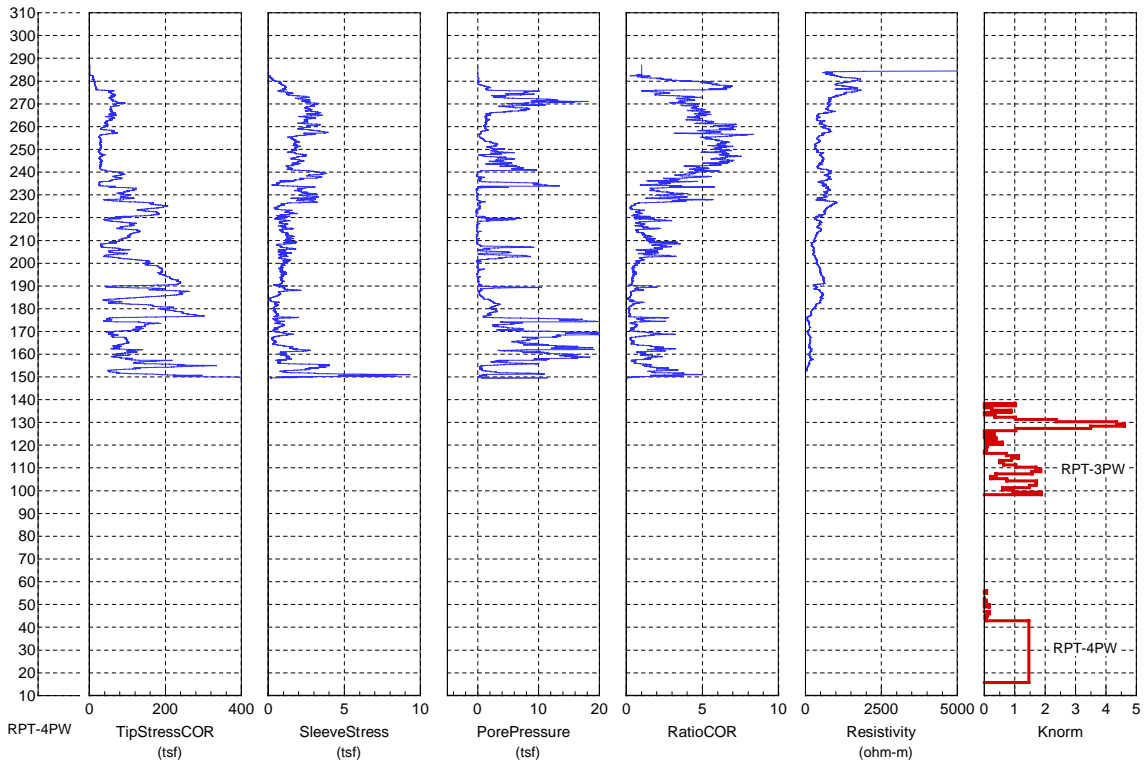
Figure 31   Comparison of CPT data to EBF horizontal conductivity distribution relative to screen-averaged conductivity for RPT-3PW and RPT-4PW.

This page intentionally left blank

Appendix A – RPC-1PW field data

Well ID	Top of Screen From Grade (ft)	Bottom of Screen From Grade (ft)	Screen Length (ft)	Casing Diameter (inch)	Approx. Water Level From TOC (ft)	Survey Elev. TOC (ft-msl)	Survey Elev. Conc Pad (ft-msl)	TOC to Conc Pad (ft)
RPC-1PW	19.5	34.5	15	2	32.7	307.56	305.24	2.32

	Probe Date	.5" 3/27/00	.5" 3/27/00
Station	Depth Below Toc	Ambient Instrument Response	y = 0.0024x2 + 0.7838x Ambient Calibrated Flow (l/min)
4			
3			
2	34.82'	-0.035	-0.0274
1	35.82'	-0.029	-0.0227
0	36.82'	-0.018	-0.0141

Time	Water Level (ft)
10:40	32.65

3/28/00   Ambient
14:30-15:30 Warm up meter set to 0.000

This page intentionally left blank

Appendix B – RPC-2PR field data

Well ID	Top of Screen From Grade (ft)	Bottom of Screen From Grade (ft)	Screen Length (ft)	Casing Diameter (inch)	Approx. Water Level From TOC (ft)	Survey Elev. TOC (ft-msl)	Survey Elev. Conc Pad (ft-msl)	TOC to Conc Pad (ft)	Pad Thickness (ft)	Top of Screen From TOC (ft)	Bottom of Screen From TOC (ft)	Top of Screen Elevation (ft)	Bottom of Screen Elevation (ft)
RPC-2PR	35	75	40	4	33.1	307.92	305.89	2.03	0.33	37.36	77.36	270.56	230.56

Ambient Corrected for "0"

Station	Depth Below TOC (ft)	Time (Probe Date .5" 3/28/00)	Ambient Instrument Response	Delta Time min (.5" 3/28/00)		Ambient Instrument Response Corrected for "0"	Time (.5" 3/28/00)	Dynamic Instrument Response	0.0024x2 + 0.7838x Ambient Calibrated Flow (l/min) (.5" 3/28/00)	0.0024x2 + 0.7838x Dynamic Calibrated Flow (.5" 3/28/00)
41	36.03	13:06	-0.027	164	0.02916	0.002			0.0017	
40	37.03	13:02	-0.029	160	0.02844	-0.001	16:30	5.395	-0.0004	4.2985
39	38.03	12:58	-0.022	156	0.02773	0.006	16:25	5.300	0.0045	4.2216
38	39.03	12:54	-0.023	152	0.02702	0.004	16:17	4.838	0.0032	3.8482
37	40.03	12:50	-0.026	148	0.02631	0.000	16:14	4.710	0.0002	3.7449
36	41.03	12:46	-0.025	144	0.02560	0.001	16:10	4.694	0.0005	3.7320
35	42.03	12:44	-0.026	142	0.02524	-0.001	16:07	4.695	-0.0006	3.7328
34	43.03	12:43	-0.028	141	0.02507	-0.003	16:04	4.710	-0.0023	3.7449
33	44.03	12:39	-0.026	137	0.02436	-0.002	16:01	4.731	-0.0013	3.7619
32	45.03	12:36	-0.029	134	0.02382	-0.005	15:57	4.733	-0.0041	3.7635
31	46.03	12:32	-0.030	130	0.02311	-0.007	15:54	4.714	-0.0054	3.7482
30	47.03	12:28	-0.033	126	0.02240	-0.011	15:49	4.555	-0.0083	3.6200
29	48.03	12:24	-0.037	122	0.02169	-0.015	15:47	4.464	-0.0120	3.5467
28	49.03	12:20	-0.048	118	0.02098	-0.027	15:45	4.337	-0.0212	3.4445
27	50.03	12:16	-0.050	114	0.02027	-0.030	15:42	4.271	-0.0233	3.3914
26	51.03	12:13	-0.048	111	0.01973	-0.028	15:39	4.300	-0.0222	3.4147
25	52.03	12:08	-0.055	106	0.01884	-0.036	15:37	4.218	-0.0283	3.3488
24	53.03	12:05	-0.050	103	0.01831	-0.032		4.230	-0.0248	3.3584
23	54.03	12:02	-0.054	100	0.01778	-0.036		4.229	-0.0284	3.3576
22	55.03	11:58	-0.060	96	0.01707	-0.043	15:27	3.901	-0.0336	3.0941
21	56.03	11:54	-0.072	92	0.01636	-0.056	15:25	3.694	-0.0436	2.9281
20	57.03	11:50	-0.072	88	0.01564	-0.056		3.580	-0.0442	2.8368
19	58.03	11:47	-0.073	85	0.01511	-0.058	15:19	3.454	-0.0454	2.7359
18	59.03	11:44	-0.080	82	0.01458	-0.065	15:16	3.379	-0.0513	2.6759
17	60.03	11:41	-0.075	79	0.01404	-0.061		3.330	-0.0478	2.6367
16	61.03	11:37	-0.082	75	0.01333	-0.069	15:10	3.261	-0.0538	2.5815
15	62.03	11:28	-0.075	66	0.01173	-0.063	15:08	3.233	-0.0496	2.5591
14	63.03	11:20	-0.080	58	0.01031	-0.070	15:06	3.225	-0.0546	2.5527
13	64.03	11:12	-0.080	50	0.00889	-0.071	15:03	3.110	-0.0557	2.4608
12	65.03	11:04	-0.080	42	0.00747	-0.073	15:00	2.880	-0.0568	2.2773
11	66.03	10:56	-0.080	34	0.00604	-0.074	14:58	2.790	-0.0580	2.2055
10	67.03	10:53	-0.080	31	0.00551	-0.074	14:56	2.755	-0.0584	2.1776
9	68.03	10:50	-0.080	28	0.00498	-0.075	14:54	2.643	-0.0588	2.0883
8	69.03	10:47	-0.080	25	0.00444	-0.076	14:52	2.140	-0.0592	1.6883
7	70.03	10:44	-0.082	22	0.00391	-0.078	14:50	1.360	-0.0612	1.0704
6	71.03	10:42	-0.078	20	0.00356	-0.074	14:48	1.291	-0.0583	1.0159
5	72.03	10:39	-0.075	17	0.00302	-0.072	14:46	1.212	-0.0564	0.9535
4	73.03	10:36	-0.071	14	0.00249	-0.069		1.126	-0.0537	0.8856
3	74.03	10:34	-0.057	12	0.00213	-0.055	14:42	0.795	-0.0430	0.6246
2	75.03	10:32	-0.017	10	0.00178	-0.015		0.151	-0.0119	0.1184
1	76.03	10:26	-0.014	4	0.00071	-0.013	14:37	0.115	-0.0104	0.0902
0	77.03	10:24	-0.011	2	0.00036	-0.011	14:33	0.090	-0.0083	0.0706
-1	78.03	10:22	-0.004	0	0.00000	-0.004	14:30	-0.001	-0.0031	-0.0008

3/28/00

Time	Water Level (ft)	Bucket 16.8L Fill in sec	Field Measured Flow (L/min)
7:52	33.15		
9:30	33.14'		
13:52	33.05'		
14:17	33.85'		
14:22	33.85'	233.5	4.32
14:27		236	4.27
14:30	33.85'		
14:45	33.86'		
15:00		231.5	4.35
15:08	33.85'		
15:27		234	4.31
15:55	33.94'		
16:02		235	4.29
16:23			
16:25		234	4.31
16:31		234	4.31

3/28/00 Ambient
Warm up 9:10-10:00 - meter set to 0.000
13:22 Probe removed / plugged reading -0.032 reset to 0.000

Times in *itallics* for ambient test estimated

Dynamic
16.40 Probe removed / plugged reading 0.000

Correction for "0"

Start Time - Stop Time = 180 min
Total Delta "0"= -.032

This page intentionally left blank

Appendix C – RPC-3PW field data

Well ID	Top of Screen From Grade (ft)	Bottom of Screen From Grade (ft)	Screen Length (ft)	Casing Diameter (inch)	Approx. Water Level From TOC (ft)	Survey Elev. TOC (ft-msl)	Survey Elev. Conc Pad (ft-msl)	TOC to Conc Pad (ft)	Pad Thickness (ft)	Top of Screen From TOC (ft)	Bottom of Screen From TOC (ft)	Top of Screen Elevation (ft)	Bottom of Screen Elevation (ft)
RPC-3PW	105	145	40	4	53.7	309.14	307.58	1.56	0.33	106.89	146.89	202.25	162.25

Ambient Corrected for "0"

	Probe Date	.5" 3/29/00		.5" 3/29/00			.5" 3/30/00		1.0" 3/31/00		.5" 3/29/00	.5" 3/30/00	1.0" 3/31/00
Station	Depth Below TOC	Time	Ambient Instrument Response	Delta Time min	Delta (ml)	Ambient Instrument Response Corrected for "0"	Time	Dynamic Flow 1 Instrument Response	Time	Dynamic Flow 2 Instrument Response	0.0024x2 + 0.7838x Ambient Calibrated Flow (l/min)	0.0024x2 + 0.7838x Dynamic Calibrated Flow (l/min)	y = 0.9797x + 0.1097 Dynamic Calibrated Flow (l/min)
42	105.16	12:32	-0.015	164	0.01500	0.00000					0.0000		
41	106.16	12:29	-0.015	161	0.01473	-0.00027	16:39	6.679	10:49	14.75	-0.0002	5.3421	14.56
40	107.16	12:25	-0.015	157	0.01436	-0.00064	16:36	6.694		14.82	-0.0005	5.3543	14.63
39	108.16	12:20	-0.015	152	0.01390	-0.00110	16:32	6.678	10:44	14.86	-0.0009	5.3412	14.67
38	109.16	12:17	0.026	149	0.01363	0.03963	16:29	1.606		8.24	0.0311	1.2650	8.18
37	110.16	12:13	-0.021	145	0.01326	-0.00774	16:23	5.555	10:39	14.33	-0.0061	4.4281	14.15
36	111.16	12:06	-0.025	138	0.01262	-0.01238	16:20	6.031	10:35	14.58	-0.0097	4.8144	14.39
35	112.16	12:03	-0.036	135	0.01235	-0.02365	16:16	6.040	10:33	14.55	-0.0185	4.8217	14.36
34	113.16	11:59	-0.034	131	0.01198	-0.02202	16:12	6.176	10:30	14.58	-0.0173	4.9323	14.39
33	114.16	11:55	-0.030	127	0.01162	-0.01838	16:08	6.125	10:25	14.53	-0.0144	4.8908	14.34
32	115.16	11:52	-0.035	124	0.01134	-0.02366	16:03	6.234	10:22	14.61	-0.0185	4.9795	14.42
31	116.16	11:48	-0.036	120	0.01098	-0.02502	15:58	6.050	10:18	14.58	-0.0196	4.8298	14.39
30	117.16	11:44	-0.033	116	0.01061	-0.02239	15:54	6.043	10:15	14.58	-0.0175	4.8241	14.39
29	118.16	11:42	-0.030	114	0.01043	-0.01957	15:49	6.002	10:13	14.56	-0.0153	4.7908	14.37
28	119.16	11:38	-0.034	110	0.01006	-0.02394	15:45	5.832	10:10	14.45	-0.0188	4.6528	14.27
27	120.16	11:34	-0.035	106	0.00970	-0.02530	15:42	5.824	10:08	14.50	-0.0198	4.6463	14.32
26	121.16	11:31	-0.033	103	0.00942	-0.02358		5.897	10:06	14.48	-0.0185	4.7055	14.30
25	122.16	11:25	-0.029	97	0.00887	-0.02013		5.916	10:04	14.50	-0.0158	4.7210	14.32
24	123.16	11:20	-0.034	92	0.00841	-0.02559		5.683	10:00	14.33	-0.0201	4.5318	14.15
23	124.16	11:17	-0.040	89	0.00814	-0.03186	15:41	5.733	9:57	14.30	-0.0250	4.5724	14.12
22	125.16	11:14	-0.072	86	0.00787	-0.06413	15:39	5.209	9:54	13.84	-0.0503	4.1479	13.67
21	126.16	11:11	-0.108	83	0.00759	-0.10041	15:37	4.957	9:52	13.36	-0.0787	3.9443	13.20
20	127.16	11:07	-0.136	79	0.00723	-0.12877	15:34	4.863	9:50	13.04	-0.1009	3.8684	12.88
19	128.16	11:04	-0.141	76	0.00695	-0.13405	15:31	4.939	9:46	13.09	-0.1050	3.9297	12.93
18	129.16	11:00	-0.138	72	0.00659	-0.13141	15:27	4.908	9:45	13.06	-0.1030	3.9047	12.90
17	130.16	10:56	-0.140	68	0.00622	-0.13378	15:23	4.929	9:42	13.08	-0.1048	3.9217	12.92
16	131.16	10:52	-0.138	64	0.00585	-0.13215	15:21	4.768	9:40	12.97	-0.1035	3.7917	12.82
15	132.16	10:46	-0.137	58	0.00530	-0.13170	15:18	4.625	9:37	12.74	-0.1032	3.6764	12.59
14	133.16	10:42	-0.137	54	0.00494	-0.13206	15:16	4.591	9:35	12.71	-0.1035	3.6490	12.56
13	134.16	10:39	-0.140	51	0.00466	-0.13534	15:13	4.517	9:32	12.60	-0.1060	3.5894	12.45
12	135.16	10:36	-0.139	48	0.00439	-0.13461	15:11	4.457	9:28	12.50	-0.1055	3.5411	12.36
11	136.16	10:33	-0.138	45	0.00412	-0.13388	15:07	4.545	9:26	12.43	-0.1049	3.6119	12.29
10	137.16	10:30	-0.132	42	0.00384	-0.12816	15:05	4.370	9:24	12.08	-0.1004	3.4710	11.94
9	138.16	10:27	-0.130	39	0.00357	-0.12643	15:02	4.241	9:22	11.93	-0.0991	3.3673	11.80
8	139.16	10:23	-0.110	35	0.00320	-0.10680	14:59	3.257	9:20	9.85	-0.0837	2.5783	9.76
7	140.16	10:20	-0.109	32	0.00293	-0.10607	14:55	3.044	9:18	9.14	-0.0831	2.4081	9.06
6	141.16	10:16	-0.105	28	0.00256	-0.10244	14:50	2.950	9:16	8.73	-0.0803	2.3331	8.66
5	142.16		-0.107	24	0.00220	-0.10480	14:47	2.889	9:14	8.60	-0.0821	2.2844	8.54
4	143.16	10:07	-0.092	19	0.00174	-0.09026	14:45	2.660	9:13	7.93	-0.0707	2.1019	7.88
3	144.16	10:03	-0.079	15	0.00137	-0.07763	14:43	2.275	9:11	6.71	-0.0608	1.7956	6.68
2	145.16	9:59	-0.061	11	0.00101	-0.05999	14:40	1.750	9:10	5.02	-0.0470	1.3790	5.03
1	146.16	9:56	-0.038	8	0.00073	-0.03727	14:36	1.100	9:08	3.20	-0.0292	0.8651	3.24
0	147.16	9:53	-0.006	5	0.00046	-0.00554	14:30	-0.004	9:07	0.00	-0.0043	-0.0031	0.11
-1	148.16	9:48	-0.005	0	0.00000	-0.00500	14:28	-0.004	9:05	0.00	-0.0039	-0.0031	0.11

3/29/00 — Ambient
Warm up 7:43-9:30 - meter set to 0.000
12:35 Probe removed / plugged reading -0.015 reset to 0.000
Station 38 reading reverified
Ambient "0" correction =.015/164= 0.000091463 ml/min

3/30/00 — Dynamic
Warm up 13:00-14:04 - meter set to 0.000
17:05 Probe removed / plugged reading -0.005

3/31/00 — Dynamic
Warm up 7:24-8:24 - meter set to 0.000

3/29/00

Time	Water Level (ft)	Time to Fill Bucket 16.8L (sec)	Field Measured Flow (L/min)
7:42	53.7'		
10:25	53.7'		
13:20	53.75'		

3/30/00

Time	Water Level (ft)	Time to Fill Bucket 16.8L (sec)	Field Measured Flow (L/min)
13:00	53.65'		
14:20	53.72'		
14:25	53.72'	196	5.14
14:28		195	5.17
14:30	53.74'		
15:06	53.74'		
15:30		193	5.22
16:00	53.82'		
16:07		193	5.22
16:43		194	5.20
16:44	53.79'		

3/31/00

Time	Water Level (ft)	Time to Fill Bucket 16.8L (sec)	Field Measured Flow (L/min)
7:30	53.69'		
8:40	53.87'		
8:46		70	14.40
8:47	53.88'		
8:53		70	14.40
8:57		69	14.61
9:02	53.88'	69	14.61
9:32	53.92'	69.5	14.50
10:01	53.95'		
10:13	53.95'		
10:20		69	14.61
10:50	53.96		
10:52		69.5	14.50
10:59	53.7		

Appendix D – RPT-2PW field data

Well ID	Top of Screen From Grade (ft)	Bottom of Screen From Grade (ft)	Screen Length (ft)	Casing Diameter (inch)	Approx. Water Level From TOC (ft)	Survey Elev. TOC (ft-msl)	Survey Elev. Conc Pad (ft-msl)	TOC to Conc Pad (ft)	Pad Thickness (ft)	Top of Screen From TOC (ft)	Bottom of Screen From TOC (ft)	Top of Screen Elevation (ft)	Bottom of Screen Elevation (ft)
RPT-2PW	78	93	15	4	28.6	289.91	287.66	2.25	0.33	80.58	95.58	209.33	194.33

Probe Date	.5" 4/5/00		.5" 4/5/00		.5" 4/5/00	.5" 4/5/00		4/5/00		
Station	Depth Below TOC (FT)	Time	Ambient Instrument Response	Time	Dynamic Instrument Response	y = 0.0024x2 + 0.7838x Ambient Calibrated Flow (l/min)	y = 0.0024x2 + 0.7838x Dynamic Calibrated Flow (l/min)	Time	Water Level (ft)	Bucket 16.8L Fill in (sec)	Field Measured Flow (L/min)
								7:40	28.59		
								12:46	28.55		
	70.00			14:47	5.032		4.005	13:05	35.30		
								13:09	35.70		
16	79.58	12:45	0.000	14:44	5.030	0.0000	4.003	13:13	35.85		
15	80.58	12:40	0.000	14:40	5.036	0.0000	4.008	13:19	36.00		
14	81.58	12:38	-0.002	14:37	4.71	-0.0016	3.745	13:27	36.13		
13	82.58	12:35	-0.004	14:33	4.041	-0.0031	3.207	13:34	36.20		
12	83.58	12:33	-0.009	14:30	3.875	-0.0071	3.073	13:47	36.40		
11	84.58	12:32	-0.015	14:23	3.503	-0.0118	2.775	13:50		249	4.05
10	85.58	12:30	-0.022	14:21	3.184	-0.0172	2.520	14:06	36.53		
9	86.58	12:27	-0.023	14:19	2.88	-0.0180	2.277	14:12		251	4.02
8	87.58	12:24	-0.024	14:17	2.709	-0.0188	2.141	14:21		252	4.00
7	88.58	12:21	-0.023	14:14	2.458	-0.0180	1.941	14:24	36.65		
6	89.58	12:18	-0.022	14:10	2.086	-0.0172	1.645	14:49		252.5	3.99
5	90.58	12:16	-0.020	14:08	1.636	-0.0157	1.289	14:50			
4	91.58	12:14	-0.017	14:05	1.303	-0.0133	1.025				
3	92.58	12:12	-0.012	14:01	0.929	-0.0094	0.730				
2	93.58	12:10	-0.002	13:58	0.078	-0.0016	0.061				
1	94.58	12:09	0.000	13:56	0.031	0.0000	0.024				
0	95.00	12:07	-0.005	13:53	0.023	-0.0039	0.018				

3/31/00

Ambient
95.00 Lowest possible position probe/ packer could be set
Warm up 9:30-12:05 - meter set to 0.000
Station 16 in casing "0" verified at 0.000

Dynamic
Dynamic test with .5" probe followed ambient rezero not required
15:00 Probe removed and plugged reading -0.004

This page intentionally left blank

Appendix E – RPT-3PW field data

Well ID	Top of Screen From Grade (ft)	Bottom of Screen From Grade (ft)	Screen Length (ft)	Casing Diameter (inch)	Approx. Water Level From TOC (ft)	Survey Elev. TOC (ft-msl)	Survey Elev. Conc Pad (ft-msl)	TOC to Conc Pad (ft)	Pad Thickness (ft)	Top of Screen From TOC (ft)	Bottom of Screen From TOC (ft)	Top of Screen Elevation (ft)	Bottom of Screen Elevation (ft)
RPT-3PW	149	189	40	4	53.6	289.83	287.64	2.19	0.33	151.52	191.52	138.31	98.31

Station	Probe Date Depth Below TOC (ft)	1.0" 4/3/00 Time	Dynamic Instrument Response	.5" 4/3/00 Time	Ambient Instrument Response	1.0" 4/3/00 y =0.9797x + 0.1097 Dynamic Calibrated Flow (l/min)	.5" 4/3/00 0.0024x2 + 0.7838x Ambient Calibrated Flow (l/min)	4/3/00 Time	Water Level (ft)	Bucket fill 16.8L in (sec)	Field Measured Flow (L/min)
41	150.48	14:41	14.34	17:47	0.000	14.159	0.0000	11:51	53.57		
40	151.48	14:38	14.34	17:43	0.000	14.159	0.0000	12:00	59.7		
39	152.48	14:35	13.86	17:39	-0.165	13.688	-0.1293	12:13	60.25		
38	153.48	14:33	13.89	17:36	-0.177	13.718	-0.1387	12:16		71	14.20
37	154.48	14:30	13.8	17:33	-0.181	13.630	-0.1418	12:23		70.5	14.30
36	155.48	14:27	13.47	17:30	-0.200	13.306	-0.1567	12:24	60.38		
35	156.48	14:23	13.55	17:27	-0.204	13.385	-0.1598	12:33	60.51		
34	157.48	14:16	13.42	17:24	-0.209	13.257	-0.1637	12:36		71	14.20
33	158.48	14:12	13.04	17:22	-0.225	12.885	-0.1762	12:40	60.6		
32	159.48	14:07	12.15	17:19	-0.267	12.013	-0.2091	12:50	60.67		
31	160.48	14:03	10.51	17:16	-0.358	10.406	-0.2803	12:53		71	14.20
30	161.48	13:59	8.76	17:14	-0.462	8.692	-0.3616	13:02		71	14.20
29	162.48	13:55	7.44	17:12	-0.537	7.399	-0.4202	13:10	60.85		
28	163.48	13:52	7.04	17:10	-0.573	7.007	-0.4483	13:21	60.9		
27	164.48	13:49	7.05	17:08	-0.580	7.017	-0.4538	13:22		71	14.20
26	165.48	13:46	6.94	17:05	-0.578	6.909	-0.4522	13:32	60.96		
25	166.48	13:44	6.94	17:02	-0.582	6.909	-0.4554	13:42	61.03		
24	167.48	13:41	6.80	16:59	-0.584	6.772	-0.4569	13:56		71	14.20
23	168.48	13:39	6.78	16:57	-0.593	6.752	-0.4639	14:08	61.13		
22	169.48	13:36	6.57	16:55	-0.590	6.546	-0.4616	14:39		71	14.20
21	170.48	13:34	6.53	16:53	-0.597	6.507	-0.4671	14:41	61.27		
20	171.48	13:31	6.51	16:51	-0.590	6.488	-0.4616	15:28	54.6		
19	172.48	13:19	6.50	16:49	-0.582	6.478	-0.4554	15:42	54.47		
18	173.48	13:27	6.54	16:46	-0.578	6.517	-0.4522	15:57	54.3		
17	174.48	13:24	6.30	16:44	-0.554	6.282	-0.4335	16:23	54.26		
16	175.48	13:22	5.91	16:42	-0.534	5.900	-0.4179	16:45	54.19		
15	176.48	13:20	5.60	16:40	-0.521	5.596	-0.4077	17:04	54.13		
14	177.48	13:18	5.43	16:38	-0.504	5.429	-0.3944	17:52	54.07		
13	178.48	13:16	5.22	16:36	-0.484	5.224	-0.3788				
12	179.48	13:13	4.86	16:34	-0.470	4.871	-0.3679				
11	180.48	13:11	4.28	16:33	-0.433	4.303	-0.3389				
10	181.48	13:09	3.64	16:31	-0.396	3.676	-0.3100				
9	182.48	13:07	3.10	16:30	-0.362	3.147	-0.2834				
8	183.48	13:05	2.97	16:29	-0.354	3.019	-0.2772				
7	184.48	13:02	2.90	16:27	-0.348	2.951	-0.2725				
6	185.48	12:59	2.65	16:25	-0.328	2.706	-0.2568				
5	186.48	12:56	2.10	16:23	-0.241	2.167	-0.1888				
4	187.48	12:54	1.56	16:21	-0.151	1.638	-0.1183				
3	188.48	12:51	1.06	16:20	-0.108	1.148	-0.0846				
2	189.48	12:49	0.86	16:18	-0.087	0.952	-0.0682				
1	190.48	12:46	0.54	16:16	-0.060	0.639	-0.0470				
0	191.48	12:44	0.00	16:14	-0.002	0.110	-0.0016				
-1	192.48	12:42	0.00	16:12	-0.002	0.110	-0.0016				

4/3/00 Dynamic
Warm up 10:42-11:42 1" probe meter set to 0.000

Ambient
Warm up 14:50-15:50 1/2" probe meter set to 0.000
17.47 After final reading probe raised into casing and "0" at 0.000

This page intentionally left blank

Appendix F – RPT-4PW field data

Well ID	Top of Screen From Grade (ft)	Bottom of Screen From Grade (ft)	Screen Length (ft)	Casing Diameter (inch)	Approx. Water Level From TOC (ft)	Survey Elev. TOC (ft-msl)	Survey Elev. Conc Pad (ft-msl)	TOC to Conc Pad (ft)	Pad Thickness (ft)	Top of Screen From TOC (ft)	Bottom of Screen From TOC (ft)	Top of Screen Elevation (ft)	Bottom of Screen Elevation (ft)
RPT-4PW	231.4	271.4	40	6	94.00	289.72	287.5	2.22	0.33	233.95	273.95	55.77	15.77

	Probe Date	.5" 3/31/00		1.0" 4/3/00		.5" 3/31/00	1.0" 4/3/00
Station	Depth Below TOC	Time	Ambient Instrument Response	Time	Dynamic Instrument Response	y = 0.0024x2 + 0.7838x Dynamic Calibrated Flow (l/min)	y = 0.9797x + 0.1097 Dynamic Calibrated Flow (l/min)
44				10:35	13.72		13.55
42	233.82						
41	234.82	17:21	0.003	10:31	13.70	0.0024	13.53
40	235.82	17:10	0.005	10:24	13.74	0.0039	13.57
39	236.82	17:06	0.000	10:18	13.74	0.0000	13.57
38	237.82	17:00	0.000	10:12	13.74	0.0000	13.57
37	238.82	16:55	0.000	10:06	13.72	0.0000	13.55
36	239.82	16:50	0.000	10:01	13.73	0.0000	13.56
35	240.82	16:45	-0.005	9:55	13.67	-0.0039	13.50
34	241.82	16:44	0.000	9:51	13.69	0.0000	13.52
33	242.82	16:20	0.000	9:47	13.72	0.0000	13.55
32	243.82	16:07	0.000	9:43	13.66	0.0000	13.49
31	244.82	16:01	0.000	9:40	13.63	0.0000	13.46
30	245.82	15:56	0.000	9:35	13.62	0.0000	13.45
29	246.82	15:54	0.000	9:30	13.60	0.0000	13.43
n/a	n/a		n/a		n/a		
n/a	n/a		n/a		n/a		
0	0		0		0		

		3/31/00	
Time	Water Level (ft)	Time to fill Bucket 16.8L (sec)	Field Measured Flow (L/min)
11:59	94.00		
16:53	94.00		

		4/3/00	
8:02	94.00'		
9:11	96.20'		
9:14		75.5	13.35
9:21		75	13.44
9:25	96.17'		
9:29		75	13.44
9:30	96.20'		
9:42	96.20'		
9:49		75	13.44
10:02	96.20'		
10:16		74.5	13.53
10:22	96.23'		
10:33		74.5	13.53

3/31/00   Ambient
Warm up 12:08-13:19 - meter set to 0.000
station 41 After final reading probe raised into casing and "0" at 0.003
250 ' Cable could only reach to Station 29 of the screen

4/3/00   Dynamic
Warm up 8:00-8:59 1" probe meter set to 0.000
250 ' Cable could only reach to Station 29 of the screen

This page intentionally left blank

Appendix G – RPT-30PZ field data

Well ID	Top of Screen From Grade (ft)	Bottom of Screen From Grade (ft)	Screen Length (ft)	Casing Diameter (inch)	Approx. Water Level From TOC (ft)	Survey Elev. TOC (ft-msl)	Survey Elev. Conc Pad (ft-msl)	TOC to Conc Pad (ft)	Pad Thickness (ft)	Top of Screen From TOC (ft)	Bottom of Screen From TOC (ft)	Top of Screen Elevation (ft)	Bottom of Screen Elevation (ft)
RPT-30PZ	15	55	40	2	26.8	289.66	287.52	2.14	0.33	17.47	57.47	272.19	232.19

	Probe Date	.5" 4/5/00		.5" 4/6/00		.5" 4/5/00	.5" 4/6/00				4/5/00		
Station	Depth Below TOC (ft)	Ambient Time	Ambient Instrument Response	Dynamic Time	Dynamic Instrument Response	y = 0.0024x2 + 0.7838x Ambient Calibrated Flow (l/min)	y = 0.0024x2 + 0.7838x Dynamic Calibrated Flow (l/min)		Time	Water Level (ft)	Graduated Cylinder Readings (ml)	Time (sec)	Field Measured Flow (L/min)
30	27.47	17:25	0.000			0.0000			13:29	26.8			
29	28.47	17:23	-0.001			-0.0008			16:04	26.75			
28	29.47	17:21	-0.002			-0.0016			17:30	26.75			
27	30.47	17:20	-0.004			-0.0031							
26	31.47	17:18	-0.003	12:52	2.197	-0.0024	1.7336				4/6/00		
25	32.47	17:16	-0.007	12:51	2.334	-0.0055	1.8425		10:52	26.73			
24	33.47	17:15	-0.010	12:50	2.322	-0.0078	1.8329		11:00	28.74			
23	34.47	17:13	-0.009	12:48	2.356	-0.0071	1.8600		11:04	28.68			
22	35.47	17:11	-0.010	12:47	2.334	-0.0078	1.8425		11:21	28.42			
21	36.47	17:08	-0.009	12:41	2.481	-0.0071	1.9594		11:37	28.25			
20	37.47	17:06	-0.015	12:40	2.478	-0.0118	1.9570		11:52	28.39			
19	38.47	17:04	-0.015	12:30	2.527	-0.0118	1.9960		11:54	28.40			
18	39.47	17:03	-0.019	12:25	2.330	-0.0149	1.8393		11:57		1970	51.5	2.30
17	40.47	17:02	-0.025	12:23	2.279	-0.0196	1.7987		12:08		2000	57.5	2.09
16	41.47	17:01	-0.029	12:22	2.180	-0.0227	1.7201		12:09	28.25			
15	42.47	16:58	-0.038	12:21	2.096	-0.0298	1.6534		12:14		1990	57.0	2.09
14	43.47	16:57	-0.040	12:19	2.122	-0.0313	1.6740		12:17	28.30			
13	44.47	16:55	-0.046	12:17	2.147	-0.0360	1.6939		12:23		1980	56.5	2.10
12	45.47	16:54	-0.051	12:15	2.127	-0.0400	1.6780		12:31		2000	55.0	2.18
11	46.47	16:52	-0.052	12:14	2.097	-0.0408	1.6542		12:32	28.35			
10	47.47	16:50	-0.058	12:13	2.069	-0.0455	1.6320		12:40		1990	55.0	2.17
9	48.47	16:48	-0.072	12:12	1.955	-0.0564	1.5415		12:48		2000	58.0	2.07
8	49.47	16:47	-0.086	12:11	1.853	-0.0674	1.4606		12:52		2000	59.5	2.02
7	50.47	16:45	-0.095	12:10	1.794	-0.0744	1.4139						
6	51.47	16:43	-0.103	12:09	1.742	-0.0807	1.3727						
5	52.47	16:41	-0.103	12:07	1.657	-0.0807	1.3053						
4	53.47	16:39	-0.082	12:05	1.119	-0.0643	0.8801						
3	54.47	16:38	-0.072	12:04	0.792	-0.0564	0.6223						
2	55.47	16:36	-0.067	12:03	0.748	-0.0525	0.5876						
1	56.47	16:35	-0.063	12:01	0.651	-0.0494	0.5113						
0	57.47	16:33	0.000	12:00	0.015	0.0000	0.0118						
-1	58.47	16:31	0.000	11:58	0.000	0.0000	0.0000						

4/5/00   Ambient
Warm up 16:00 - 16:30 meter set to 0.000 +/- 0.001
station 30 After final reading probe raised into casing and "0" at 0.000

4/5/00   Dynamic
Warm up 8:20 - 10:38 meter set to 0.000 +/- 0.001
Station 26 probe at the bottom of the pump

This page intentionally left blank